

NAVAL POSTGRADUATE SCHOOL

Monterey, California



THESIS

A METHODOLOGY TO MEASURE THE METAL EROSION ON RECOVERED ARMATURES

by

Ozkan Gurhan

December 2001

Thesis Advisor:
Co-advisor:

William B. Maier II
Francis Stefani

Approved for public release; distribution is unlimited

Report Documentation Page		
Report Date 19Dec2001	Report Type N/A	Dates Covered (from... to) -
Title and Subtitle A Methodology to Measure the Metal Erosion on Recovered Armatures	Contract Number	
	Grant Number	
	Program Element Number	
Author(s) Gurhan, Okan	Project Number	
	Task Number	
	Work Unit Number	
Performing Organization Name(s) and Address(es) Naval Postgraduate School Monterey, California	Performing Organization Report Number	
Sponsoring/Monitoring Agency Name(s) and Address(es)	Sponsor/Monitor's Acronym(s)	
	Sponsor/Monitor's Report Number(s)	
Distribution/Availability Statement Approved for public release, distribution unlimited		
Supplementary Notes The original document contains color images.		
Abstract		
Subject Terms		
Report Classification unclassified	Classification of this page unclassified	
Classification of Abstract unclassified	Limitation of Abstract UU	
Number of Pages 113		

THIS PAGE INTENTIONALLY LEFT BLANK

REPORT DOCUMENTATION PAGE			<i>Form Approved OMB No. 0704-0188</i>	
Public reporting burden for this collection of information is estimated to average 1 hour per response, including the time for reviewing instruction, searching existing data sources, gathering and maintaining the data needed, and completing and reviewing the collection of information. Send comments regarding this burden estimate or any other aspect of this collection of information, including suggestions for reducing this burden, to Washington headquarters Services, Directorate for Information Operations and Reports, 1215 Jefferson Davis Highway, Suite 1204, Arlington, VA 22202-4302, and to the Office of Management and Budget, Paperwork Reduction Project (0704-0188) Washington DC 20503.				
1. AGENCY USE ONLY (Leave blank)		2. REPORT DATE December 2001	3. REPORT TYPE AND DATES COVERED Master's Thesis	
4. TITLE AND SUBTITLE: Title (Mix case letters) A Methodology to Measure the Metal Erosion on Recovered Armatures			5. FUNDING NUMBERS	
6. AUTHOR(S) Gurhan, Ozkan				
7. PERFORMING ORGANIZATION NAME(S) AND ADDRESS(ES) Naval Postgraduate School Monterey, CA 93943-5000			8. PERFORMING ORGANIZATION REPORT NUMBER	
9. SPONSORING /MONITORING AGENCY NAME(S) AND ADDRESS(ES)			10. SPONSORING/MONITORING AGENCY REPORT NUMBER	
11. SUPPLEMENTARY NOTES The views expressed in this thesis are those of the author and do not reflect the official policy or position of the Department of Defense or the U.S. Government.				
12a. DISTRIBUTION / AVAILABILITY STATEMENT Approved for public release; distribution unlimited			12b. DISTRIBUTION CODE	
13. ABSTRACT (maximum 200 words) Metal erosion on railgun armatures is a life-limiting mechanism for electromagnetic guns. A methodology to measure the eroded metal and to plot erosion contours on the armatures would be helpful for optimization and development of armatures. Such a method would enable to correlate eroded mass with firing parameters. The object of our research is to develop a methodology to measure the metal erosion on recovered armatures, which were obtained from a railgun test research facility. The armature surfaces were painted a uniform white. We measured displacements from a fiducial plane with a commercial optical displacement sensor. The armatures were positioned by a computer-controlled XY table. Volume-loss contours were determined from the data. Most mass loss occurred on the lateral edges of the current-carrying surfaces of the armatures. Mass losses of 0.4-0.7 g per current carrying armature surface were inferred from our observations, but lack of information about firing parameters precluded correlations in this thesis.				
14. SUBJECT TERMS Electromagnetic Railgun, Electromagnetic Launch, Armature Erosion, Railgun Armatures			15. NUMBER OF PAGES 113	
			16. PRICE CODE	
17. SECURITY CLASSIFICATION OF REPORT Unclassified	18. SECURITY CLASSIFICATION OF THIS PAGE Unclassified	19. SECURITY CLASSIFICATION OF ABSTRACT Unclassified	20. LIMITATION OF ABSTRACT UL	

THIS PAGE INTENTIONALLY LEFT BLANK

Approved for public release; distribution is unlimited

**A METHODOLOGY TO MEASURE THE METAL EROSION ON RECOVERED
ARMATURES**

Ozkan Gurhan
1st Lieutenant, Turkish Army
B.S., Turkish Army Academy, 1996

Submitted in partial fulfillment of the
requirements for the degree of

MASTER OF SCIENCE IN PHYSICS

from the

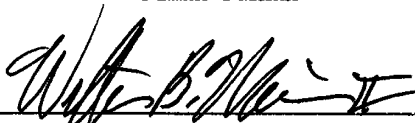
**NAVAL POSTGRADUATE SCHOOL
December 2001**

Author:

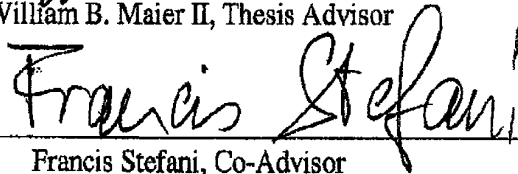


Ozkan Gurhan

Approved by:



William B. Maier II, Thesis Advisor



Francis Stefani, Co-Advisor



William B. Maier II, Chairman
Department of Physics

THIS PAGE INTENTIONALLY LEFT BLANK

ABSTRACT

Metal erosion on railgun armatures is a life-limiting mechanism for electromagnetic guns. A methodology to measure the eroded metal and to plot erosion contours on the armatures would be helpful for optimization and development of armatures. Such a method would help to correlate the eroded projectile mass with firing parameters. The object of this research is to develop a methodology to measure the metal erosion on recovered aluminum armatures from a test research facility. The armature surfaces were painted a uniform white. We measured displacements from a fiducial plane with a commercial optical displacement sensor. The armatures were positioned by a computer controlled XY translation table. Volume-loss contours were determined from the data. Most mass loss occurred on the lateral edges of the current-carrying surfaces of the armatures. Mass losses of 0.4-0.7 g per current carrying armature surface were inferred from our observations, but lack of information about firing parameters precluded correlations in this thesis.

THIS PAGE INTENTIONALLY LEFT BLANK

TABLE OF CONTENTS

I.	INTRODUCTION.....	1
A.	HISTORY	1
B.	MILITARY APPLICATIONS OF RAILGUN	1
C.	CURRENT LIMITATIONS WITH THE LATEST DEVELOPMENTS	3
D.	THE OBJECTIVE OF THE THESIS	4
II.	THE THEORY	5
A.	THE OPERATION OF RAILGUN	5
B.	ARMATURE AND RAIL CONSIDERATIONS.....	5
C.	METAL EROSION ON THE ARMATURES	6
III.	A METHODOLOGY TO MEASURE THE METAL EROSION ON THE RECOVERED ARMATURES	9
A.	THE ARMATURES	9
B.	THE MEASUREMENT APPARATUS.....	10
1.	The LED Type Optical Displacement Sensor.....	12
2.	The MAXY4009W1-S4 Assembled X-Y Tables	13
3.	Stepper Motors.....	15
4.	Stepper Motor Controllers (Indexers)	15
5.	Calibrator	15
6.	Control Terminal	15
C.	THE METHODOLOGY	15
1.	Preparation of the Armatures and the Sensor Head Before Measuring.....	16
2.	Running the VB Code and Positioning the Tables to the Initial Scan Point	17
3.	Scanning.....	18
IV.	RESULTS.....	19
A.	THE MEASURED DATA.....	19
1.	Armature 10 (Surface A);	19
a.	Unpainted Surface Data	19
b.	Painted Surface Data	21
c.	Correction	22
d.	Calculation of Eroded mass.....	27
2.	Armature 10 (Surface B);.....	28
a.	Unpainted Surface Data	28
b.	Painted Surface Data	29
c.	Correction	31
d.	Calculation of Eroded Mass	34
3.	Armature 11 (Surface A).....	35
a.	Unpainted Surface Data	35

<i>b. Painted Surface Data</i>	36
<i>c. Correction</i>	38
<i>d. Calculation of Eroded Mass</i>	41
4. Armature 11 (Surface B)	41
<i>a. Unpainted Surface Data</i>	41
<i>b. Painted Surface Data</i>	43
<i>c. Correction</i>	44
<i>d. Calculation of Eroded Mass</i>	47
5. Armature 18 (Surface A)	48
<i>a. Unpainted Surface Data</i>	48
<i>b. Painted Surface Data</i>	49
<i>c. Correction</i>	51
<i>d. Calculation of Eroded Mass</i>	54
6. Armature 18 (Surface B)	54
<i>a. Unpainted Surface Data</i>	54
<i>b. Painted Surface Data</i>	56
<i>c. Correction</i>	57
<i>d. Calculation of Eroded Mass</i>	60
7. Armature 19 (Surface A)	61
<i>a. Unpainted Surface Data</i>	61
<i>b. Painted Surface Data</i>	62
<i>c. Correction</i>	64
<i>d. Calculation of Eroded Mass</i>	67
8. Armature 19 (Surface B)	67
<i>a. Unpainted Data</i>	67
<i>b. Painted Surface Data</i>	69
<i>c. Correction</i>	70
<i>d. Calculation of Eroded Mass</i>	73
V. UNCERTAINTIES	75
A CONTROL ARMATURE SURFACE	75
B. COMPARISON OF MASS LOSSES	75
VI. CONCLUSIONS	77
VII. FUTURE WORK	79
APPENDIX A	81
LIST OF REFERENCES	93
INITIAL DISTRIBUTION LIST	95

LIST OF FIGURES

Figure 1.	Lorentz Force	5
Figure 2.	The measured armatures	9
Figure 3.	The measurement set.....	11
Figure 4.	MAXY4009W1-S4 Assembled X-Y Tables	14
Figure 5.	The initial position of the LED light on the armature surface	17
Figure 6.	Initial position of the LED light.....	17
Figure 7.	Scanning route	18
Figure 8.	(3-D) Surface plot of 10A	19
Figure 9.	(3-D) Erosion contours of 10A	20
Figure 10.	(2-D) Erosion contours of 10A	20
Figure 11.	(3-D) Surface plot of 10A	21
Figure 12.	(3-D) Erosion contours of 10A	21
Figure 13.	(2-D) Erosion contours of 10A	22
Figure 14.	Lines for correction plane	23
Figure 15.	Linear fitting of the line for 49th column for 10A.....	23
Figure 16.	Linear fitting of the line for 26th row for 10A.....	24
Figure 17.	The reference system of the plane equation.....	24
Figure 18.	Translated reference system.....	25
Figure 19.	Corrected 3-D surface plot of 10A.....	25
Figure 20.	Corrected 3-D erosion contours of 10A.....	26
Figure 21.	Corrected 2-D erosion contours of 10A.....	26
Figure 22.	Incremental integration volumes.....	27
Figure 23.	(3-D) Surface plot of 10B	28
Figure 24.	(3-D) Erosion contours of 10B	28
Figure 25.	(2-D) Erosion contours of 10B	29
Figure 26.	(3-D) Surface plot of 10B	29
Figure 27.	(3-D) Erosion contours of 10B	30
Figure 28.	(2-D) Erosion contours of 10B	30
Figure 29.	Lines for correction plane	31
Figure 30.	Linear fittings for the 26 th row and 59 th column	32
Figure 31.	Corrected 3-D surface plot of 10B.....	32
Figure 32.	Corrected (3-D) erosion contours of 10B	33
Figure 33.	Corrected (2-D) erosion contours of 10B	33
Figure 34.	(3-D) Surface plot of 11A	35
Figure 35.	(3-D) Erosion contours of 11A	35
Figure 36.	(2-D) Erosion contours of 11A	36
Figure 37.	(3-D) Surface plot of 11A.....	36
Figure 38.	(3-D) Erosion contours of 11A	37

Figure 39.	(2-D) Erosion contours of 11A	37
Figure 40.	Lines for correction plane of 11A	38
Figure 41.	Linear fittings for the 26 th row and 55 th column	39
Figure 42.	Corrected (3-D) surface plot of 11A	39
Figure 43.	Corrected (3-D) erosion contours of 11A	40
Figure 44.	Corrected (2-D) erosion contours of 11A	40
Figure 45.	(3-D) Surface plot of 11B	41
Figure 46.	(3-D) Erosion contours of 11B	42
Figure 47.	(2-D) Erosion contours of 11B	42
Figure 48.	(3-D) Surface plot of 11B	43
Figure 49.	(3-D) Erosion contours of 11B	43
Figure 50.	(2-D) Erosion contours of 11B	44
Figure 51.	Lines for correction plane of 11B	44
Figure 52.	Linear fittings of the line equations	45
Figure 53.	Corrected 3-D surface plot of 11B	46
Figure 54.	Corrected (3-D) erosion contours of 11B	46
Figure 55.	Corrected (2-D) erosion contours of 11B	47
Figure 56.	(3-D) Surface plot of 18A	48
Figure 57.	(3-D) Erosion contours of 18A	48
Figure 58.	(2-D) Erosion contours of 18A	49
Figure 59.	(3-D) Surface plot of 18A	49
Figure 60.	(3-D) Erosion contours of 18A	50
Figure 61.	(2-D) Erosion contours of 18A	50
Figure 62.	Lines for correction plane of 18A	51
Figure 63.	Linear fittings of the line equations for 18A	52
Figure 64.	Corrected (3-D) surface plot of 18A	52
Figure 65.	Corrected (3-D) erosion contours of 18A	53
Figure 66.	Corrected (2-D) erosion contours of 18A	53
Figure 67.	(3-D) Surface plot of 18B	54
Figure 68.	(3-D) Erosion contours of 18B	55
Figure 69.	(2-D) Erosion contours of 18B	55
Figure 70.	(3-D) Surface plot of 18B	56
Figure 71.	(3-D) Erosion contours of 18B	56
Figure 72.	(2-D) Erosion contours of 18B	57
Figure 73.	Lines for correction plane of 18B	57
Figure 74.	Linear fittings of the line equations for 18B	58
Figure 75.	Corrected (3-D) surface plot of 18B	59
Figure 76.	Corrected (3-D) erosion contours of 18B	59
Figure 77.	Corrected (2-D) erosion contours of 18b	60
Figure 78.	(3-D) Surface plot of 19A	61
Figure 79.	(3-D) Erosion contours of 19A	61
Figure 80.	(2-D) Erosion contours of 19A	62
Figure 81.	(3-D) Surface plot of 19A	62
Figure 82.	(3-D) Erosion contours of 19A	63
Figure 83.	(2-D) Erosion contours of 19A	63

Figure 84.	Lines for correction plane of 19A.....	64
Figure 85.	Linear fittings of the line equations for 19A.....	65
Figure 86.	Corrected (3-D) surface plot of 19A.....	65
Figure 87.	Corrected (3-D) erosion contours of 19A.....	66
Figure 88.	Corrected (2-D) erosion contours of 19A.....	66
Figure 89.	(3-D) Surface plot of 19B.....	67
Figure 90.	(3-D) Erosion contours of 19B.....	68
Figure 91.	(2-D) Erosion contours of 19B.....	68
Figure 92.	(3-D) Surface plot of 19B.....	69
Figure 93.	(3-D) Erosion contours of 19B.....	69
Figure 94.	(2-D) Erosion contours of 19B.....	70
Figure 95.	Lines for correction plane of 19A.....	70
Figure 96.	Linear fittings of the line equations for 19B.....	71
Figure 97.	Corrected (3-D) surface plot of 19B.....	72
Figure 98.	Corrected (3-D) surface plot of 19B.....	72
Figure 99.	Corrected (2-D) erosion plot of 19B.....	73
Figure 100.	(3-D) Surface plot of unfired armature.....	75

THIS PAGE INTENTIONALLY LEFT BLANK

LIST OF TABLES

Table 1.	Performance Parameters for a notional land attack railgun from [4].	3
Table 2.	Sensor Head Specifications	13
Table 3.	Controller Specifications	13
Table 4.	Physical Specifications of X-Y Tables	14
Table 5.	Mass losses for each armature surface	76

THIS PAGE INTENTIONALLY LEFT BLANK

ACKNOWLEDGMENTS

I would like to thank my thesis advisor, Bill Maier and my co-advisor Francis Stefani for their technical assistance and guidance. They gave me inspiration during my thesis research and provided numerous ideas of how to go about this project. I owe a special debt of gratitude to Don Snyder who was always available throughout the design and construction of the measurement test bench. I also want to thank George Jaksha for his expert machining service. My lab colleagues Mark Adamy and Allan Feliciano helped me understand the fundamentals of railgun theory.

Finally and most importantly my deepest gratitude goes to my wife Ebru for her loving support and understanding. Without her, I simply would not have been able to do this thesis.

THIS PAGE INTENTIONALLY LEFT BLANK

I. INTRODUCTION

A. HISTORY

The main motivation for developing weapons throughout history has been to launch projectiles to higher velocities and to longer distances. Higher speeds enable longer ranges, shorter flight times and more accuracy on the target. Electromagnetic (EM) launch technology is a strong candidate for providing this type of improvement in weapon technology. Railguns, one type of an electromagnetic launcher, can accelerate projectiles to speeds that exceed those of conventional ordnance since the driving mechanisms is not tied to the sound speed of the propellant gases. Since the start of railgun research in the 1970's at The Australian National University, the technology has progressed to the point that it is now considered an advanced weapon system on the battlefield, which will be mounted on various weapon platforms in the near future.

Richard Marshall at the Australian National University first tested railguns in the 1970's. His railgun was 5 m long and used 1.6 MA current to accelerate a 3 g projectile to 6 km/s. Railgun research became important when the U.S. President Ronald Reagan initiated the "Strategic Defense Initiative"(SDI) in the mid 80's. Since then, EM gun research has been done at various test facilities, including Eglin Air Force Base in Florida, The Institute of Advanced Technology in Austin/Texas, The Greenfarm Facility in San Diego/California, and the Army Research Laboratory in Aberdeen, Maryland.

Focused research on technical challenges and on the physics of electromagnetic launchers continues to show promise. Fundamental problems in railgun research include compact pulsed power supplies, barrel and armature design considerations, integrated launch packages, and advanced materials.

B. MILITARY APPLICATIONS OF RAILGUN

Railgun research in the Army is currently focused on developing a "tank killer" gun capable of defeating reactive armor through direct-fire engagement with high velocity projectiles (2-3 km/s) [1]. The Army hopes the railgun will be the main weapon system of tanks. Mounted on the tanks, with its higher initial velocity and higher kinetic energy, a railgun would provide a higher penetration into enemy armor and bunkers. In

addition to its high potential kill rate, a tank-mounted railgun would also increase the survivability of the Main Battle Tank. The explosive ammunition propellants increase the vulnerability of the tank when hit. If the hit is on the ammo storage shelves, the kill probability of both the tank and its crew is very high. However mounting a railgun on the tank removes the need to use chemical explosive propellants, greatly reducing the kill probability.

Considering the tactical limitations on the battlefield, the maximum number of ammunition rounds carried on any weapon platform is an important constraint on the effectiveness calculations. Railgun armatures and projectiles are lighter and smaller than the classical ammunition. Railgun would permit more rounds of ammunition to be carried on the battlefield.

The U.S. Navy is also considering railguns as a future weapon system on its ships. Railguns can be effectively used for indirect fire support of military operations in littorals. In the last few years, the Navy has become interested in the use of an electromagnetic gun for long-range shore bombardment [2]. “The goal is to increase the ship-to-shore standoff distance, improve ship survivability in combat situations, and provide lethal support for Maritime ground forces in a timely fashion” [3]. The Navy is also trying to put electric propulsion ships into service. An EM launcher can use the same electric power on such a ship. Some proposed typical parameters for a Naval railgun are given in Table 1.

Range	550 to 750 km.
Projectile Mass	60 to 70 kg.
Barrel Length	≤ 15 m.
Muzzle Velocity	2.5 to 3.5 km/s
Impact Velocity	1.5 to 2.5 km/s
Firing Rate	6 rounds/min.
Power Use (at max range and rate)	≈ 60 MW
Time of Flight (at max range)	≈ 8 Min
Cost	$\leq \$5,000$ per round

Table 1. Performance Parameters for a notional land attack railgun from [4]

C. CURRENT LIMITATIONS WITH THE LATEST DEVELOPMENTS

The effectiveness of a railgun both on land weapon platforms and on naval vessels mostly depends upon overcoming several technical challenges.

The main problems of railguns are barrel life, erosion on armatures and bore degradation. The high current density through the armature makes material selection and design considerations critical points in railgun research. The high current density on the armature and the rails may result in arcing at the armature-rail interface. Because of the arcing, pitting occurs along the rails, and the barrel life is reduced dramatically. A sudden transition from low voltage to high voltage on the interface is one indication of arcing between rails and projectile. Another problem is the large power supply needed to fire a railgun. The optimal and less voluminous power supply that has been designed for tanks is a 2.5 MJ generator with dielectric capacitors; the volume of this power supply is approximately 12.8 m^3 , which is equivalent to the total internal volume of a Russian T-72 tank.

The design of both the barrel and the armature itself are also other challenges. Large electromagnetic forces tend to separate the rails; therefore the barrel must be stiff enough to resist the resulting force.

D. THE OBJECTIVE OF THE THESIS

The objective of this thesis is to develop a methodology to measure the metal erosion on recovered armatures. The recovered armatures are obtained from a 50 mm square bore railgun [8].

The measurement apparatus is modeled and constructed in Naval Postgraduate School, Monterey, California.

II. THE THEORY

A. THE OPERATION OF RAILGUN

A simple electromagnetic launcher consists of two current-carrying parallel rails with a conductive armature between the rails and a power supply. The current passing through the rails and the armature generates a magnetic field between the rails. The armature and rails experiences a force called the **Lorentz Force**. According to the right hand rule, the Lorentz Force imparts a separating force on the rails and an axially directed accelerated force on the armature.

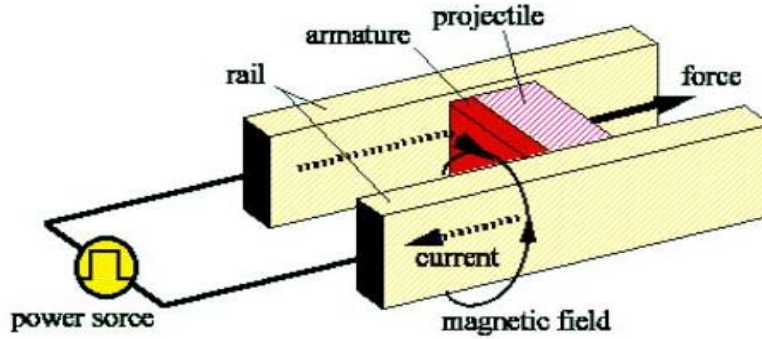


Figure 1. Lorentz Force

The force experienced by the armature is:

$$F = \frac{1}{2} L' i^2 \quad (2.1)$$

Where L' is the “Inductance Gradient” and i is the current.

B. ARMATURE AND RAIL CONSIDERATIONS

The main purpose of railgun research is to have a fieldable electromagnetic gun on weapons platforms. Unlike the classical ordinary guns, the driving force for railgun projectiles is electromagnetic rather than propellant gas pressure. Obviously the design and geometry of any railgun is different from other ordinary guns in many ways.

An objective in barrel design is to maximize i and L' , while keeping the barrel strong enough to resist the electromagnetic forces pushing the rails apart. The inductance

gradient is dependent on geometry of the rails [9]. Because the numerical value of inductance gradient is small ($0.5 \times 10^{-6} \frac{\mu\text{H}}{\text{m}}$), the current must be high to obtain useful velocities. A major challenge in designing railguns is the handling of these high currents, particularly at the armature rail interfaces [5].

The current from the power supply must travel along the rails and through the conductive armature.

The interface between armature and rails for the armatures investigated in this thesis was initially metal-to metal. Solid nonarcing armatures are preferred for military applications provided that they can remain nonarcing up to the required velocities and do not cause unacceptable rail damage.

C. METAL EROSION ON THE ARMATURES

Current research on railguns is focused on understanding and improving the way solid armatures perform. Solid armatures are ideally suited for military applications in which the muzzle speed is less than 3 km/s provided they can remain nonarcing to and do not cause unacceptable rail damage. Solid armatures operate ideally with metal-on-metal sliding contact throughout the launch. In this mode they are characterized by low power dissipation due to the low resistance of metals. Aluminum is the preferred armature material for its combination of low mass density, and high strength and electrical conductivity.

To date the performance of solid armatures remains less than ideal due to a phenomenon called “transition to arcing contact”. “Transition”, which occurs at the armature-rail interface, is a complex phenomenon whose reasons are still not completely understood. Transition is the abrupt change from low-voltage sliding electrical contact between rails and armature, typically involving a stable liquid film at the interface, to high voltage contact involving a plasma arc.

The electrical contact between the armature and the rails may not remain solid as the armature accelerates down the rails. A region of gross melting develops along the perimeter of the armature. The molten metal maintains good electrical contact but as the

armature travels along the rails and gains velocity, electrical contact may be broken, possibly because melted metal is ejected from the armature due to the electromagnetic forces inside the barrel. The ejection of the melted material results in erosion of the armature at the armature-rail interface. This can lead to the establishment of a pinch force tending to lift off the armature from the rails and ultimately loss of electrical contact. The loss of contact causes a sudden change in voltage on the interface from a low voltage of typically twenty-five volts or less to hundreds of volts. At this stage, the transition from a liquid film between the armature and the rails to a plasma arc on the armature-rail interface has occurred.

The majority of published work on transition has focused on modeling this process, sometimes called the current melt wave, or current melt wave erosion. Most models have attempted to correlate the amount of erosion damage with conditions under which the armature transitions. Although most melt wave models contain reasonable assumptions about the physics of the erosion front, they are unable to predict transition because of other factors not included in the models cause transition in addition to the wear state of the armature. It is thus difficult to establish the validity of the published models based on transition data alone. A more direct test of the models could be made by comparing the amount of eroded material predicted by the models with observed melt-wave erosion patterns on recovered armatures. Accordingly, the objective of this thesis is to develop a technique for making accurate surface measurements of erosion patterns on recovered railgun armatures.

The armatures [8] that we used in this research were launched and recovered from the 50 mm square bore railgun. The armatures were fired at velocities not greater than 700 or 800 m/sec and recovered by using a “soft catch” technique that did not effect the erosion patterns on the surface, although in some cases there was some bending of the trailing arms because the armature tumbled prior to impact. The erosion on these armatures is mostly on the lateral edges of the electrical contact face, as predicted by the current wave models, therefore it is a reasonable assumption that the metal loss on the perimeters is the result of electrical erosion from the current melt wave.

THIS PAGE INTENTIONALLY LEFT BLANK

III. A METHODOLOGY TO MEASURE THE METAL EROSION ON THE RECOVERED ARMATURES

The development of railgun armatures for a fieldable electromagnetic launcher could benefit from the close examination and study of fired and recovered armatures. Characteristics of electromagnetic launch, both electrical erosion and viscous armature wear are observable in armatures after firing. The erosion contours and some significant effects of high electromagnetic forces can be observed on a recovered armature. The erosion mechanisms on the rail/armature interface are best understood if the firing parameters are correlated with metal mass losses on the interfaces. A study of a method to measure armature metal loss will obviously need well-recovered armatures.

A. THE ARMATURES

The armatures [8] we used in the method are recovered from a 50 mm square bore railgun and are shown in Figure 4. These armatures were fired with speeds less than 700 or 800 m/sec. There is obviously no way to recover an armature that was shot at high speeds without some additional deformation. Measurements can only be made on armatures that are reasonably undeformed. If they have suffered serious damage after exiting the barrel, there is no way to discern material lost within the barrel from deformation suffered after the armature leaves the rails.



Figure 2. The measured armatures

B. THE MEASUREMENT APPARATUS

The method we used in our measurements employ a commercial optical device to measure displacement and a translation table with computer-controlled motors. Figure 3 shows:

- The LED type optical displacement sensor
 - a) Sensor Head
 - b) General purpose controller
- Assembled X-Y Tables
- Motors
- Calibrator
- Indexers
- Power Supply
- Control Terminal (A Visual Basic code was written.)
- M-EL120 Lab Jack

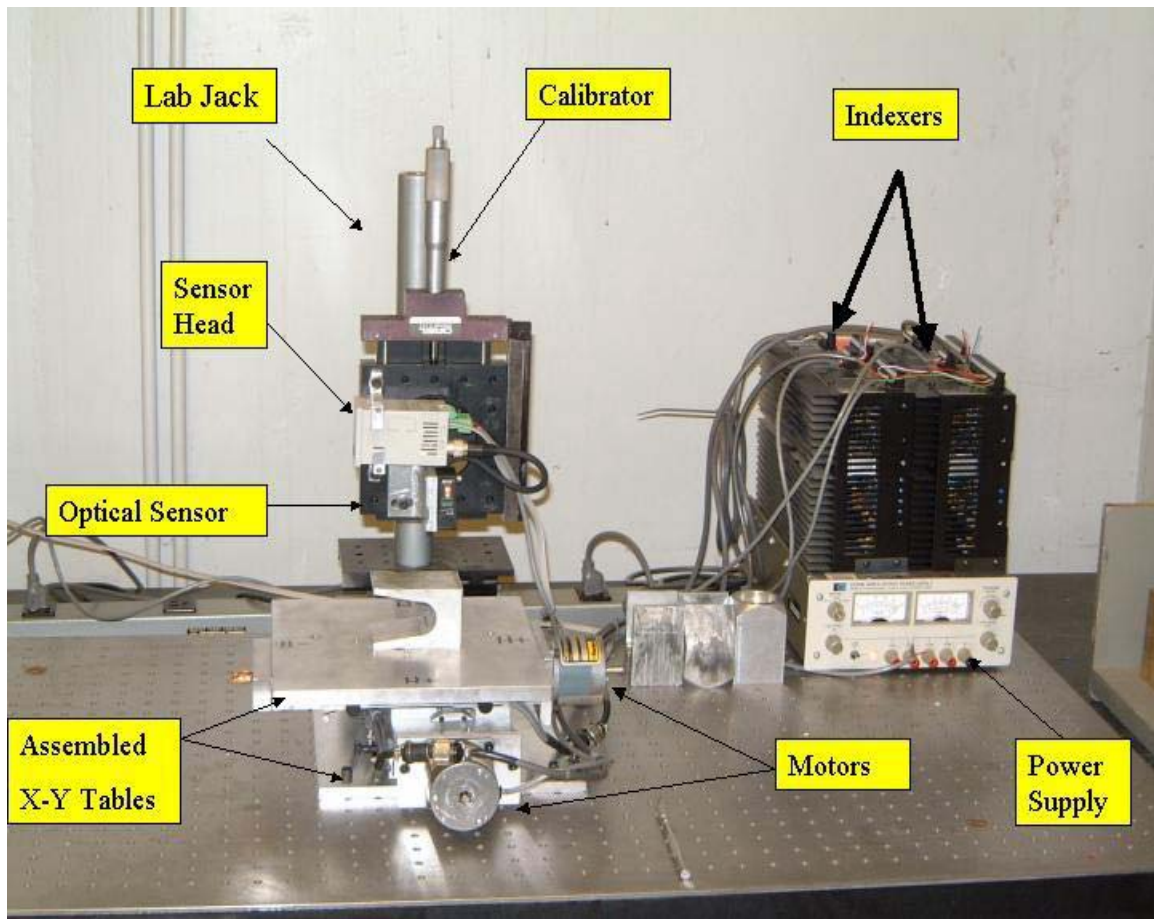


Figure 3. The measurement set

1. The LED Type Optical Displacement Sensor

The sensor is a Sunx LH-50 series LED-type optical displacement object detection sensor. It consists of

- The Sensor head
- The general-purpose controller

A position-sensitive detector (PSD) is used in the sensor head. A PSD element uses the light quantity distribution of the entire beam spot on the receiving element to determine the beam spot center and to identify this as the position of the target. However, the distribution of the light is directly affected by the surface condition of the target.

The operation of the sensor is based on the position of the reflected light on the position-sensitive detector. The light emitted from the LED is focused on the object with the optical lens forming a spot. This image is projected on the PSD by another optical lens. The position of the image on the PSD can be used to calculate the unknown distance, namely the depth.

The general-purpose controller has a screen to read the output data or the depth measurements. It also has the following elements;

- a) Comparative output indicator
- b) Emitting indicator
- c) Analog output hold indicator
- d) Jog switch
- e) Mode selection switch
- f) 5 digit LED display
- g) Connector for sensor head connection

The specification tables for both the sensor head and the controller is in Table 2 and 3.

Center measuring distance	40 mm.
Measuring range	$\pm 10\text{mm}$.
Emitting element	Red LED (modulated)(Peak wavelength 650 nm.)
Spot diameter	1.6 mm. or less
Resolution	10 μm .
Cable	0.22 mm^2 11-core composite cable, 0.2 m. long with a connector at the end.
Weight	70 g approx. (with cable), 45 g approx.(without cable)

Table 2. Sensor Head Specifications

Supply voltage	24 V DC $\pm 10\%$
Current consumption	250 mA or less (including sensor head)
Sampling frequency	5 kHz. Approx.
Display	5 digit red LED display

Table 3. Controller Specifications

2. The MAXY4009W1-S4 Assembled X-Y Tables

The X-Y tables are the main frames of the apparatus. They are made of lightweight aluminum extrusions. The tables are constructed of two crossed and inverted linear sliders, which are driven by two motors. The sliders travel on low friction polymer bearing pads. The tables include motor mounting plates, couplings, and 10 pitch lead screws. The linear sliders have adjustable outboard limits as well as fixed end-of-travel switches. There are two stepper motors connected to the tables. Each motor is connected to an indexer.

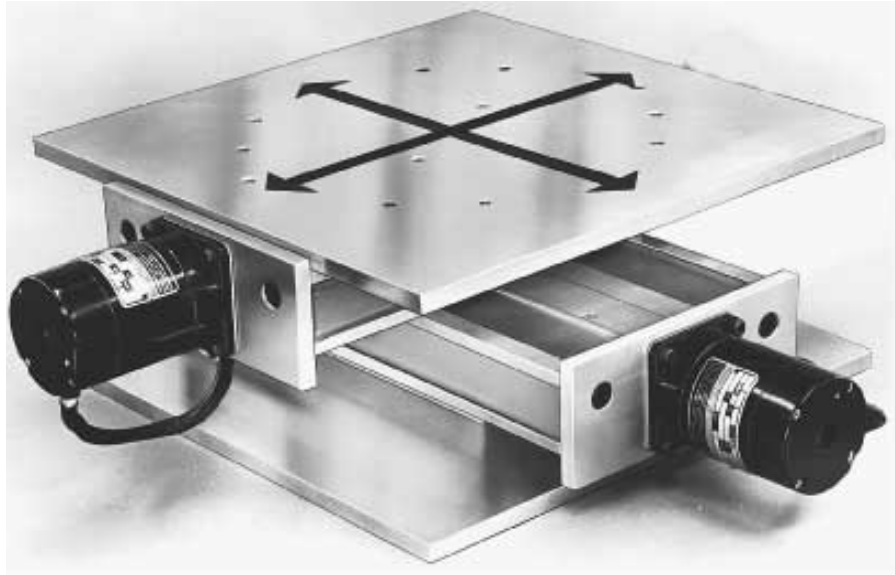


Figure 4. MAXY4009W1-S4 Assembled X-Y Tables

Travel	5"×5"
Height	4.13"
Load Capacity	25 lbs.
XL Max.	18.5"
YL Max.	18.5"
Top/Bottom Plates	9"×9"
Plate thickness Top/Bottom	0.5"/0.375"

Table 4. Physical Specifications of X-Y Tables

3. Stepper Motors

The stepper motors are connected to the X-Y tables to move the sliders in the desired direction. An indexer controls each motor.

4. Stepper Motor Controllers (Indexers)

The indexers controlled the stepper motors. An RS232 connection was made between the serial ports of the computer and the indexers to interact between the code and the motor controllers.

5. Calibrator

The calibrator was an accurate mechanical micrometer used to set the displacement between the sensor head and the armature surface to zero and to verify the depth indications of the optical displacement sensor. The sensor was calibrated for every measurement of armature surface.

6. Control Terminal

A PC was used to control the whole apparatus and to store the measured data. The stepper motor controllers were connected to the serial ports of the computer via an RS232 connection. The Visual Basic program was written to control the indexers and stepper motors. The code is given in Appendix A.

C. THE METHODOLOGY

The main purpose of the method is to have a detailed and quantitative measurement of the erosion patterns on each armature surface. The armatures were placed on the XY traveling table and displacements from an undamaged fiducial portion of the surface were measured at 1 mm spacing over the area of interest, usually about $50 \times 50 \text{ mm}$. The erosion contour plots and erosion maps of the armature faces are the outputs of our measurement methodology. We plotted the erosion maps and used them to calculate the eroded mass numerically. The recovered armatures show the effects of erosion, melting, and frictional wear on them. Each surface of the recovered armatures has both lost material and discolored nonuniformly. Because the optical displacement sensor is sensible to the color of the target area, the color variation is a critical point in our method. The armature surfaces have also been bent and tilted by forces within the

barrel or by the collection procedure. An accurate determination of the missing material mass must allow for this distortion.

1.Preparation of the Armatures and the Sensor Head Before Measuring

The surface of each armature was first cleaned with alcohol and then scanned to measure displacements. About 2500 points were measured on an area approximately $50 \times 50 \text{ mm}$ on each surface. The results of such a scan are depicted in Figure 8. The indicated displacements did not adequately reproduce the actual displacements, and the color and the texture of the surface significantly influenced the indicated displacements. The sensor also would not give any reading on some armature faces. These problems were solved by painting the armatures with a nearly uniform thickness of white paint. Other colors were tried but with less success. The variation of the data with gray paint was less than with the unpainted surface but we still had some dark and bright regions on the face that the sensor couldn't measure. Ink from felt tip pens gave a very thin coating (0.005 mm) but didn't solve the problem.

To summarize, the armatures were first cleaned with alcohol and then painted with white color before taking the measurements. The indicated distance between the sensor head and the armature was also set to zero before measurement, by adjusting the calibrator. With the cleaned and painted armature on the X-Y table, the sensor was turned on, and the armature was positioned where the LED light would fall on the middle point of the leading edge, where the surface was undamaged. Figure 5. depicts the initial position of the LED light on the armature surface.

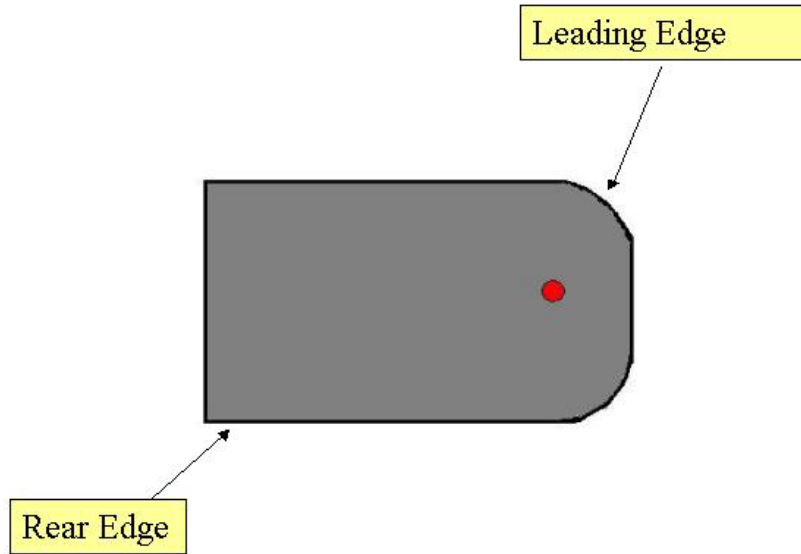


Figure 5. The initial position of the LED light on the armature surface

2. Running the VB Code and Positioning the Tables to the Initial Scan Point

After the sensor was calibrated to zero, the X-Y tables were moved to the initial scan point. As seen in Figure 5. this point is on the far left and down edge of the surface. The Visual Basic code command buttons were used to take the armature to the specified point with known motor steps, velocity and acceleration values. Those values were assigned in the program itself.

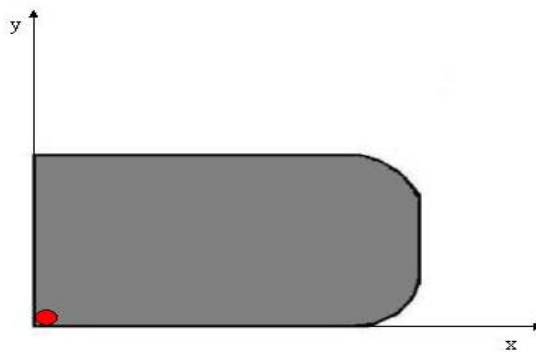


Figure 6. Initial position of the LED light

3.Scanning

After positioning the tables to the initial scanning point, the armature surface was scanned as shown in Figure 7. The algorithm of the program was;

- Read the measured depth
- Save the data to a file
- Step 1 mm.

The algorithm was executed in a loop. The number of the loop was the length of the armature length in +y direction. At the end of the loop one column was measured and the data array of this column was saved in a file. The next step after scanning one column on the armature surface was to travel 1 mm. to the right and travel downward (in -y direction). Again this downward motion of the y table was done in a loop. The same displacement that was taken in +y direction while scanning upward, was traveled in -y direction. Because there was not any erosion at the first 5-10 mm of the leading edges, this area was not scanned.

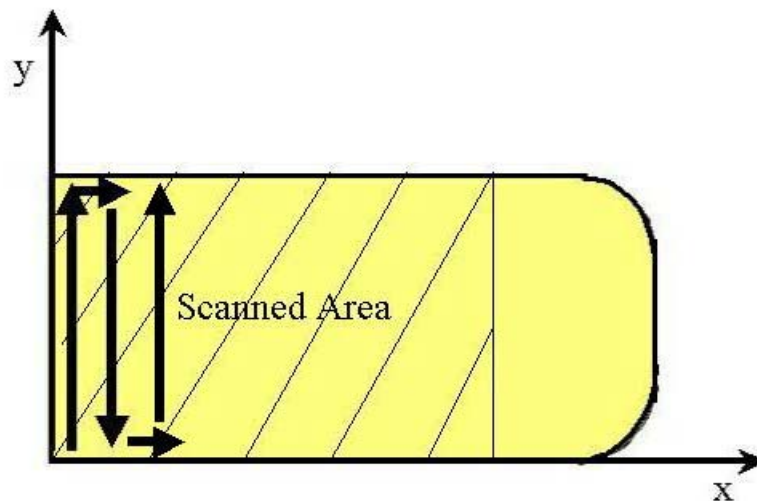


Figure 7. Scanning route

IV. RESULTS

A. THE MEASURED DATA

The surface plots and erosion contours of the painted and unpainted armature surfaces are presented in this chapter. All data manipulation and plotting was done with Matlab 6.1. The armatures were numbered 10,11,18,19. Each side of each armature was labeled as A and B.

1. Armature 10 (Surface A);

a. Unpainted Surface Data

Although the data varies with a variance of 0.237 mm, the eroded regions and erosion paths are seen on the surface plots. Much of the erosion is on the lateral edges. Unpainted data give results that are visually similar to the armatures, but that do not give an accurate measurement of material removal.

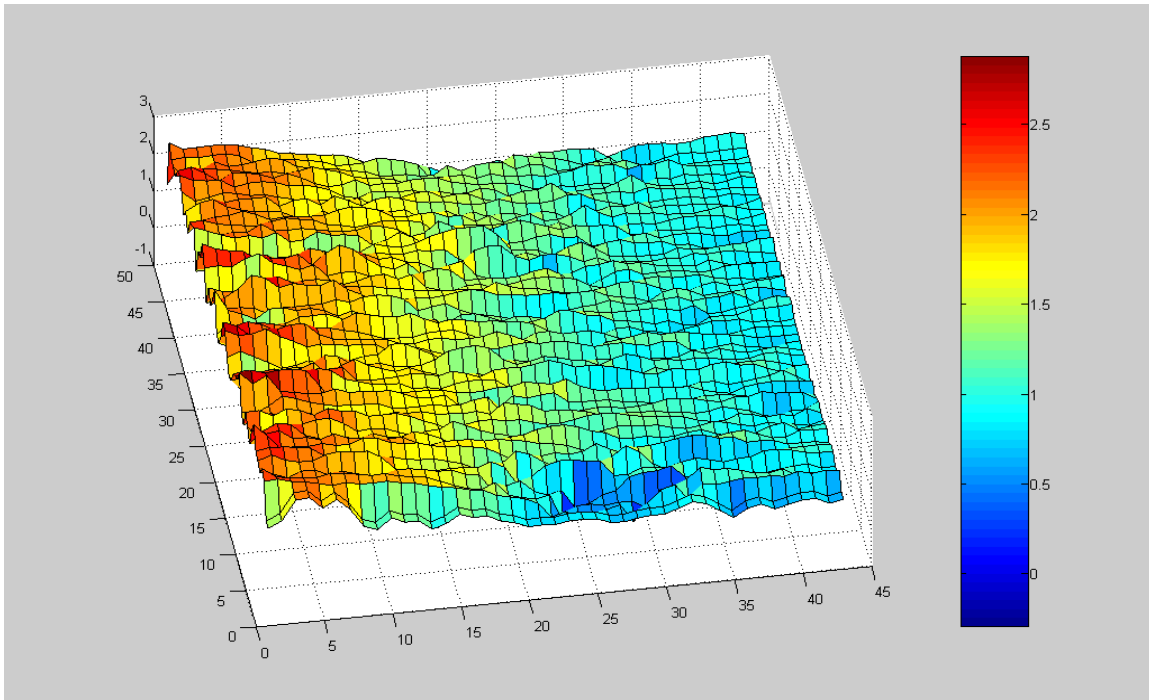


Figure 8. (3-D) Surface plot of 10A

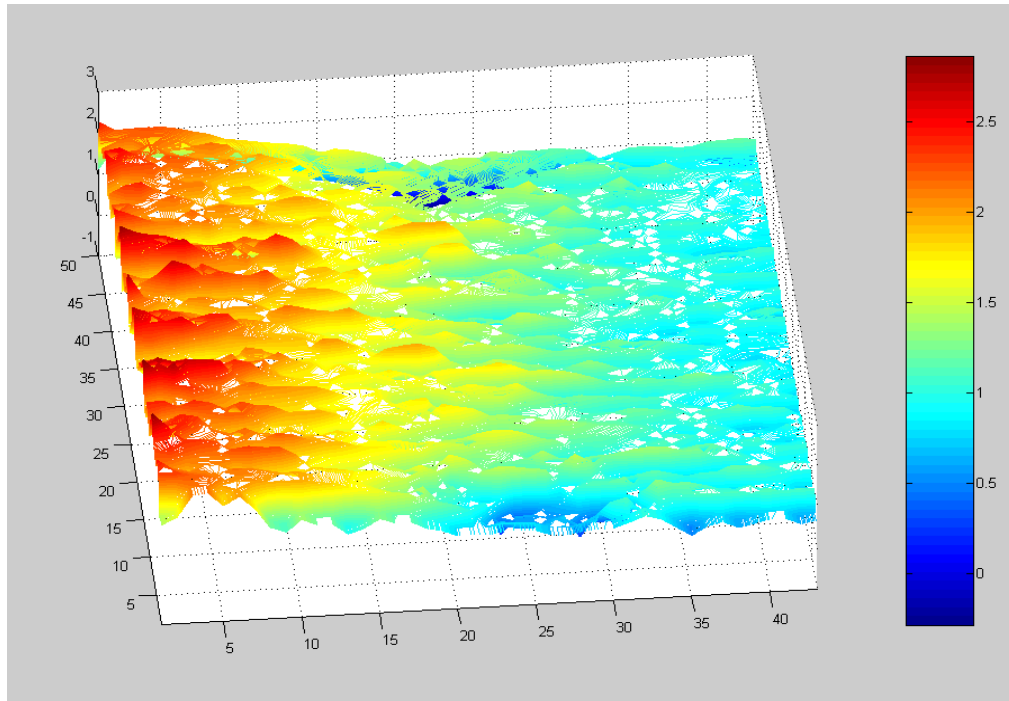


Figure 9. (3-D) Erosion contours of 10A

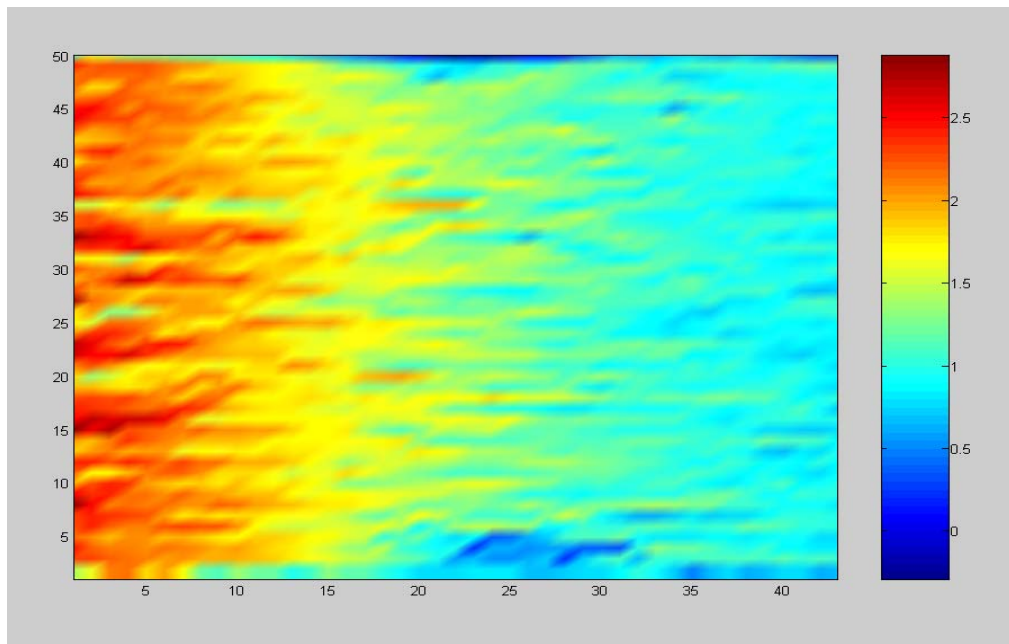


Figure 10. (2-D) Erosion contours of 10A

b. Painted Surface Data

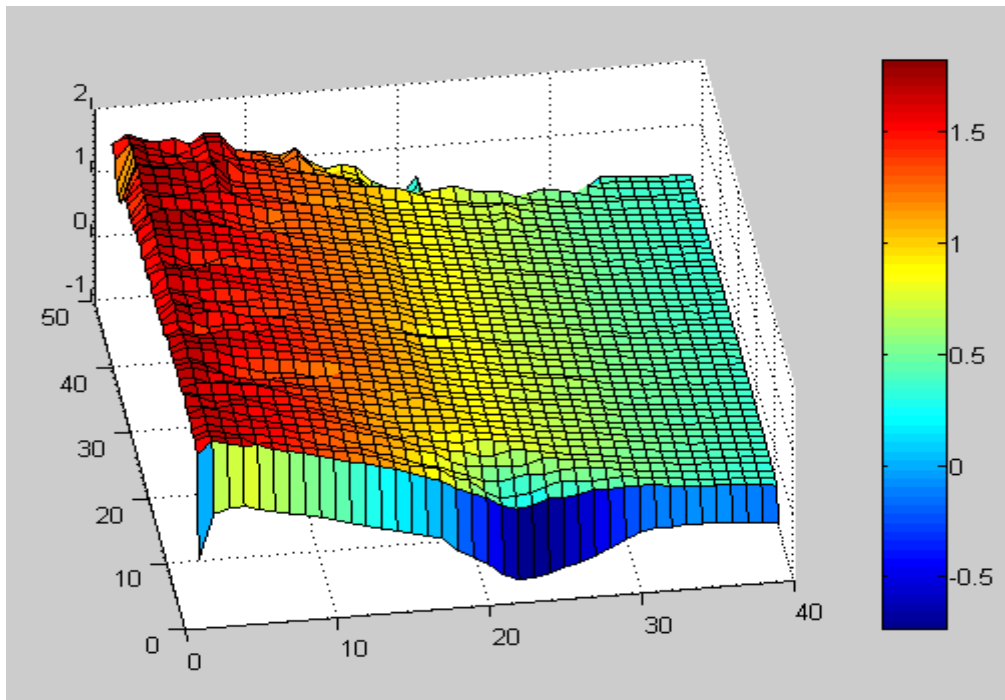


Figure 11. (3-D) Surface plot of 10A

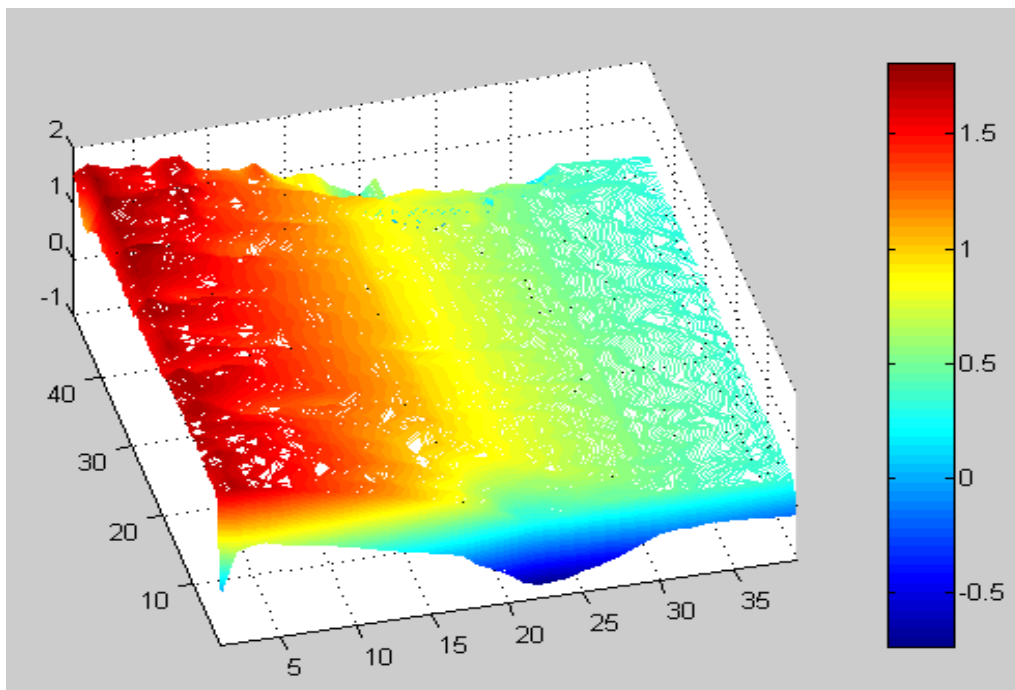


Figure 12. (3-D) Erosion contours of 10A

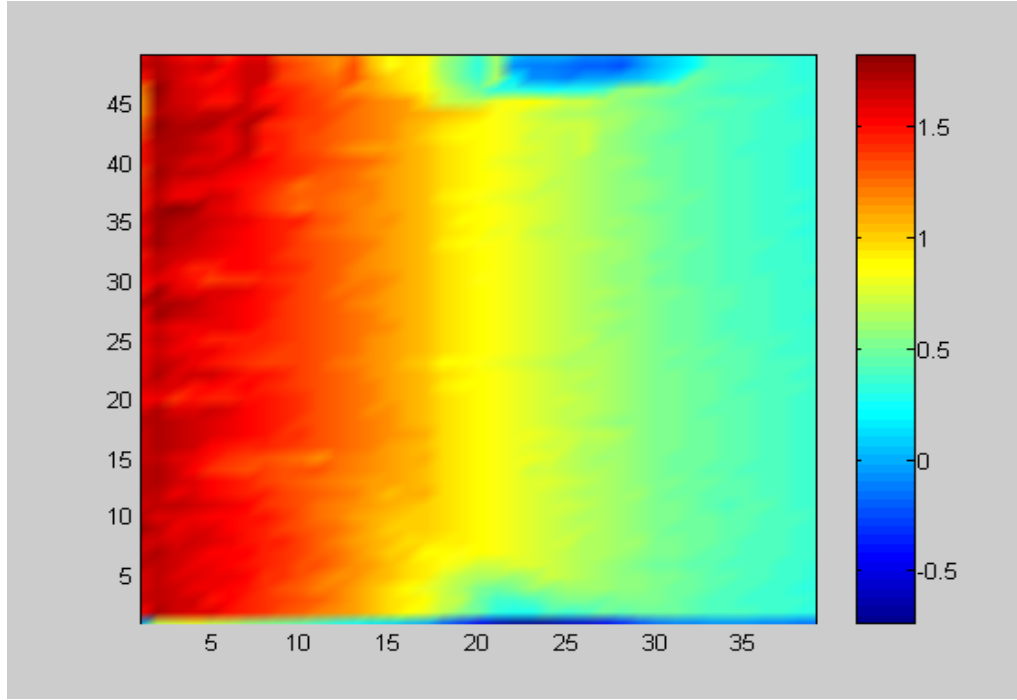


Figure 13. (2-D) Erosion contours of 10A

c. Correction

As seen in the figures of 10A, the armature is tilted upwards with an angle at the rear edges. The eroded mass on the surface, found by integrating all these data, would obviously be more than its true value. To minimize this error, the data were corrected as follows:

By inspection with naked eye, it was seen that the region between the 30th column and the leading edge was damaged. Lines that can adequately represent this particular area were selected as column 49 and the second half of 26th row as shown in Fig 16. The equations of these two lines were found by linear fitting with Matlab. The equations of the two lines;

For the 49th column;

$$y = -0.0026x + 1.612 \quad (4-1)$$

For the 26th row;

$$y = -0.039x + 1.703 \quad (4.2)$$

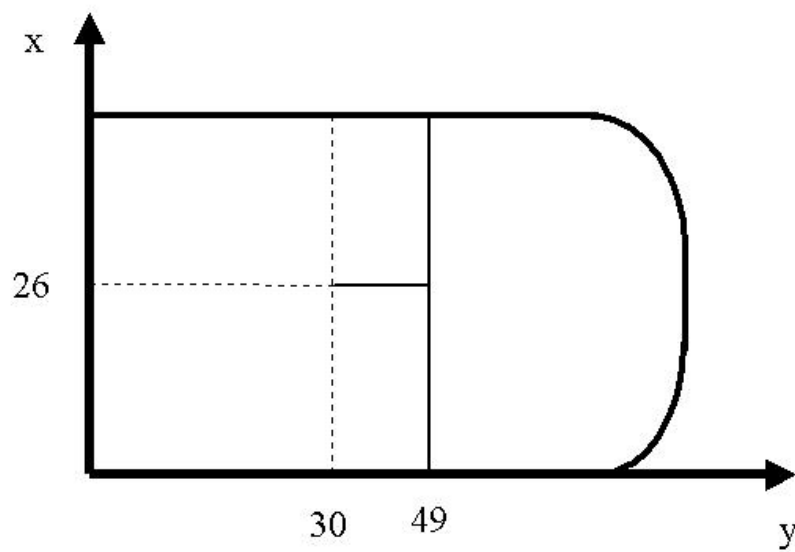


Figure 14. Lines for correction plane

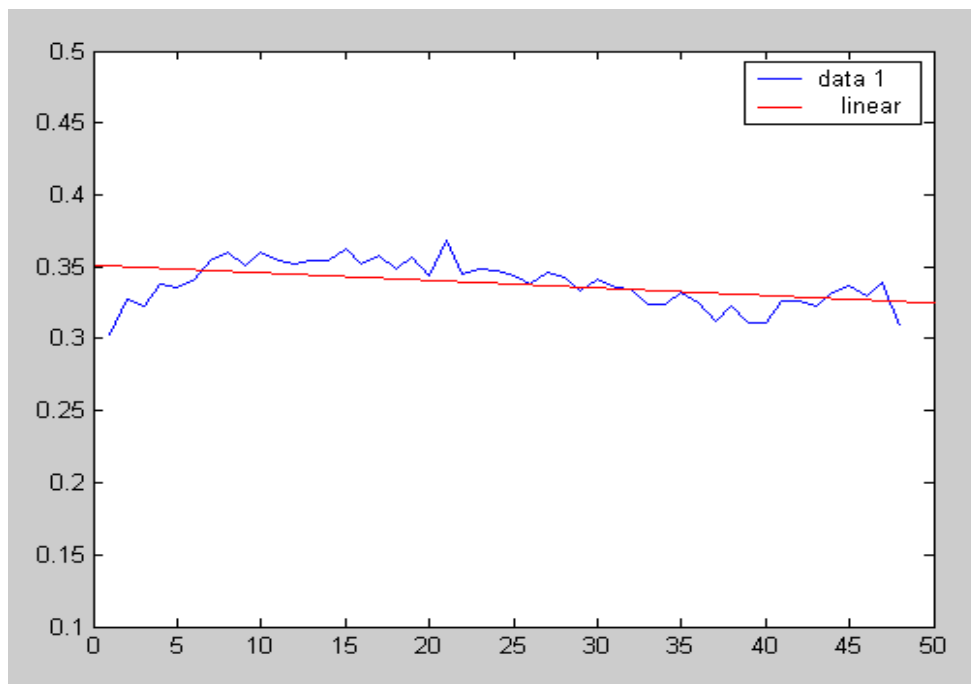


Figure 15. Linear fitting of the line for 49th column for 10A

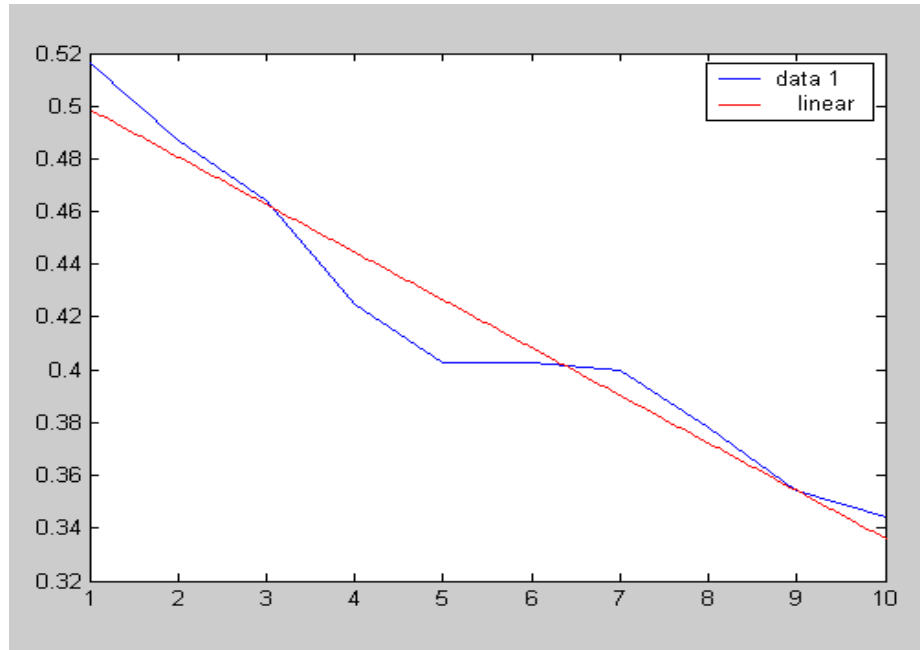


Figure 16. Linear fitting of the line for 26th row for 10A

The equation of the plane is the combination of the line equations 13 and 14.

$$z = -0.0026x - 0.039y + 1.612 \quad (4.3)$$

The reference system of plane equation is as shown in Figure 17. If the reference system is translated to that shown in Figure 18. then (4.3) becomes:

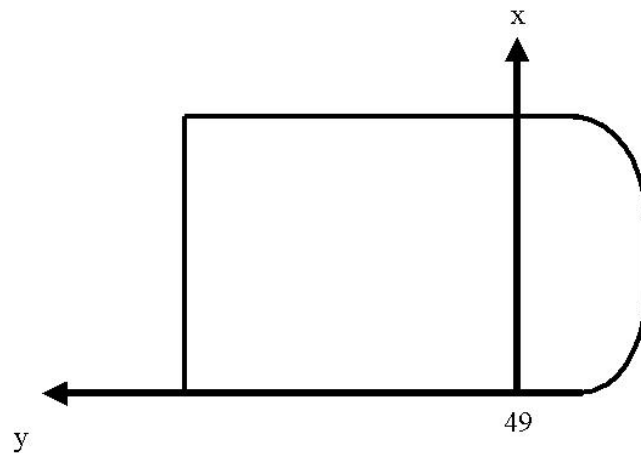


Figure 17. The reference system of the plane equation

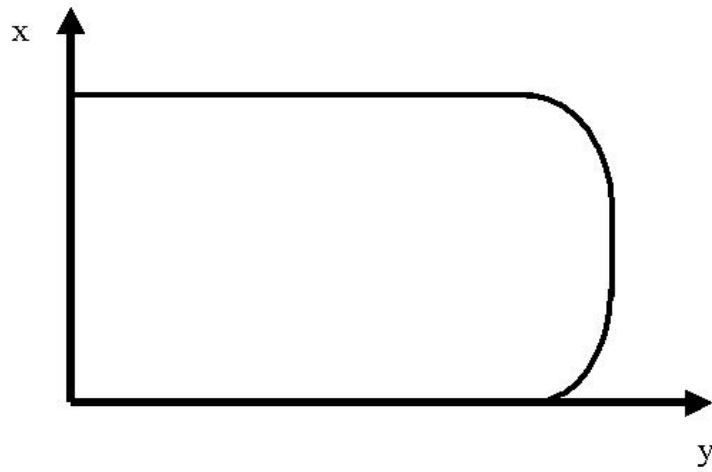


Figure 18. Translated reference system

$$z = -0.0026x - 0.039(y - 49) + 1.6 \quad (4.4)$$

$$z = f(x, y)$$

Where x is the column number and y is the row number.

The values of z corresponding to the tilted page were calculated for each element of the data matrix with a Matlab program and subtracted from the measured data. The corrected data gave a better measure of eroded mass on the surfaces. The corrected data plots are shown below.

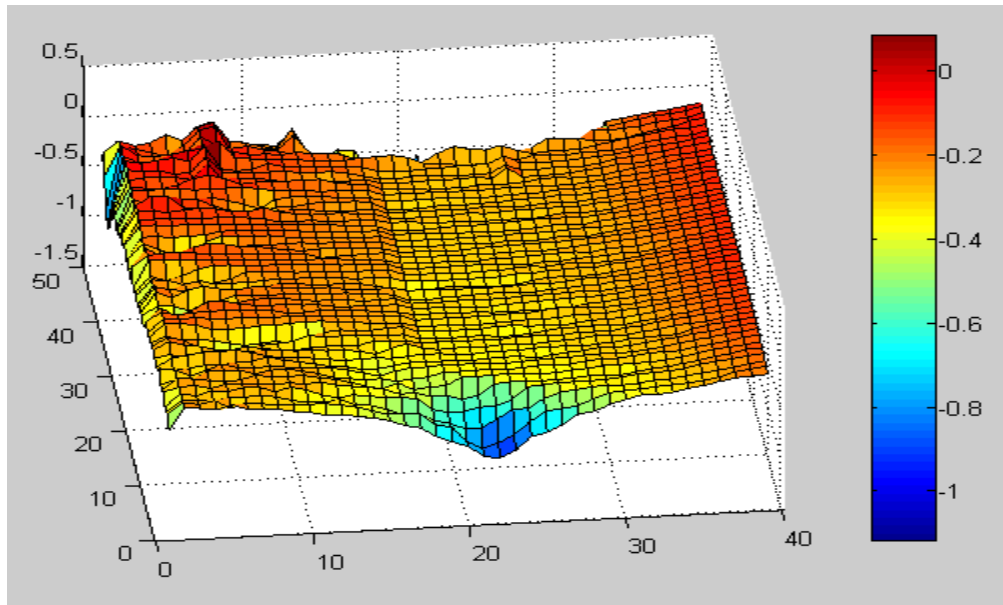


Figure 19. Corrected 3-D surface plot of 10A

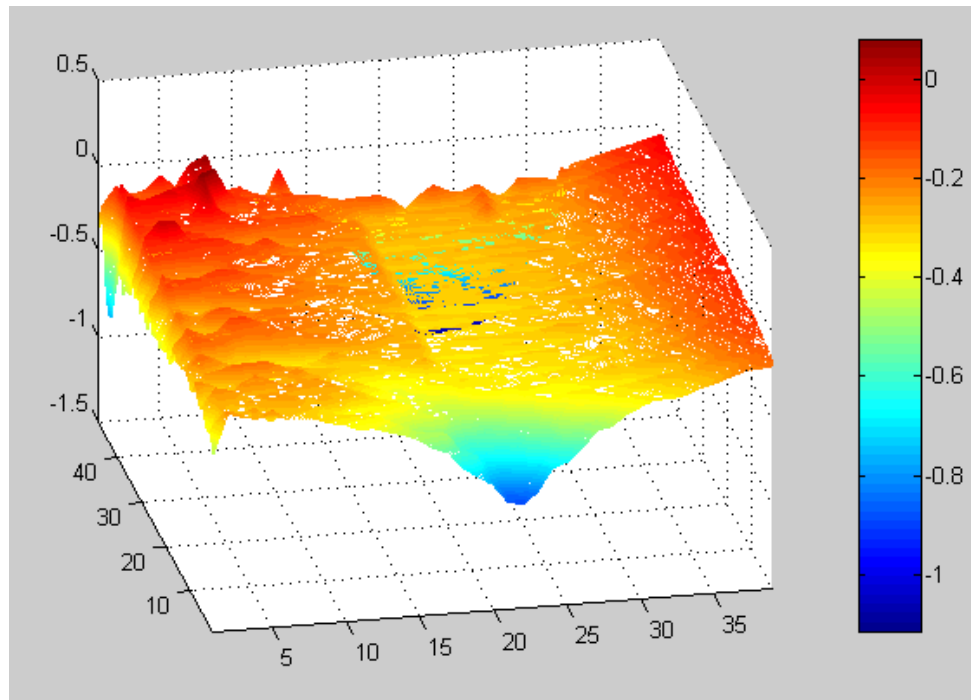


Figure 20. Corrected 3-D erosion contours of 10A

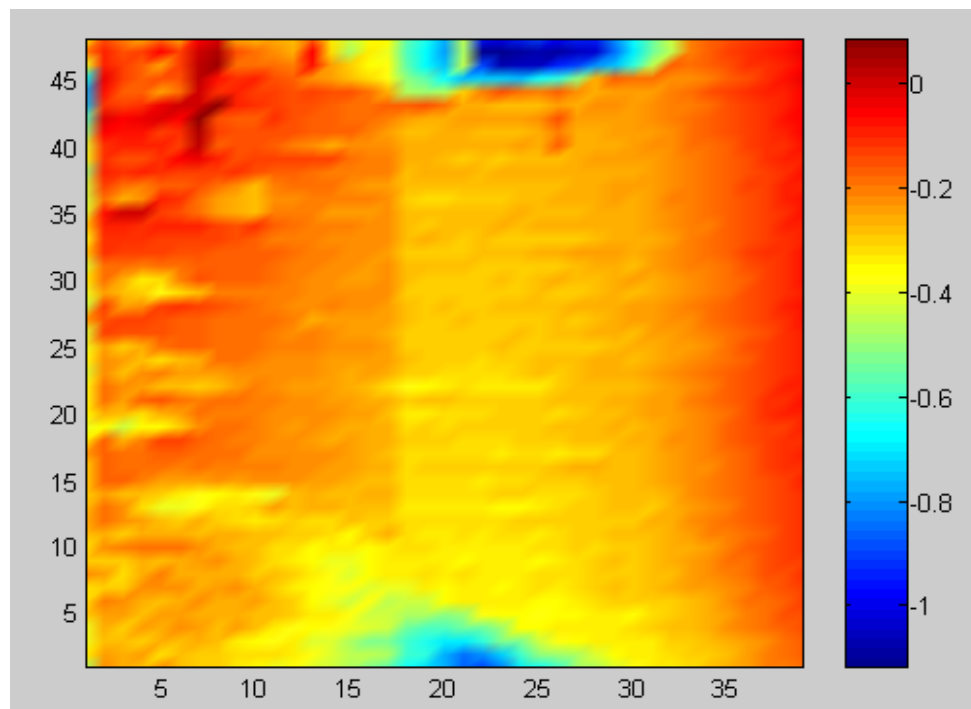


Figure 21. Corrected 2-D erosion contours of 10A

d. Calculation of Eroded mass

After the correction, the data were integrated to find the total volume lost. We assumed that each armature surface was consisted of incremental volumes. The lost volume:

$$\iiint dx dy dz \approx (1 \text{ mm}^2) \sum_k d_k$$

Where k $d_k \equiv$ measured corrected displacement at the k^{th} point.

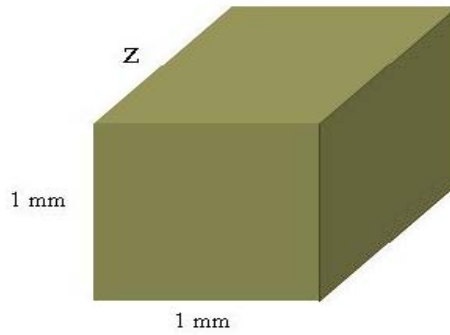


Figure 22. Incremental integration volumes

The total eroded metal volume that was lost on surface A of armature 10 was found to be 495.2536 mm^3 . If the armature is made of aluminum, then the eroded aluminum on one surface of this particular armature is;

$$m = \text{density} \times \text{volume}$$

$$\text{Where } \rho = 2.7 \frac{\text{g}}{\text{cm}^3} \text{ for aluminum}$$

$$m = 0.0027 \frac{\text{g}}{\text{mm}^3} \times 495.2536 = 1.33 \text{ g}$$

2. Armature 10 (Surface B);

a. Unpainted Surface Data

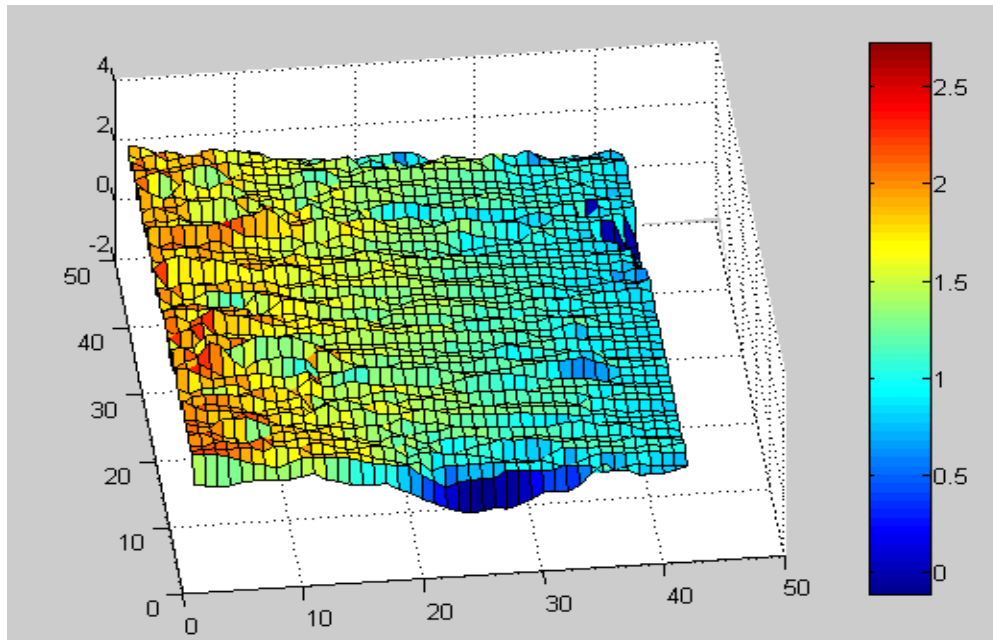


Figure 23. (3-D) Surface plot of 10B

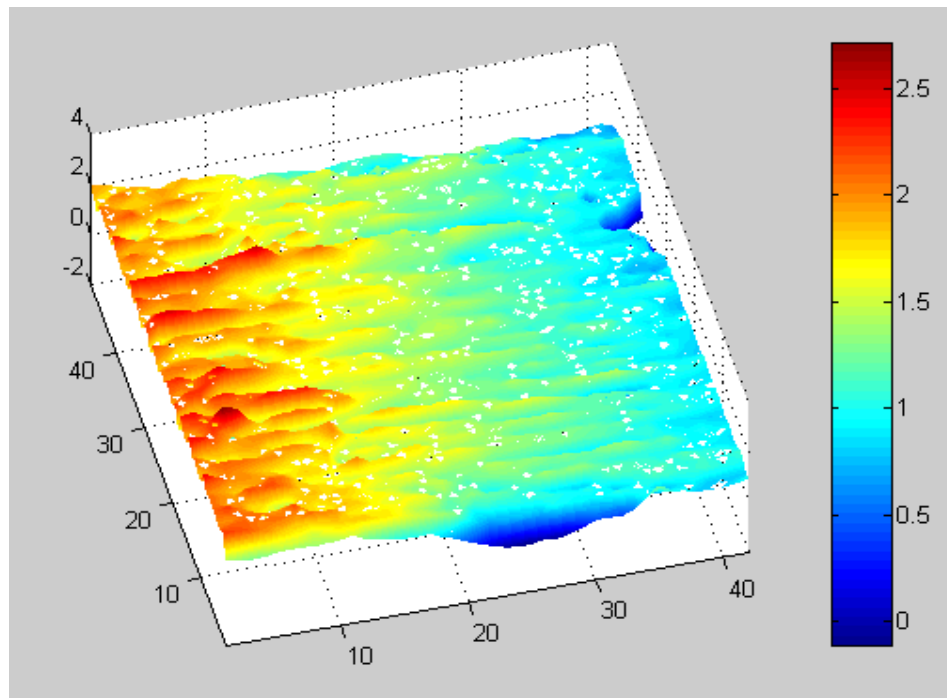


Figure 24. (3-D) Erosion contours of 10B

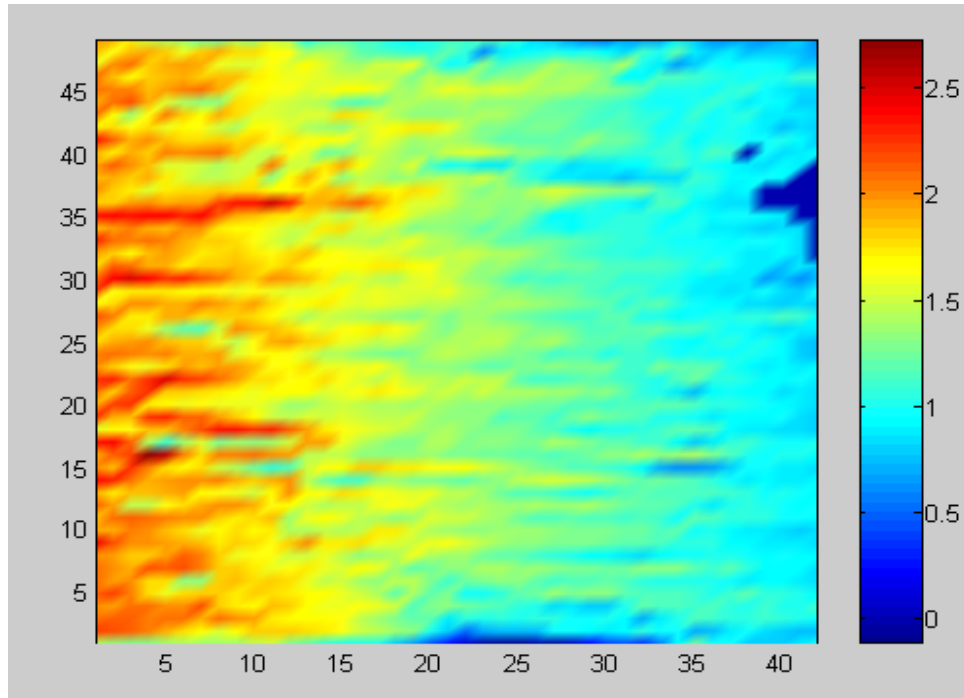


Figure 25. (2-D) Erosion contours of 10B

b. Painted Surface Data

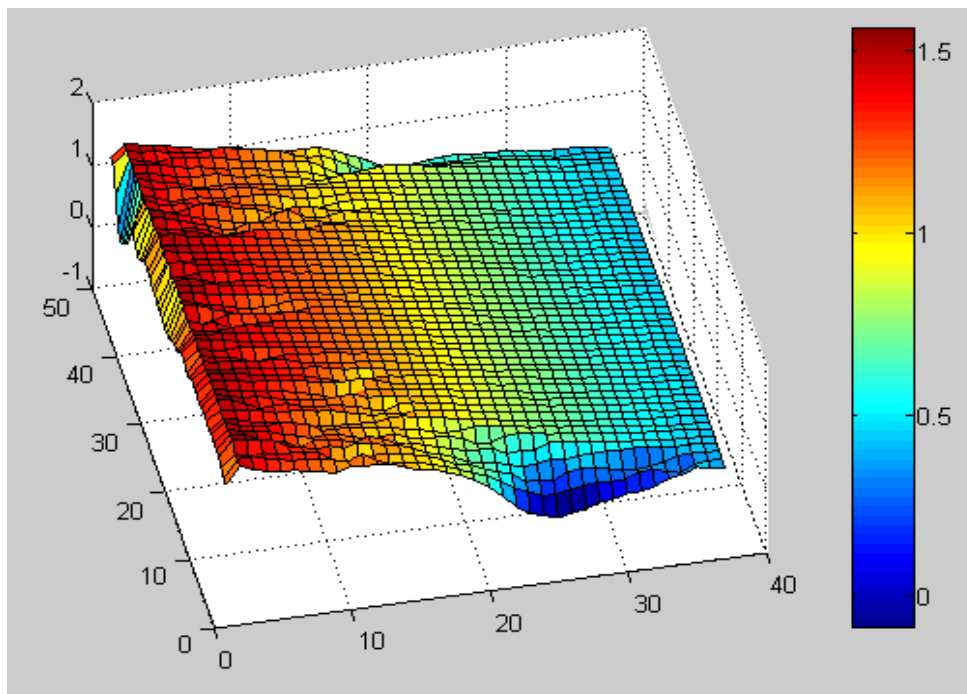


Figure 26. (3-D) Surface plot of 10B

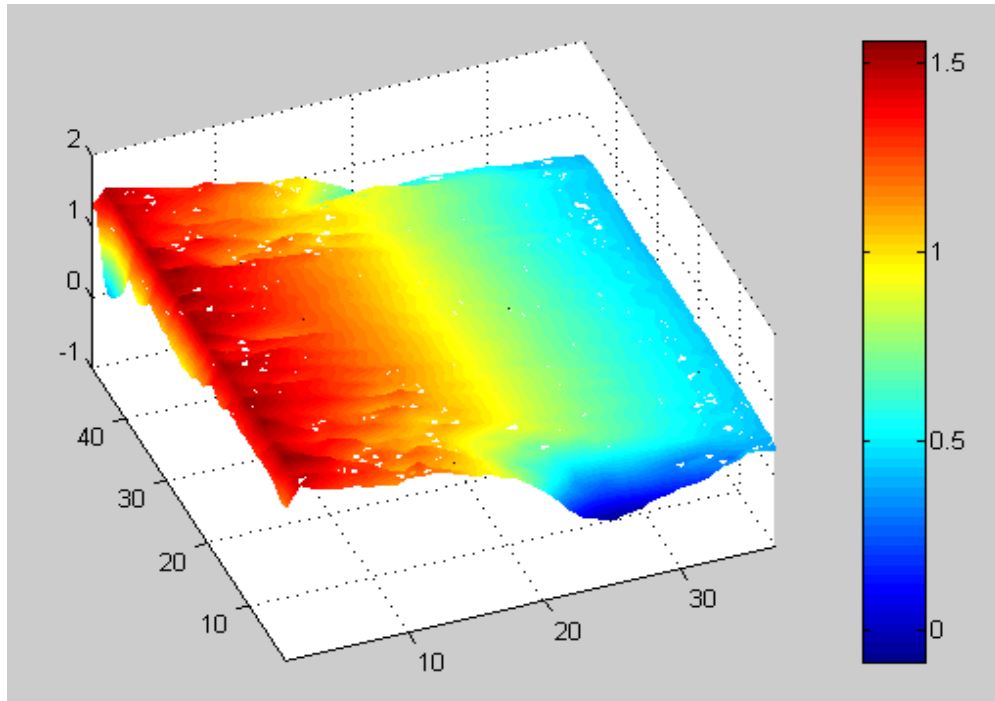


Figure 27. (3-D) Erosion contours of 10B

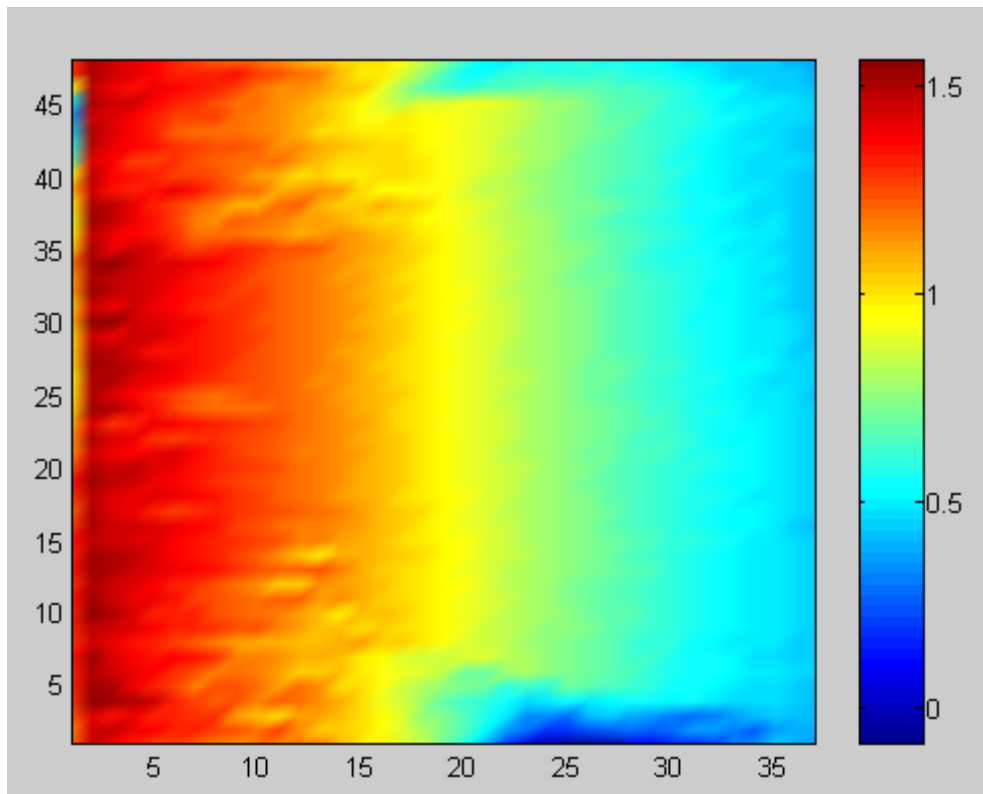


Figure 28. (2-D) Erosion contours of 10B

c. Correction

It was seen that the region between the 22nd column and the leading edge was not damaged. To represent this undamaged plane, the selected lines were the last column and the part of 26th row that lies between the 22nd column and the last column as shown in Figure 29.

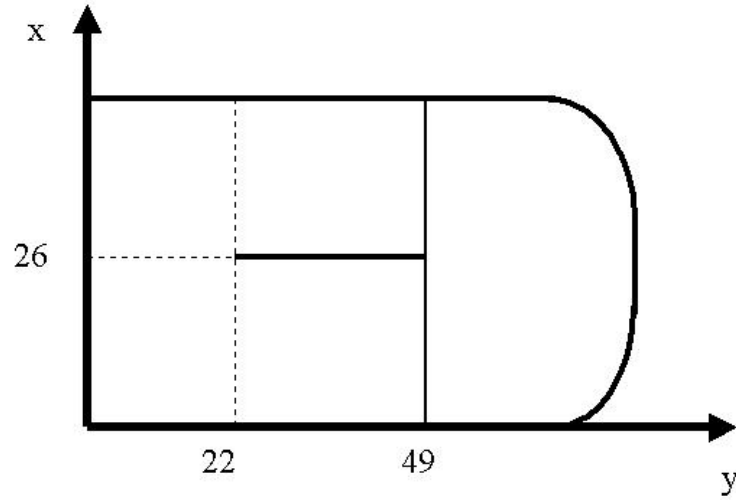


Figure 29. Lines for correction plane

The equations of two lines were obtained by linear fitting with Matlab.

For the 49th column:

$$y = -0.00011x + 0.43 \quad (4-5)$$

For the 26th row:

$$y = -0.028x + 0.86 \quad (4-6)$$

Combining line equations (4-5) and (4-6), we had the equation of the plane:

$$z = -0.00011x - 0.028y + 0.43 \quad (4-7)$$

To translate the reference system as shown in Figure 18. (4-7) is changed into:

$$z = -0.00011x - 0.028(y - 49) + 0.43 \quad (4-8)$$

The calculated values of z were subtracted from the measured data to have the corrected data plots.

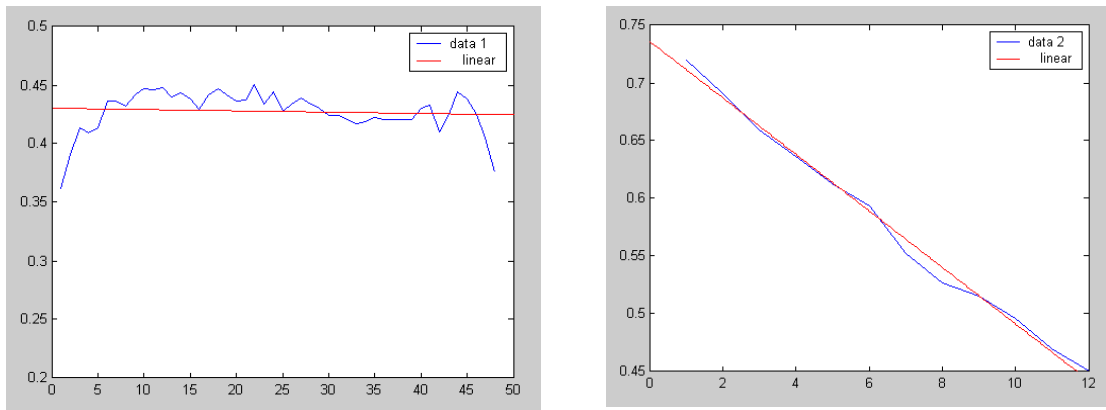


Figure 30. Linear fittings for the 26th row and 59th column

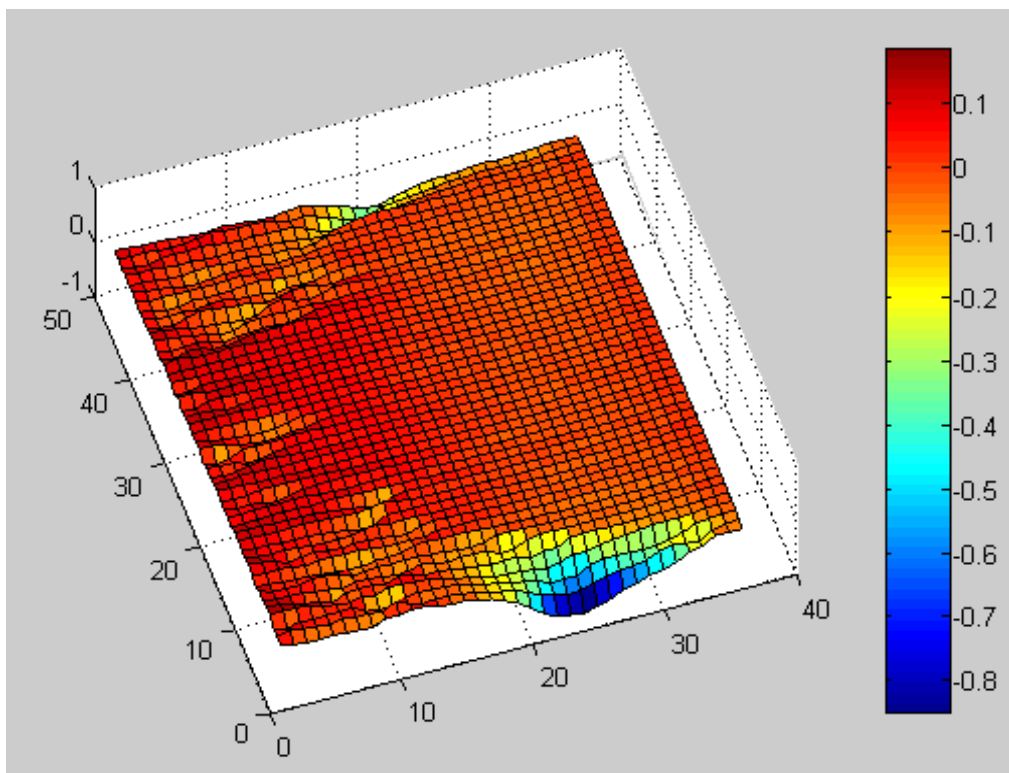


Figure 31. Corrected 3-D surface plot of 10B

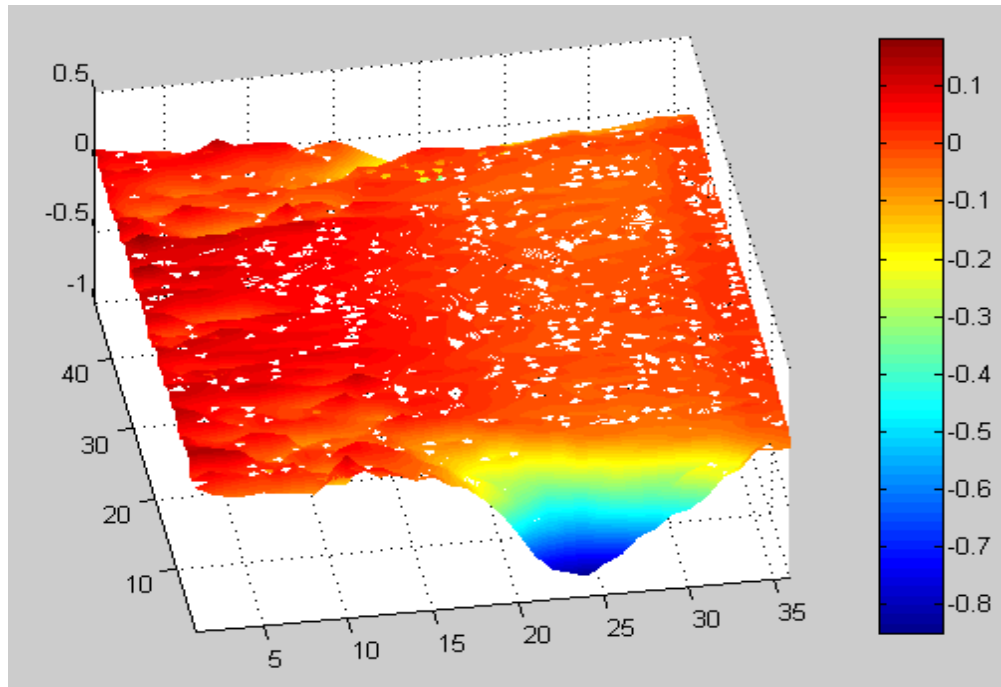


Figure 32. Corrected (3-D) erosion contours of 10B

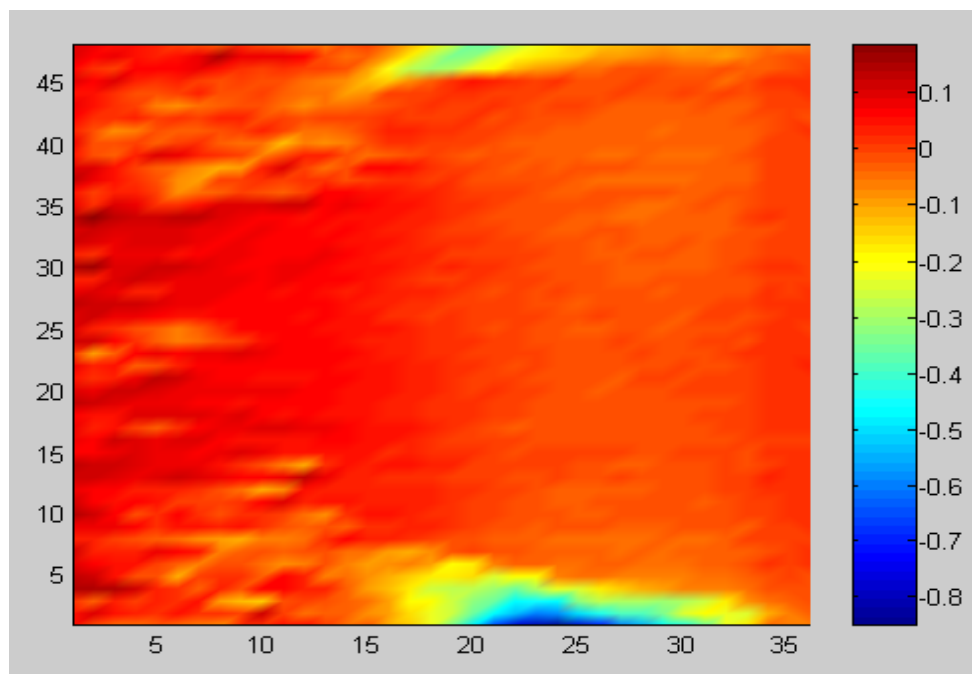


Figure 33. Corrected (2-D) erosion contours of 10B

d. Calculation of Eroded Mass

The total eroded volume that was measured on the surface B of armature 10 was found to be 34.7287 mm^3 .

$$\rho = 2.7 \frac{\text{g}}{\text{cm}^3} \text{ for aluminum}$$

$$m = 0.0027 \frac{\text{g}}{\text{mm}^3} \times 34.7287 \text{ mm}^3 = 0.0938 \text{ g}$$

3. Armature 11 (Surface A)

a. Unpainted Surface Data

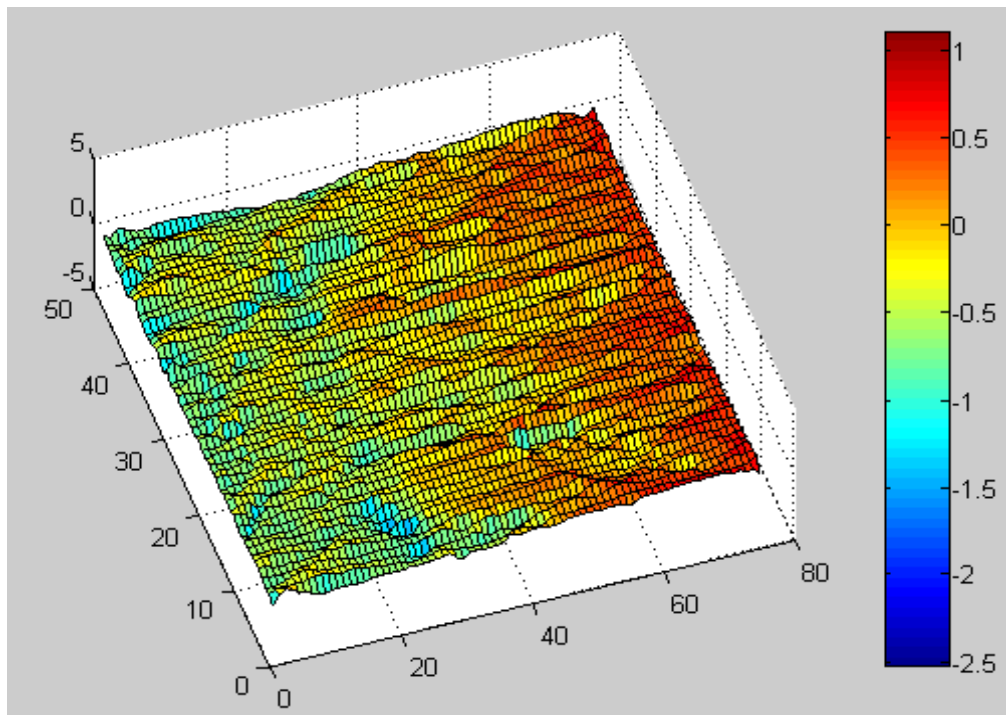


Figure 34. (3-D) Surface plot of 11A

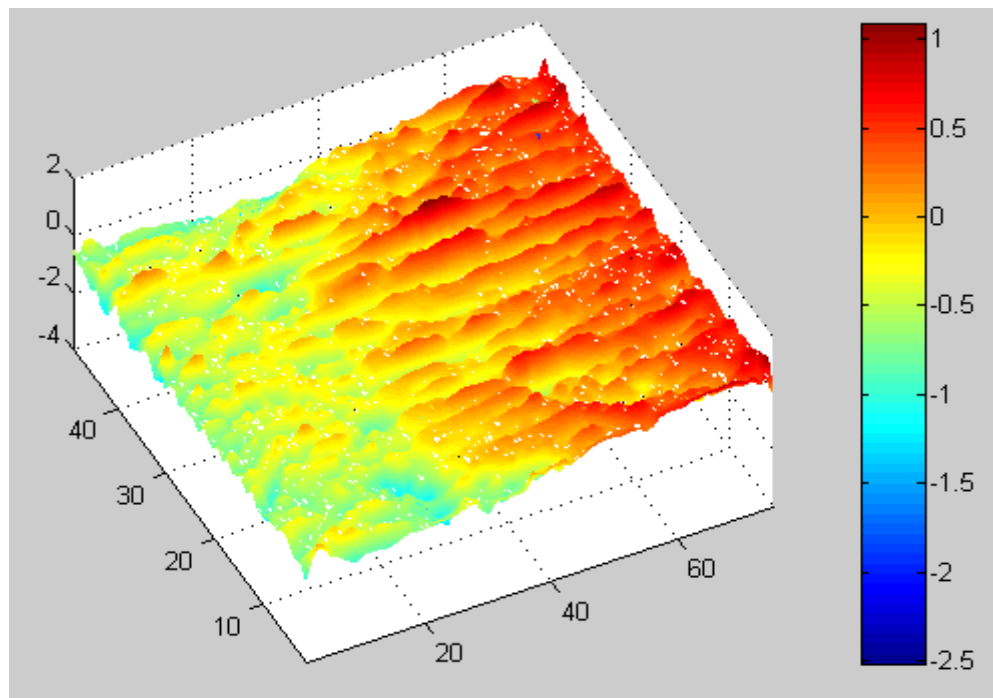


Figure 35. (3-D) Erosion contours of 11A

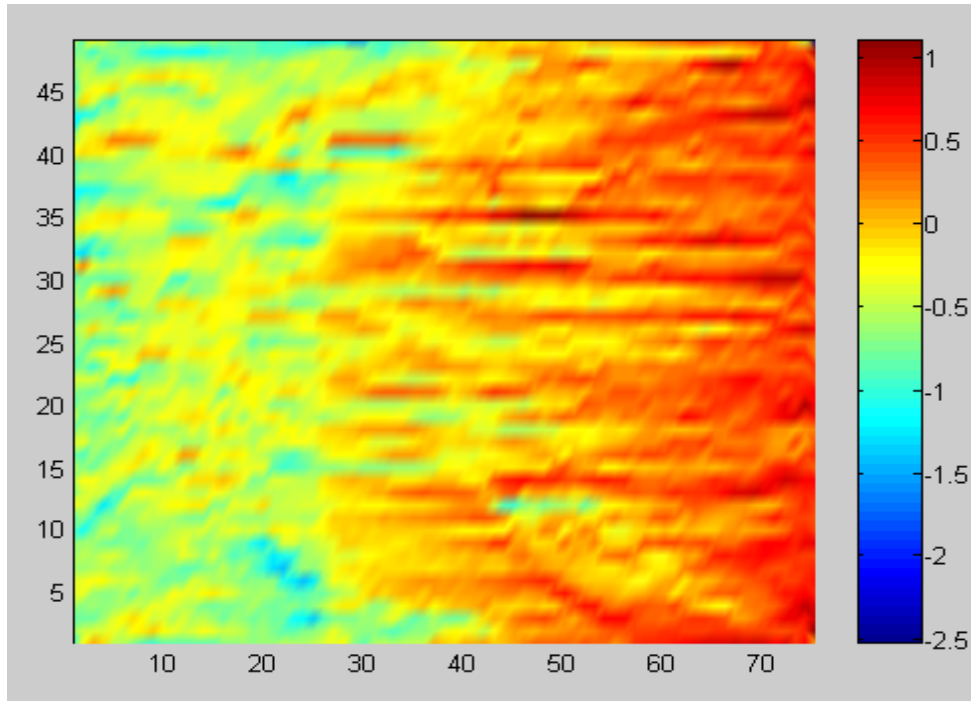


Figure 36. (2-D) Erosion contours of 11A

b. Painted Surface Data

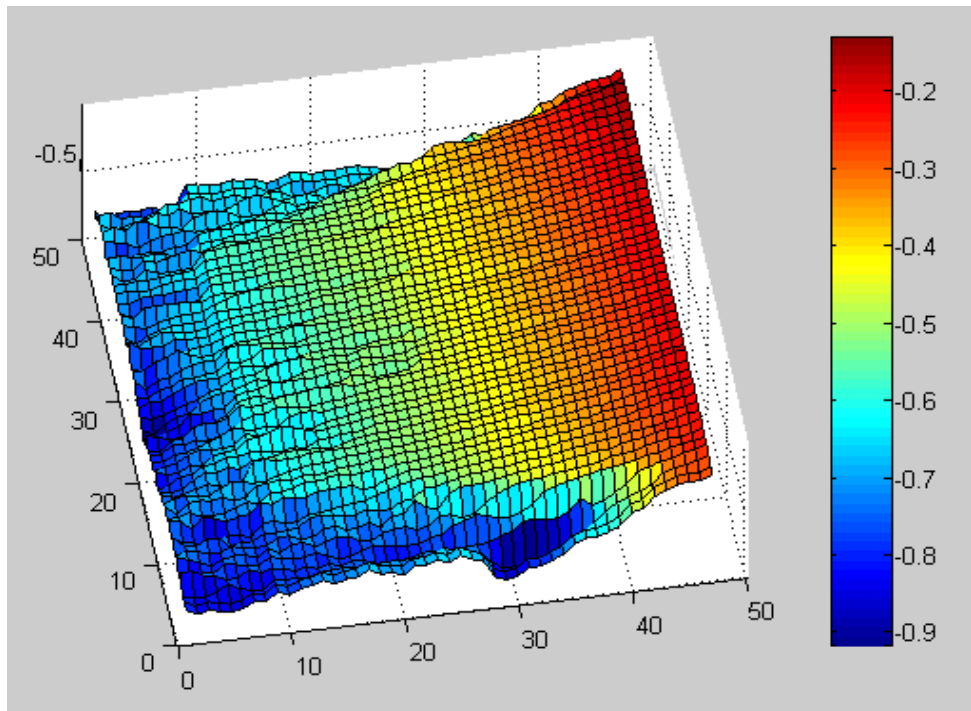


Figure 37. (3-D) Surface plot of 11A

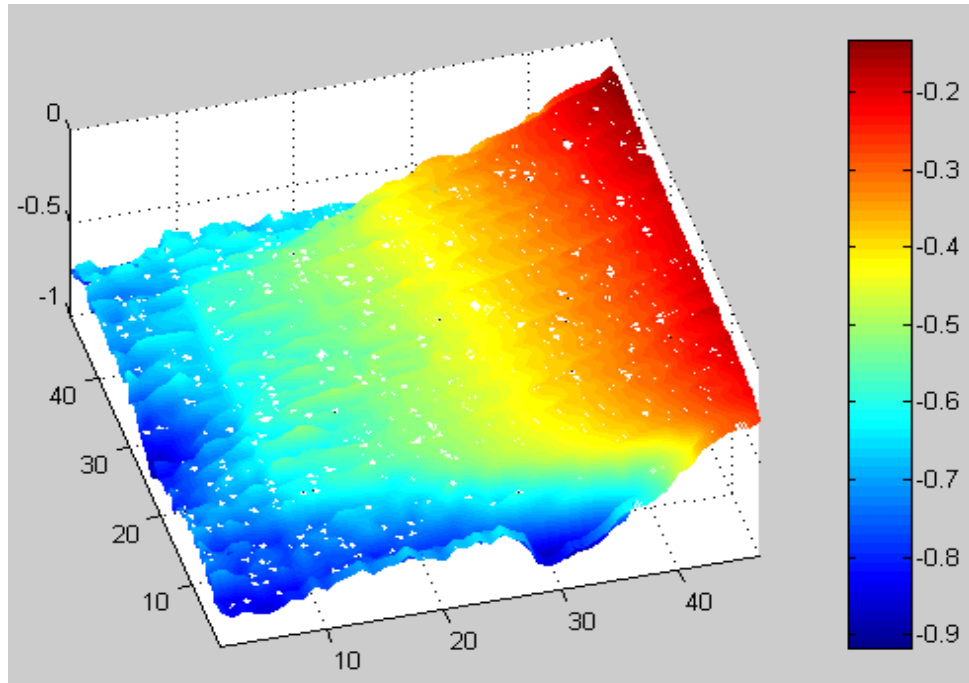


Figure 38. (3-D) Erosion contours of 11A

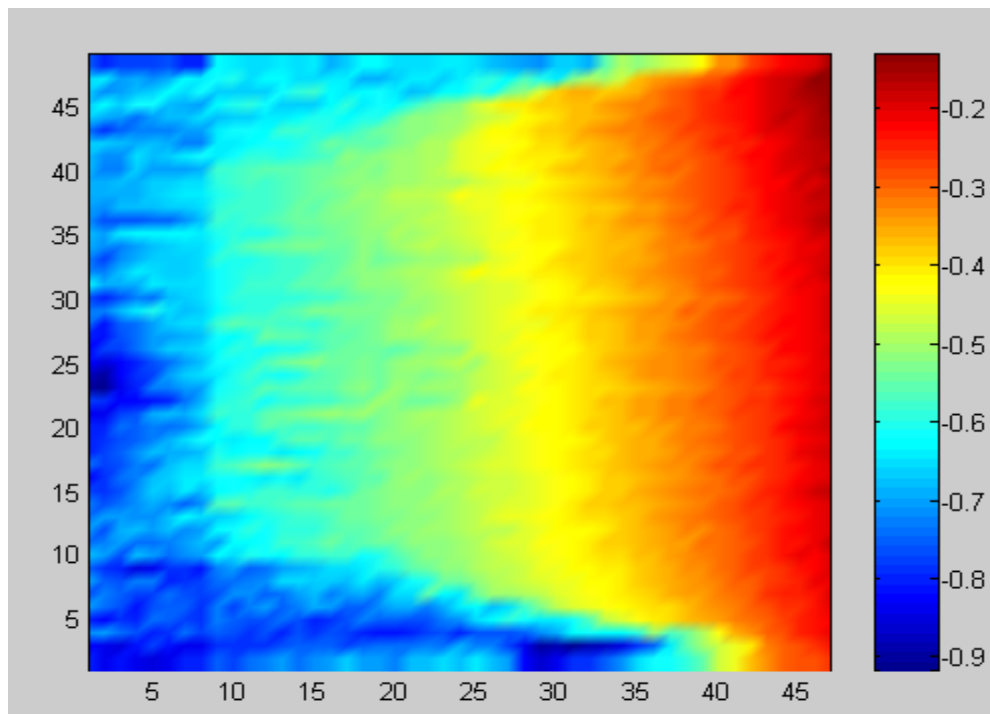


Figure 39. (2-D) Erosion contours of 11A

c. Correction

The region between the 20th column and the last column was not damaged. Lines that adequately represent the area were the part of 26th row after 20th column and column 49 as shown in Figure 40.

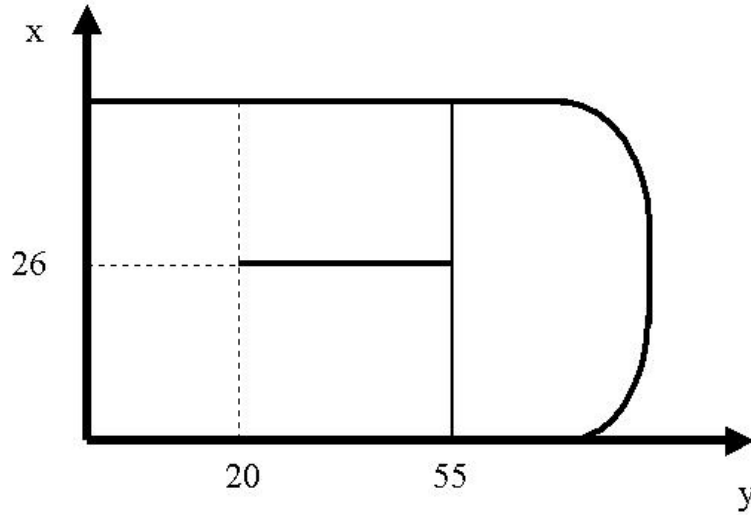


Figure 40. Lines for correction plane of 11A

The line equations:

For the 55th column:

$$y = 0.0017x - 0.23 \quad (4-9)$$

For the 26th row:

$$y = 0.013x - 0.56 \quad (4-10)$$

The combination of the two equations above gives us the plane equation.

$$z = 0.0017x + 0.013y - 0.23 \quad (4-11)$$

If the reference system is translated to that shown in Fig. 9, the plane equations becomes as follows:

$$z = 0.0017x + 0.013(y - 55) - 0.23 \quad (4-12)$$

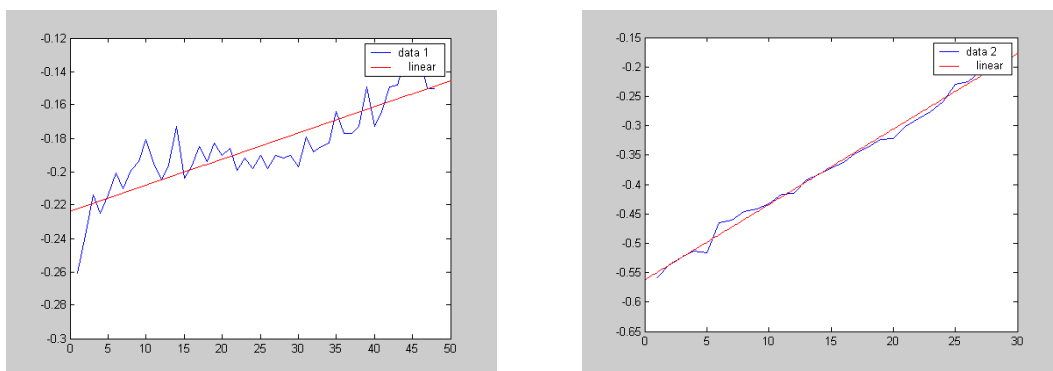


Figure 41. Linear fittings for the 26th row and 55th column

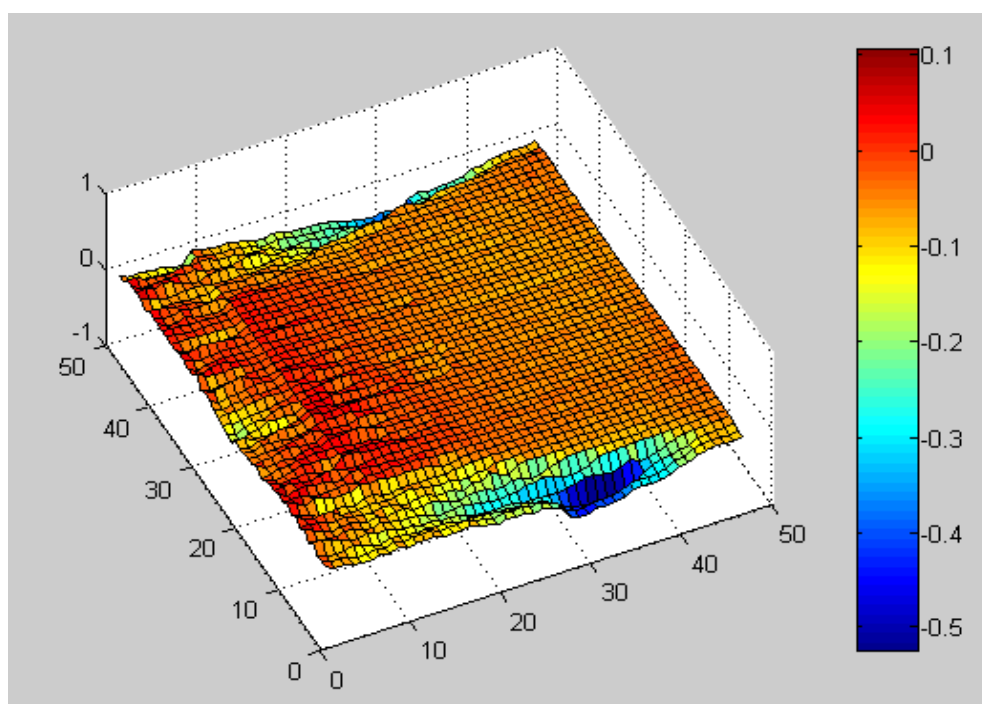


Figure 42. Corrected (3-D) surface plot of 11A

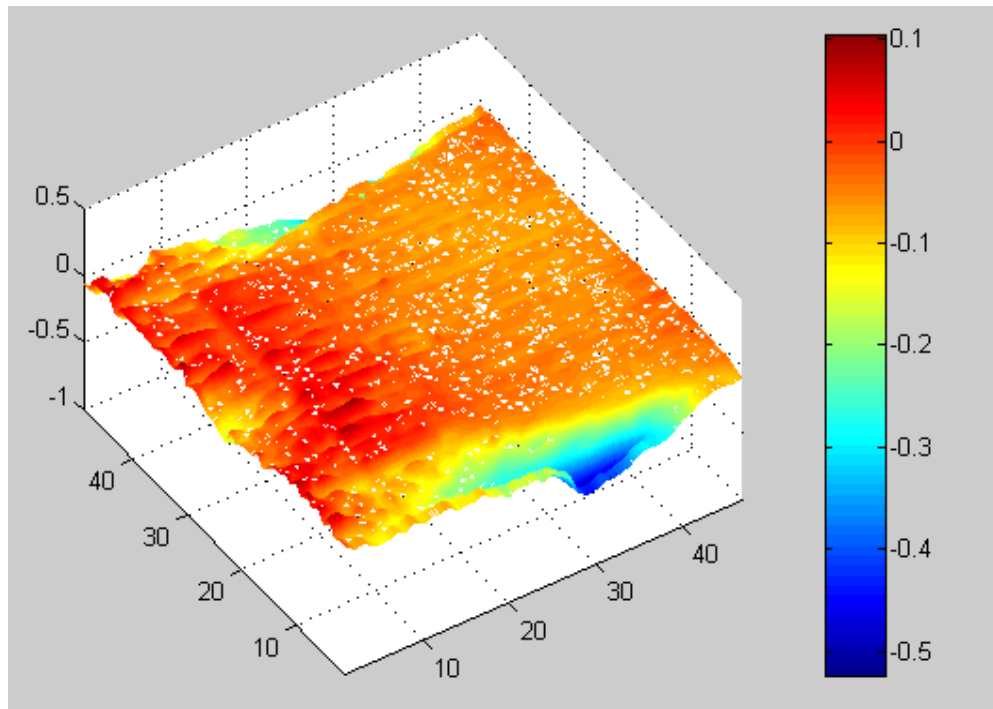


Figure 43. Corrected (3-D) erosion contours of 11A

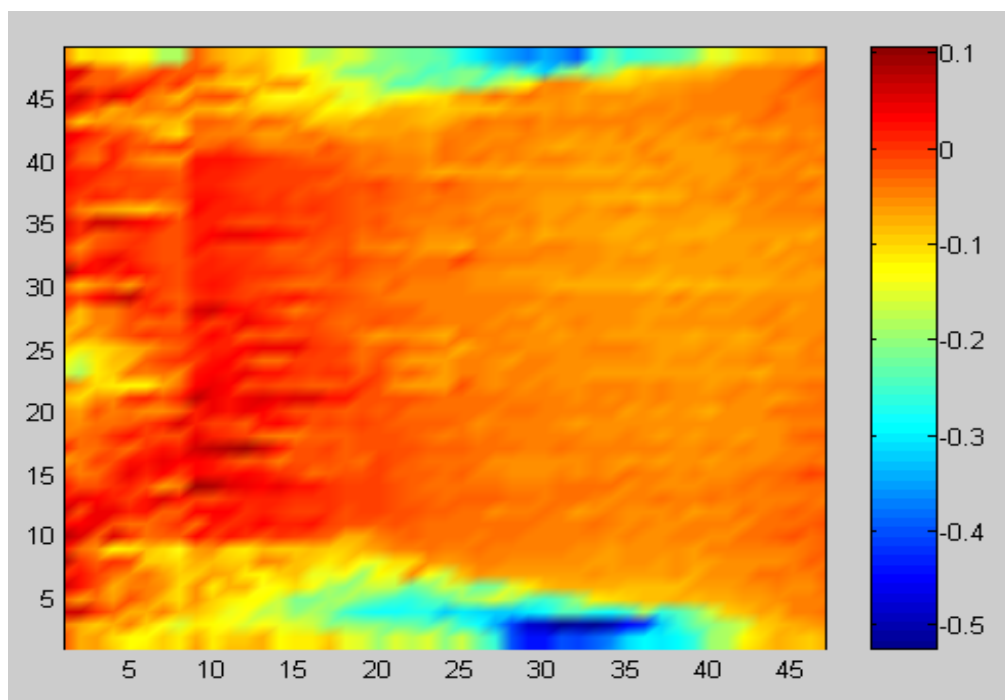


Figure 44. Corrected (2-D) erosion contours of 11A

d. Calculation of Eroded Mass

The total eroded metal volume was found to be 146.645 mm^3 .

$$\rho = 2.7 \frac{\text{g}}{\text{cm}^3}$$

$$m = 0.0027 \frac{\text{g}}{\text{mm}^3} \times 146.645 \text{ mm}^3 = 0.396 \text{ g}$$

4. Armature 11 (Surface B)

a. Unpainted Surface Data

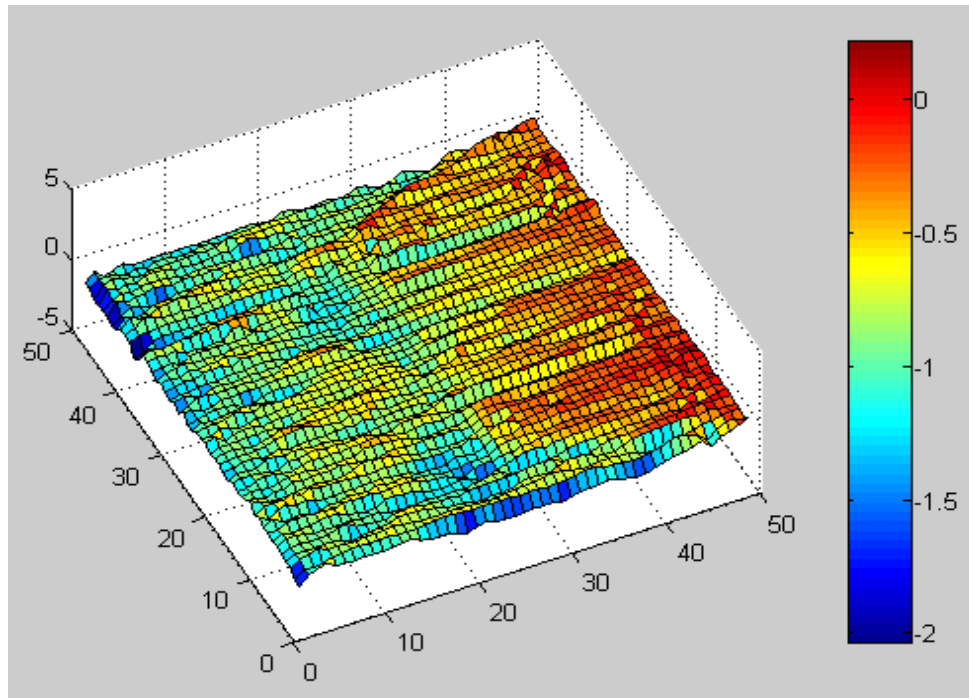


Figure 45. (3-D) Surface plot of 11B

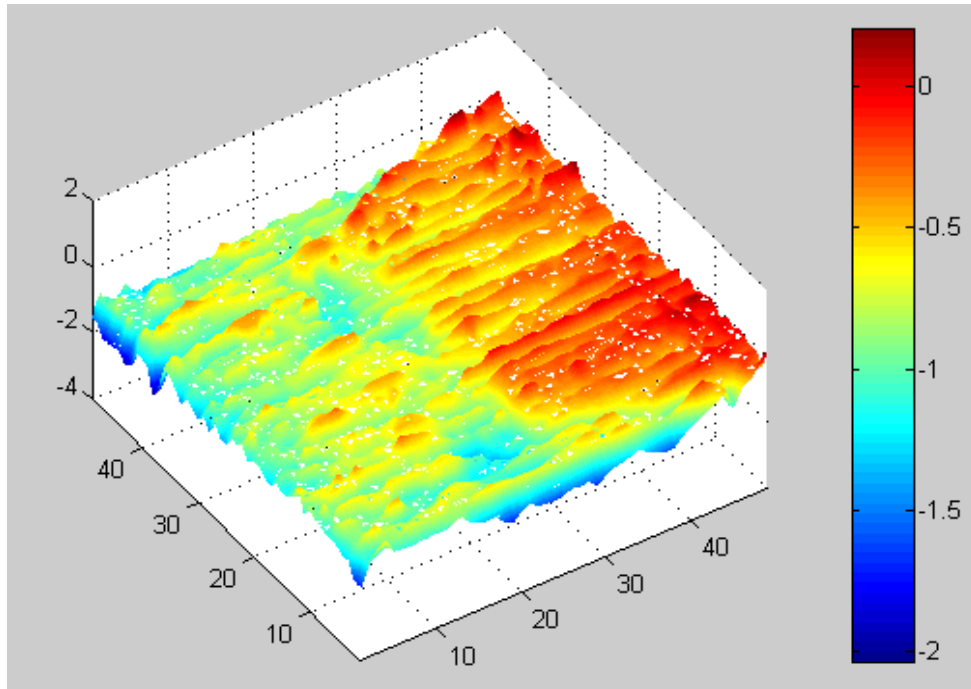


Figure 46. (3-D) Erosion contours of 11B

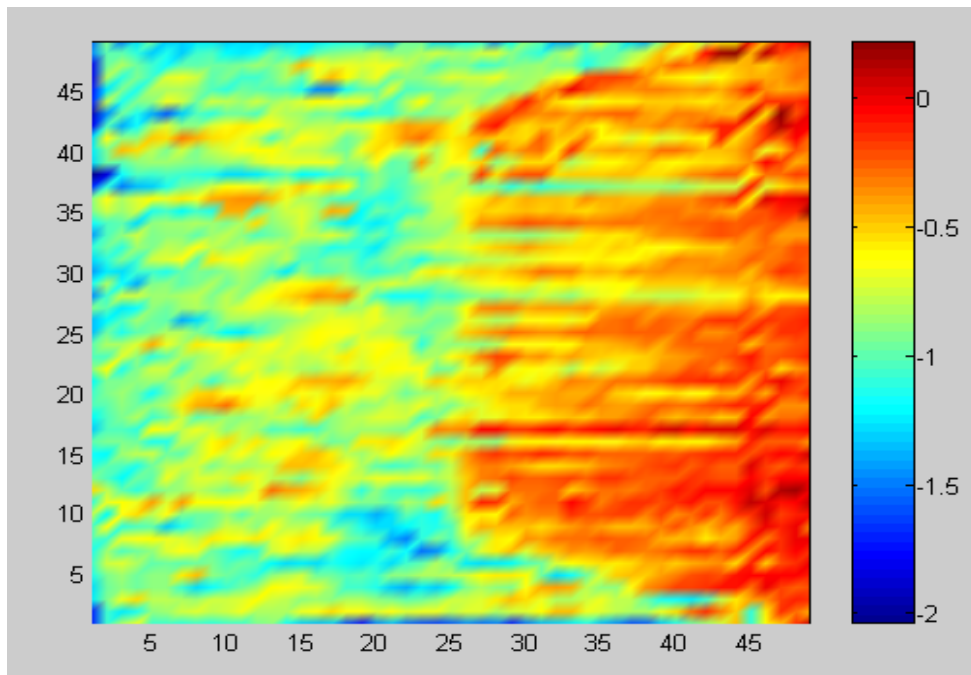


Figure 47. (2-D) Erosion contours of 11B

b. Painted Surface Data

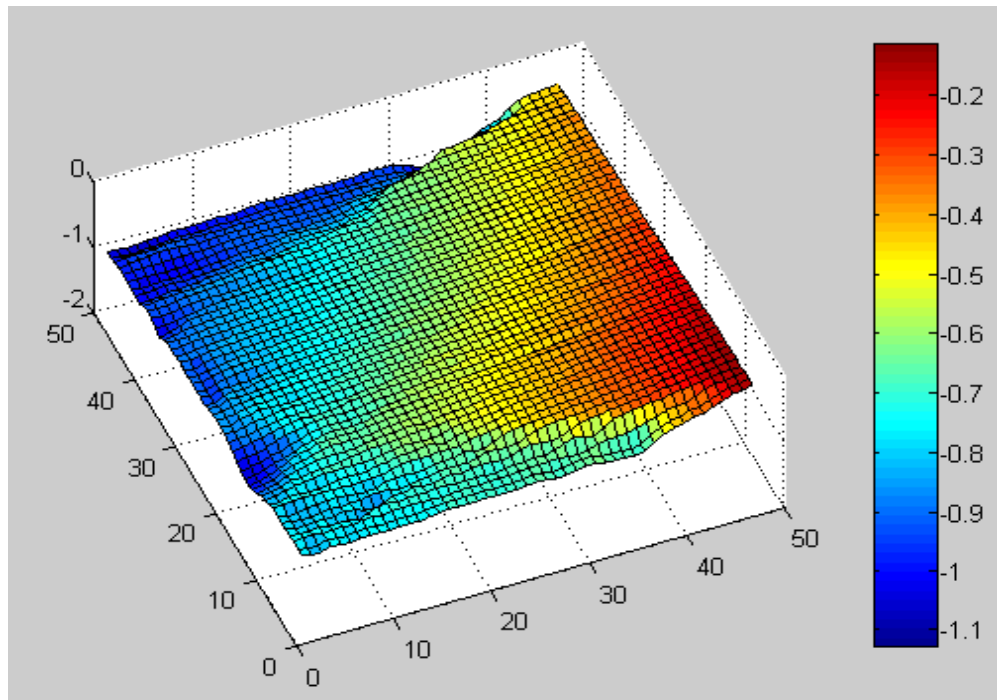


Figure 48. (3-D) Surface plot of 11B

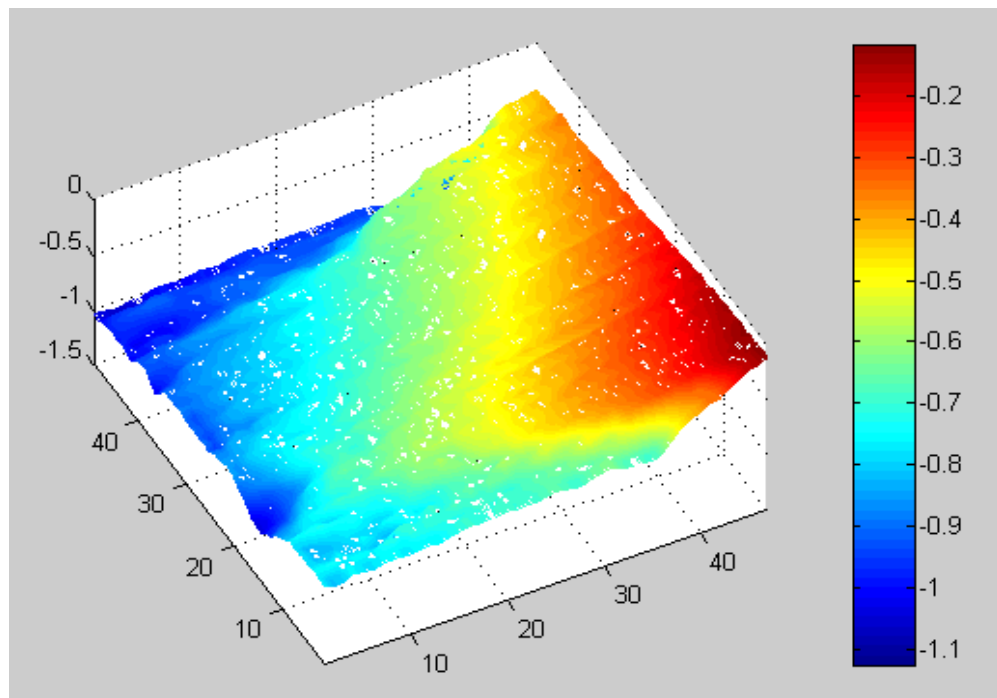


Figure 49. (3-D) Erosion contours of 11B

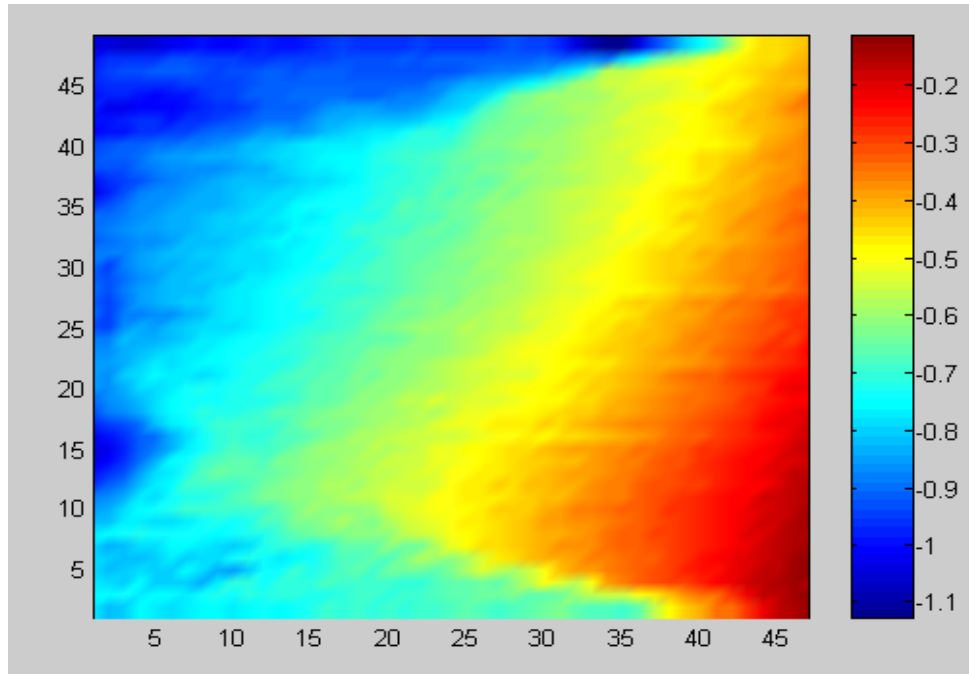


Figure 50. (2-D) Erosion contours of 11B

c. Correction

The region between the 30th column and the last column was not damaged. Lines that adequately represent the area were the part of 26th row after 30th column and column 49 as shown in Figure 51.

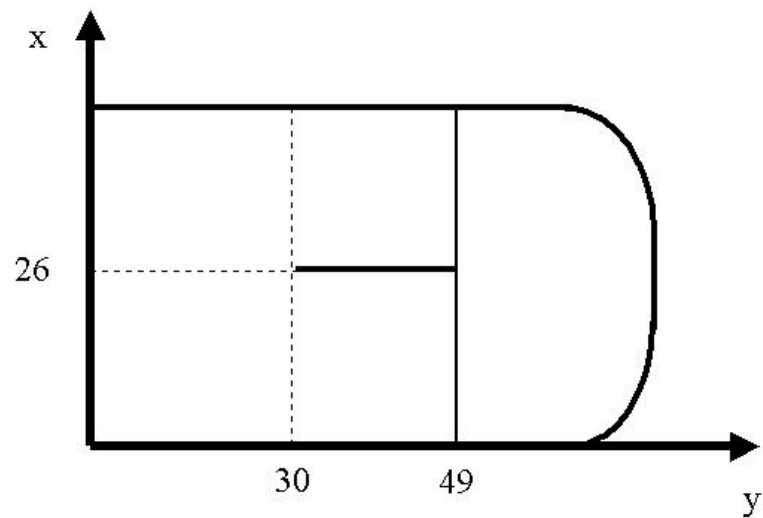


Figure 51. Lines for correction plane of 11B

For the 49th column:

$$y = -0.0067x - 0.092 \quad (4.13)$$

For 26th row:

$$y = 0.015x - 0.57 \quad (4.14)$$

The combination of the two equations above gives us the plane equation.

$$z = -0.0067x + 0.015y - 0.092 \quad (4.15)$$

If the reference system is translated to that shown in Fig. 9, the plane equations becomes as follows:

$$z = -0.0067x + 0.015(y - 49) - 0.092 \quad (4.16)$$

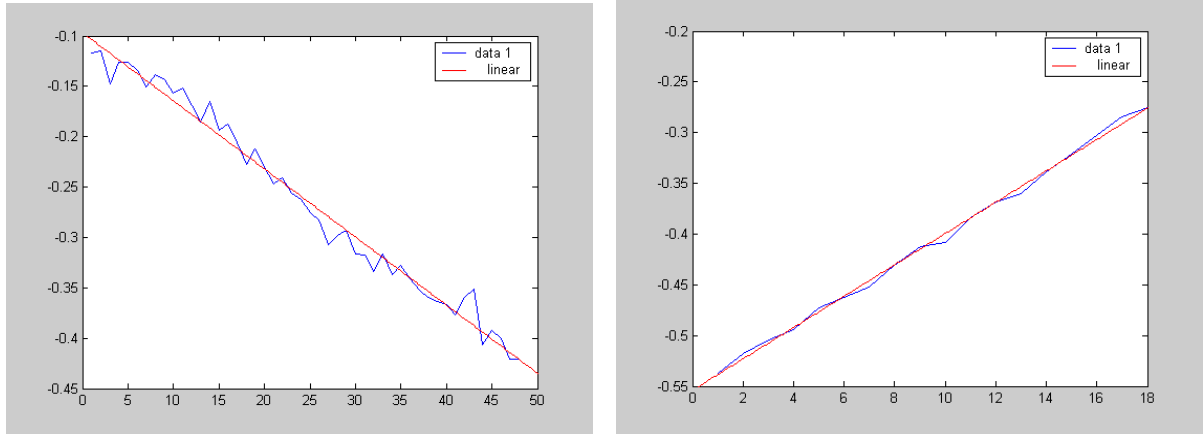


Figure 52. Linear fittings of the line equations

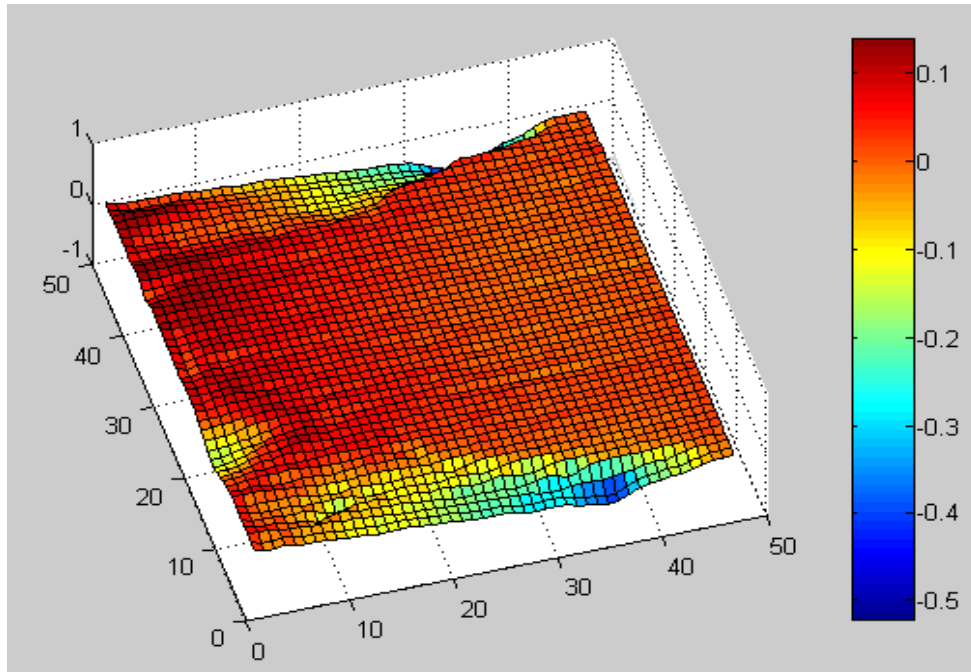


Figure 53. Corrected 3-D surface plot of 11B

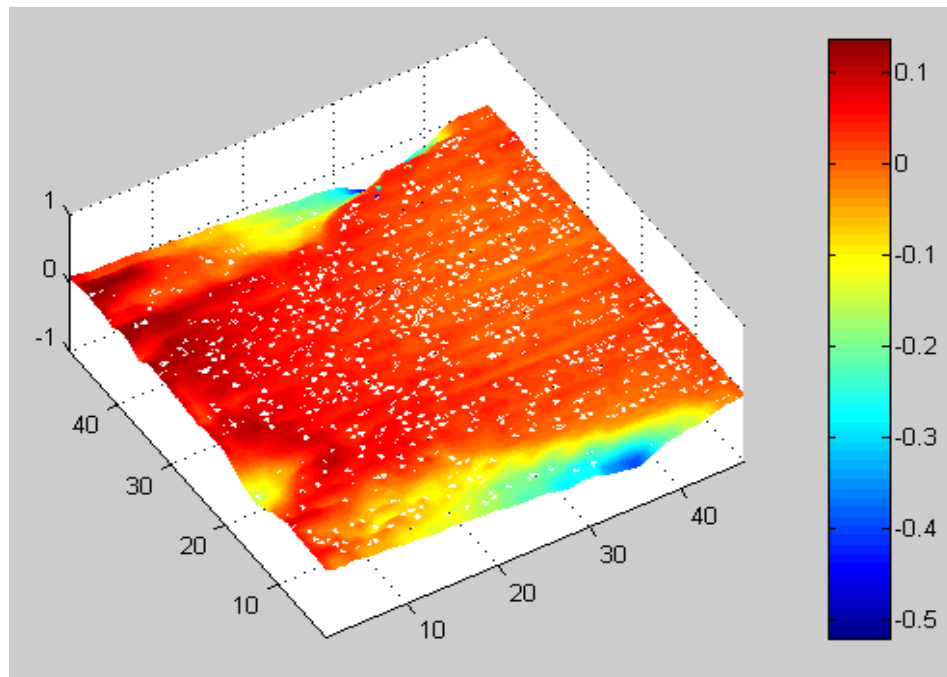


Figure 54. Corrected (3-D) erosion contours of 11B

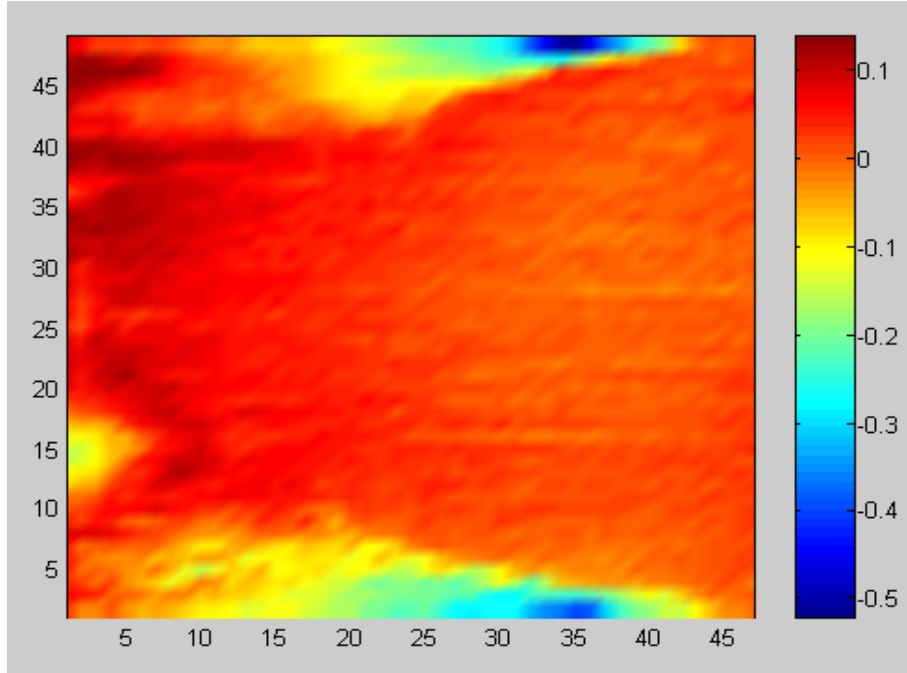


Figure 55. Corrected (2-D) erosion contours of 11B

d. Calculation of Eroded Mass

The total eroded metal volume was found to be 167.34 mm^3 .

$$\rho = 2.7 \frac{\text{g}}{\text{cm}^3}$$

$$m = 0.0027 \frac{\text{g}}{\text{mm}^3} \times 167.34 \text{ mm}^3 = 0.452 \text{ g}$$

5. Armature 18 (Surface A)

a. Unpainted Surface Data

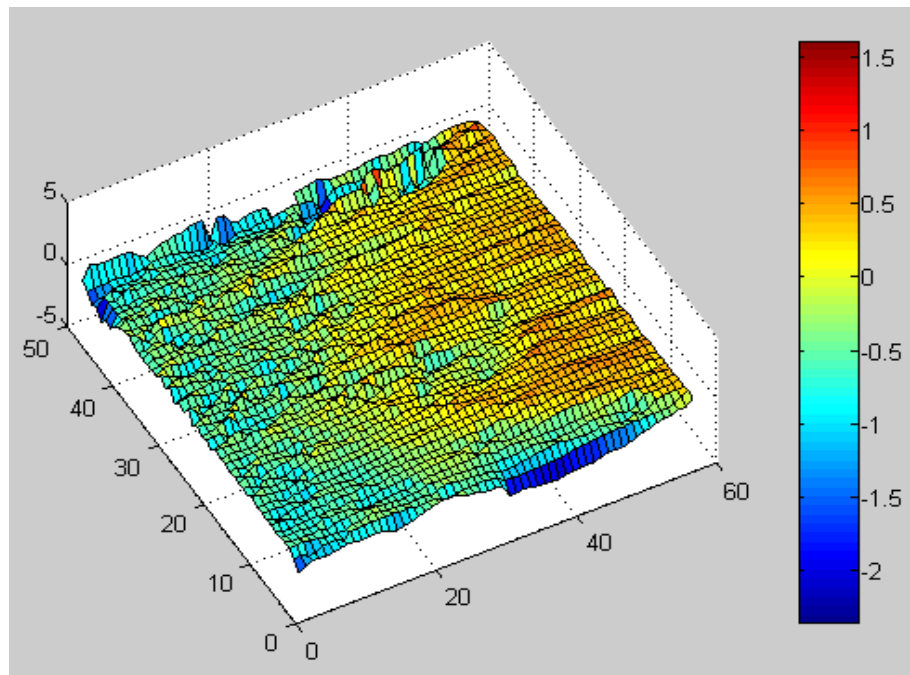


Figure 56. (3-D) Surface plot of 18A

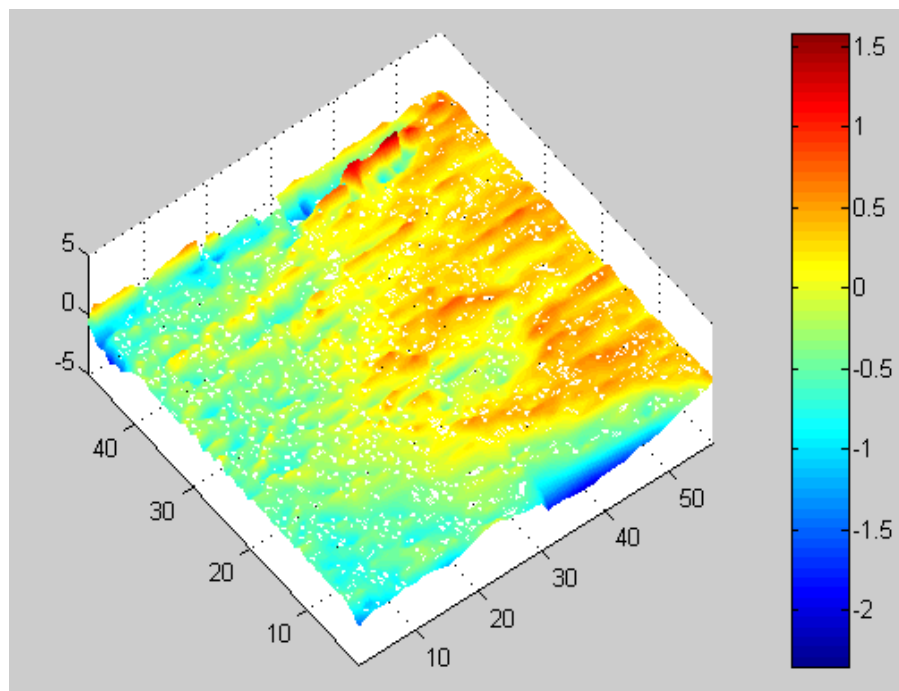


Figure 57. (3-D) Erosion contours of 18A

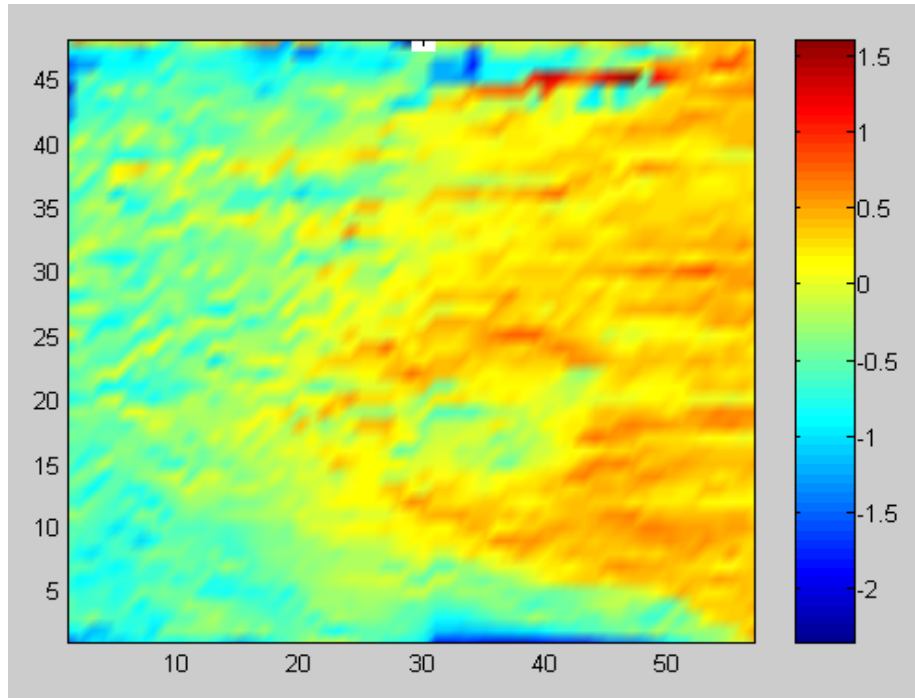


Figure 58. (2-D) Erosion contours of 18A

b. Painted Surface Data

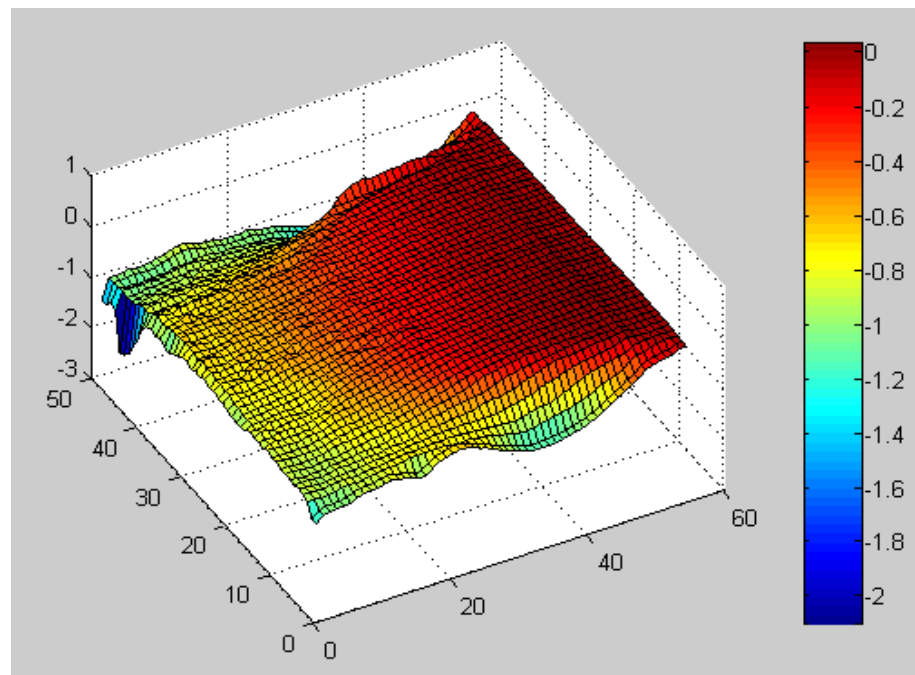


Figure 59. (3-D) Surface plot of 18A

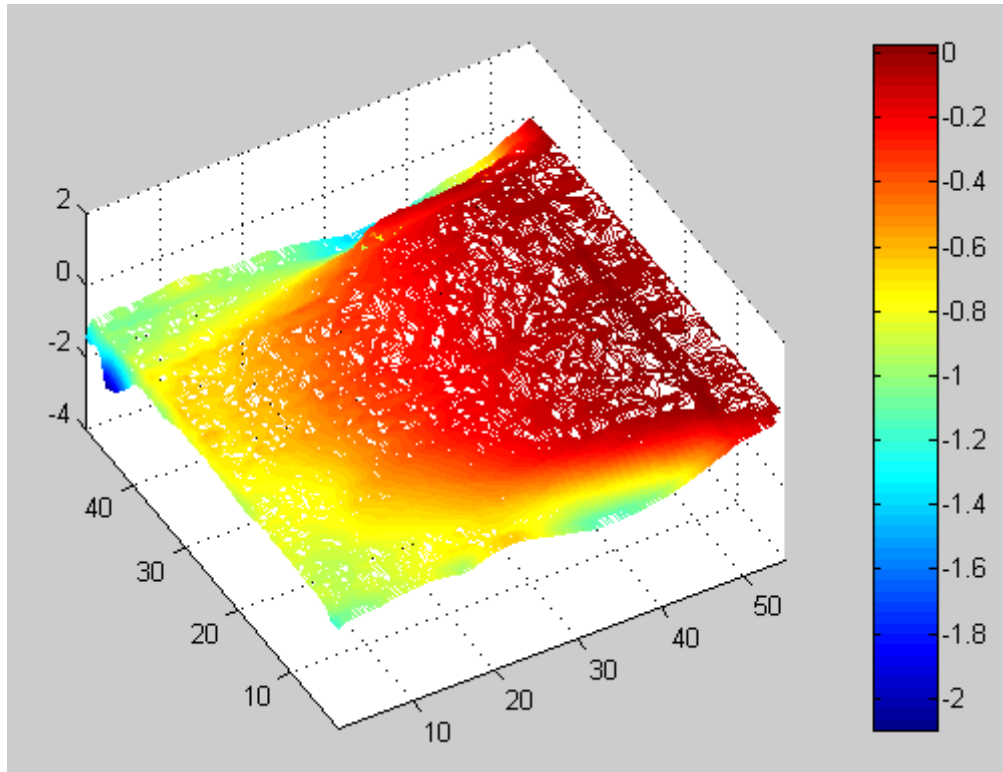


Figure 60. (3-D) Erosion contours of 18A

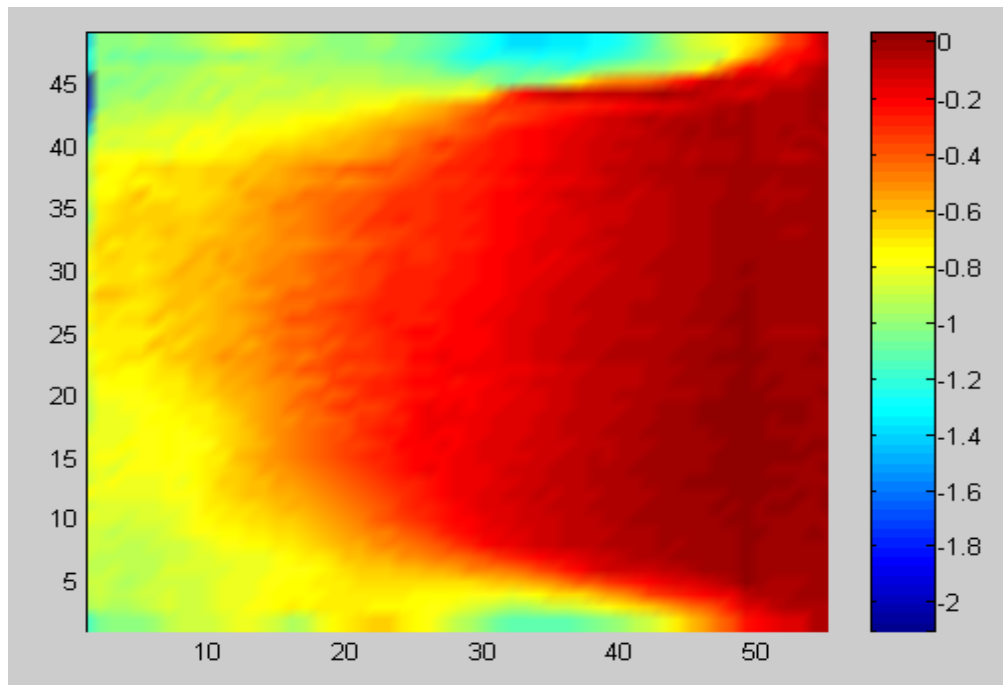


Figure 61. (2-D) Erosion contours of 18A

c. Correction

The region between the 35th column and the last column was not damaged. Lines that adequately represent the area were the part of 26th row after 35th column and column 55 as shown in Figure 6.

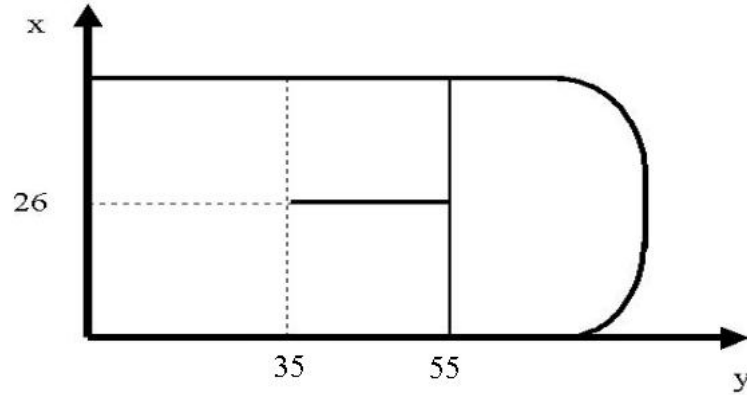


Figure 62. Lines for correction plane of 18A

For 55th column:

$$y = -0.00039x - 0.013 \quad (4-17)$$

For 26th row:

$$y = 0.0061x - 0.11 \quad (4-18)$$

The combination of the two equations above gives us the plane equation.

$$y = -0.00039x + 0.0061y - 0.013 \quad (4-19)$$

If the reference system is translated to that shown in Fig. 9, the plane equations becomes as follows:

$$z = -0.00039x + 0.0061(y - 55) - 0.018 \quad (4-20)$$

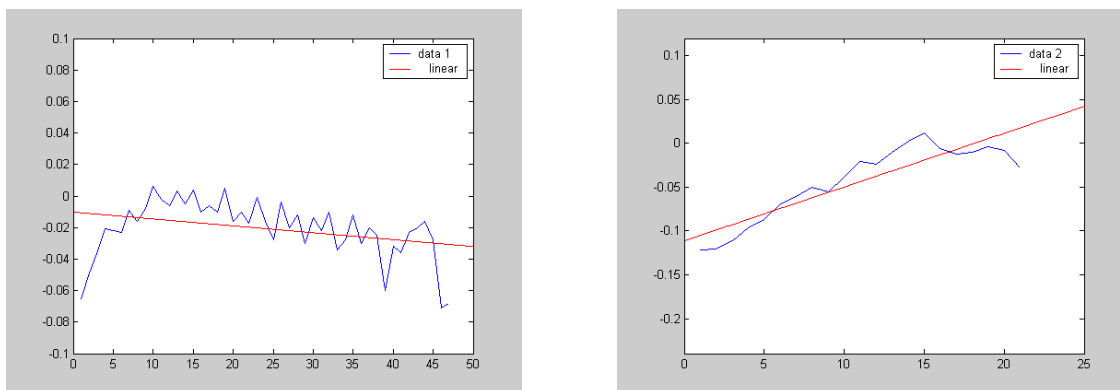


Figure 63. Linear fittings of the line equations for 18A

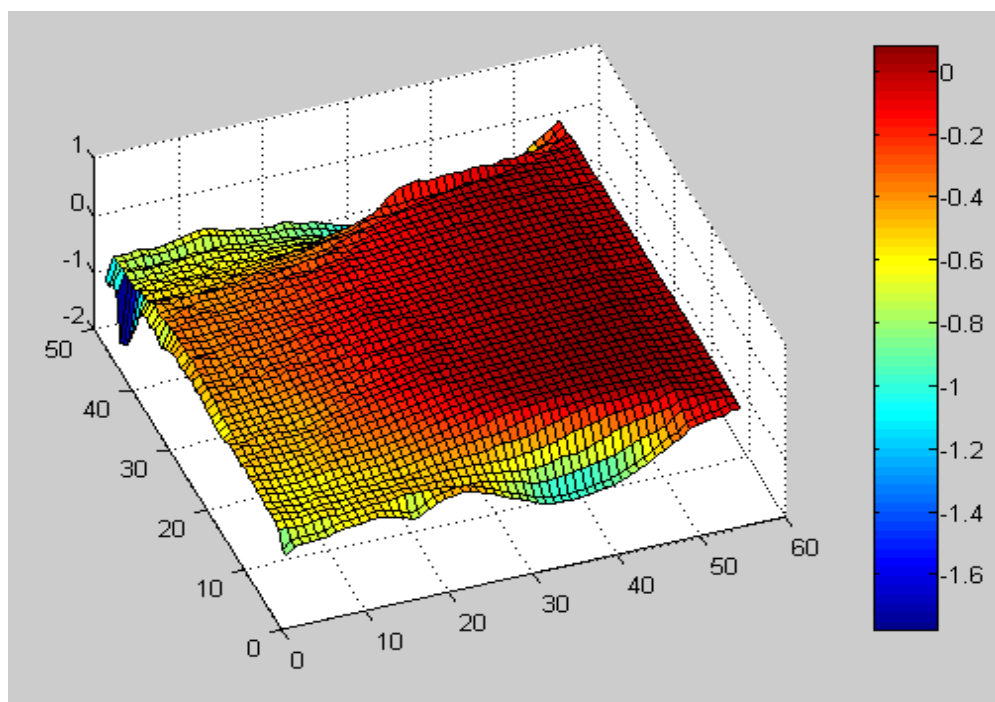


Figure 64. Corrected (3-D) surface plot of 18A

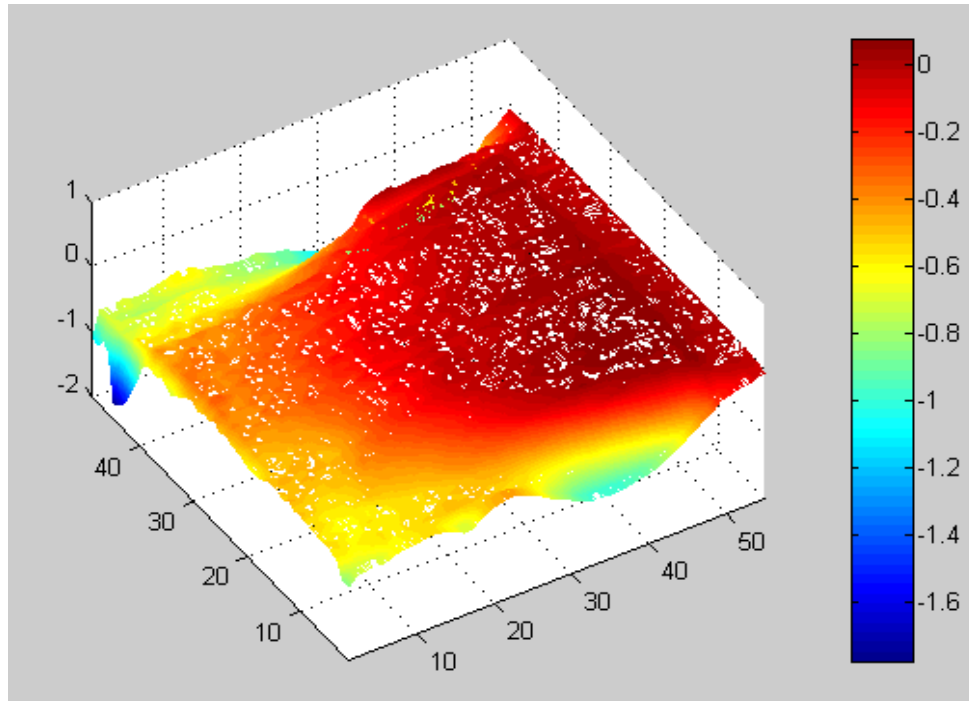


Figure 65. Corrected (3-D) erosion contours of 18A

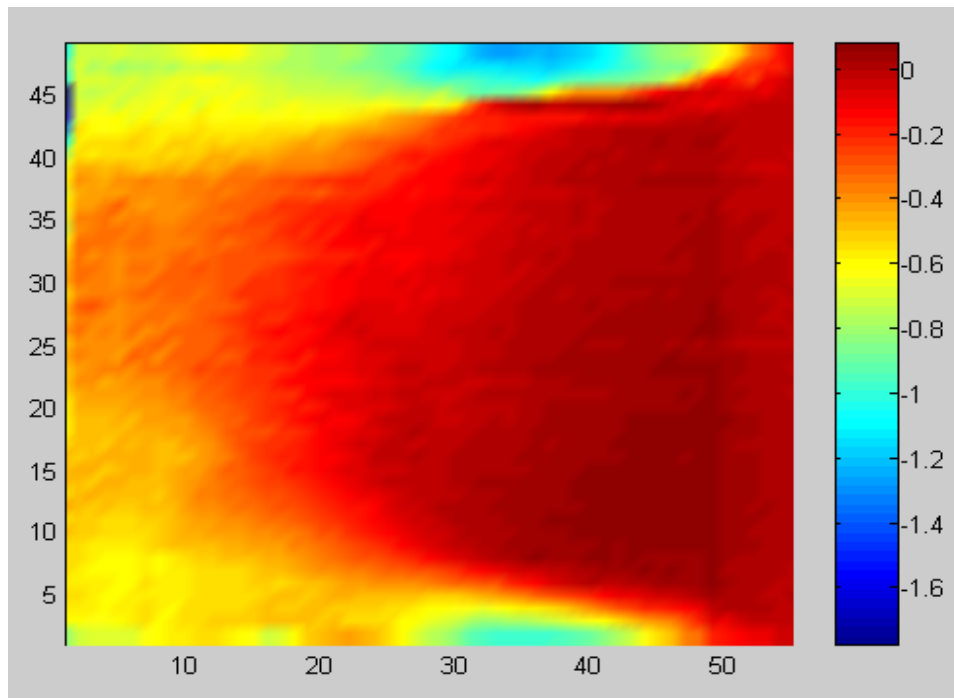


Figure 66. Corrected (2-D) erosion contours of 18A

d. Calculation of Eroded Mass

The total eroded metal volume was found to be 720.617 mm^3 .

$$\rho = 2.7 \frac{\text{g}}{\text{cm}^3}$$

$$m = 0.0027 \frac{\text{g}}{\text{mm}^3} \times 720.617 \text{ mm}^3 = 1.945 \text{ g}.$$

6. Armature 18 (Surface B)

a. Unpainted Surface Data

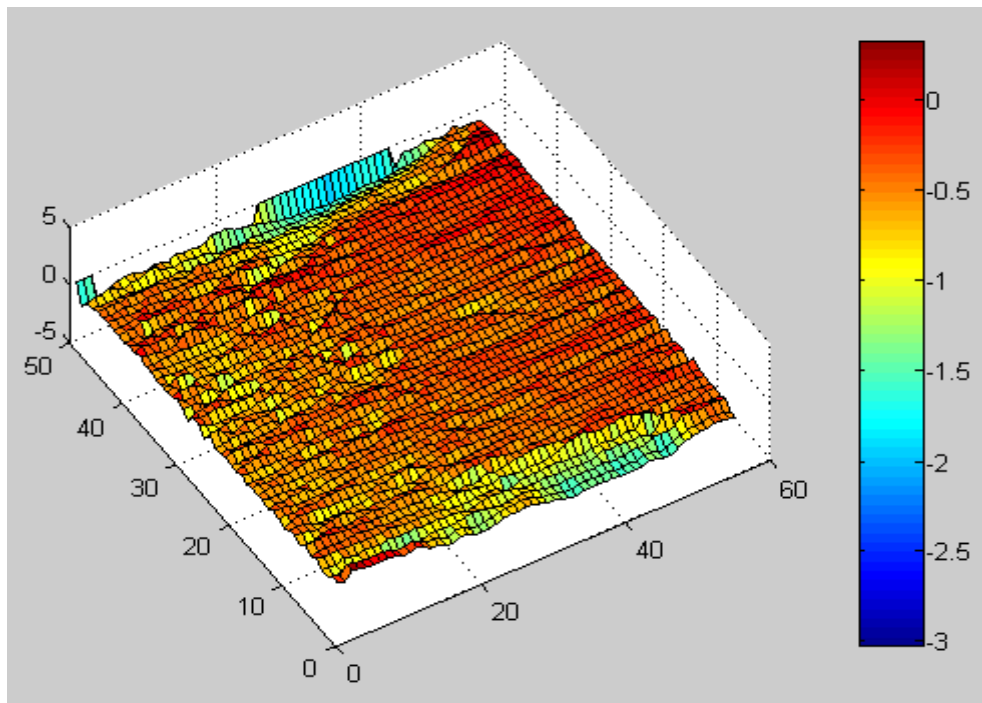


Figure 67. (3-D) Surface plot of 18B

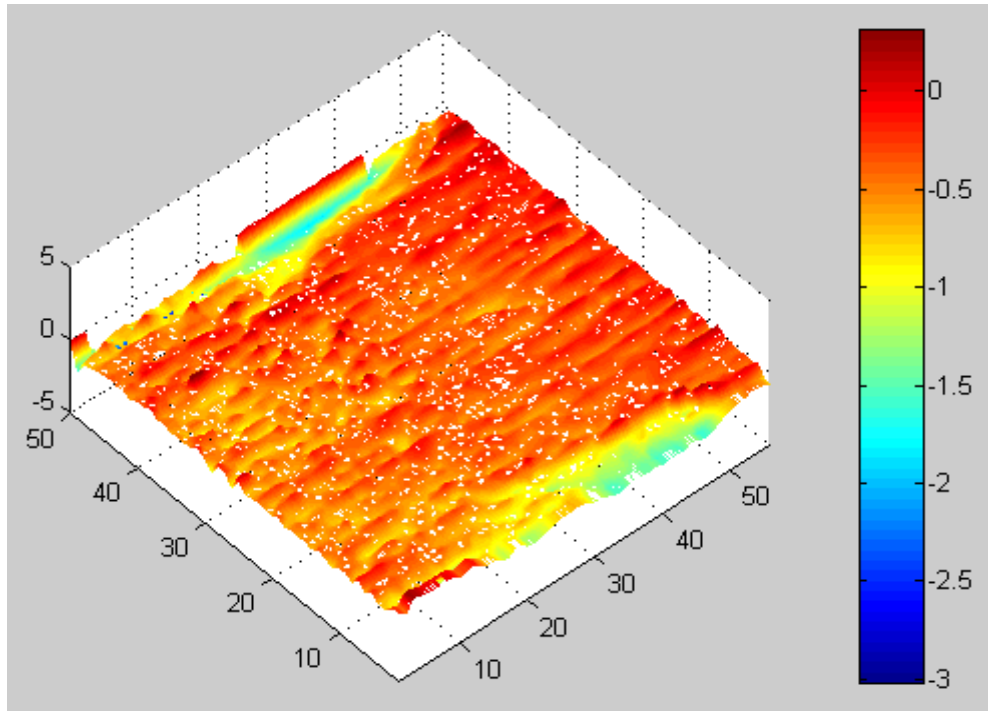


Figure 68. (3-D) Erosion contours of 18B

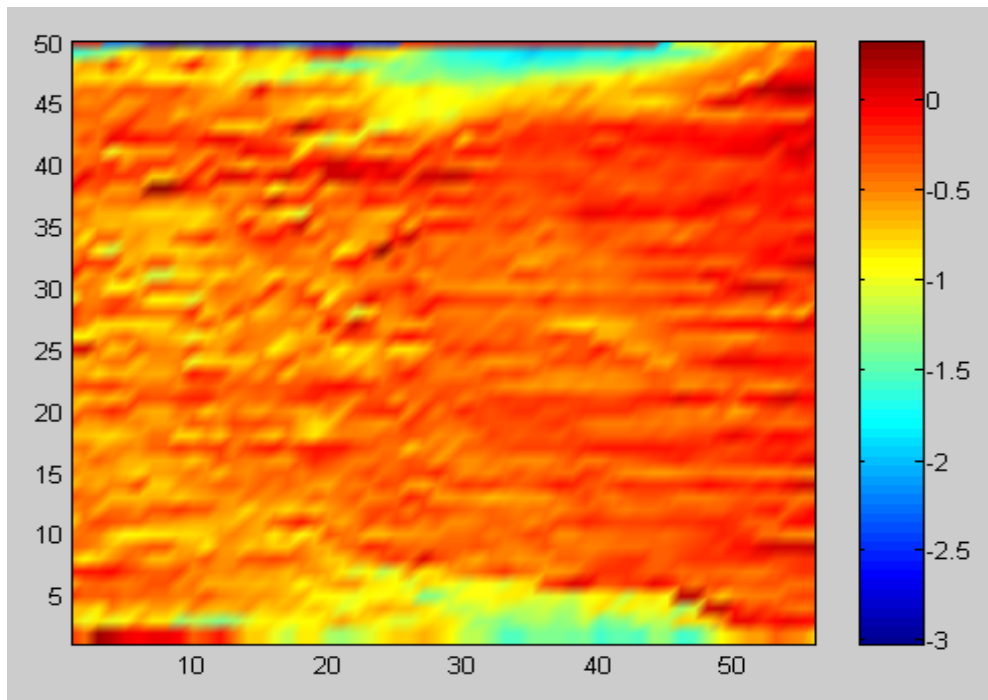


Figure 69. (2-D) Erosion contours of 18B

b. Painted Surface Data

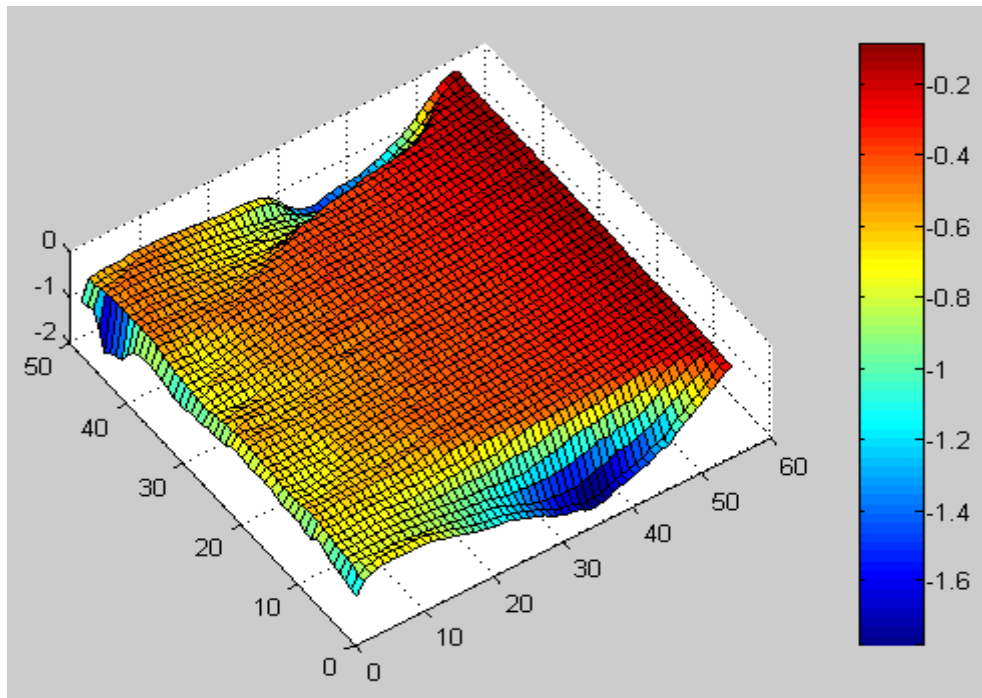


Figure 70. (3-D) Surface plot of 18B

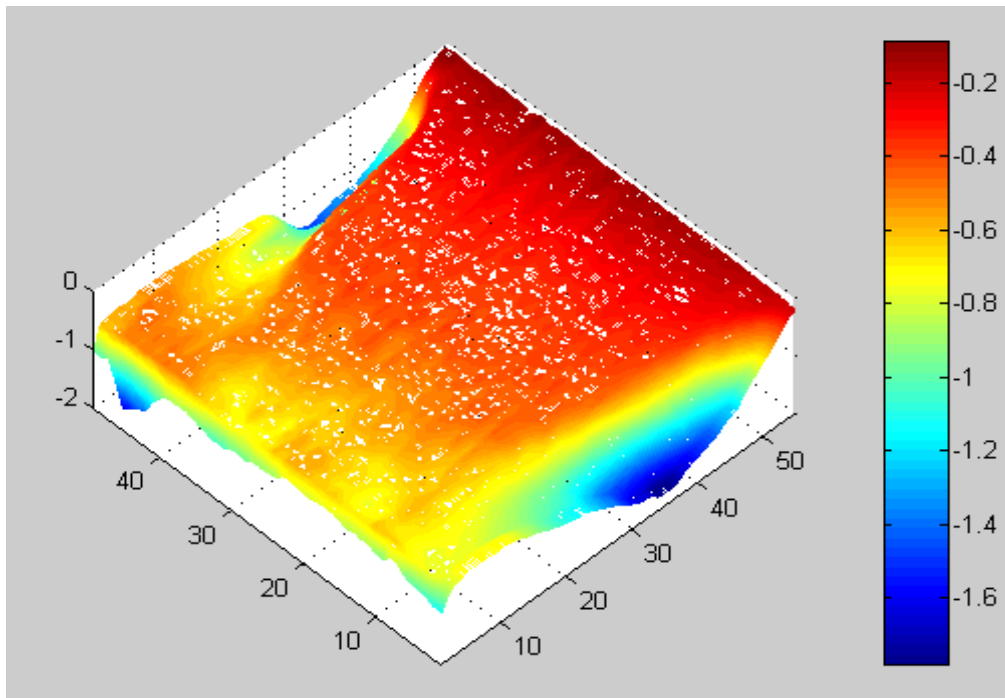


Figure 71. (3-D) Erosion contours of 18B

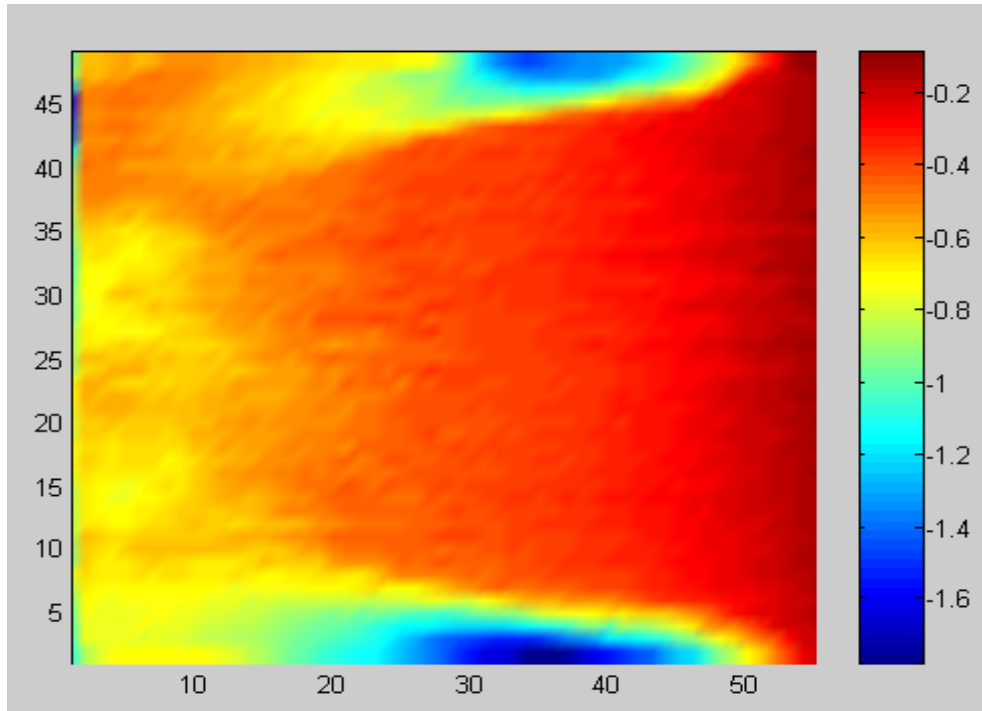


Figure 72. (2-D) Erosion contours of 18B

c. Correction

The region between the 20th column and the last column was not damaged. Lines that adequately represent the area were the part of 26th row after 20th column and column 55 as shown in Figure 73.

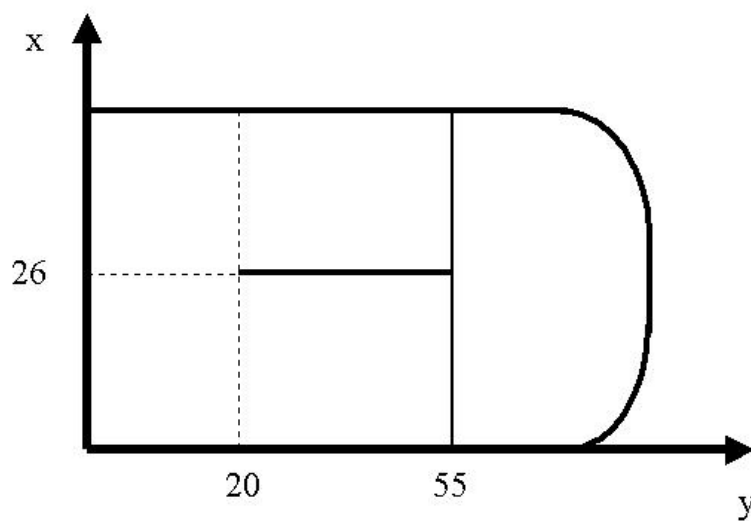


Figure 73. Lines for correction plane of 18B

For 55th column:

$$y = -0.001352x - 0.1765 \quad (4-21)$$

For 26th row:

$$y = 0.01066x - 0.5355 \quad (4-22)$$

The combination of the two equations above gives us the plane equation.

$$z = 0.001352x + 0.01066y - 0.1765 \quad (4-23)$$

If the reference system is translated to that shown in Fig. 9, the plane equations becomes as follows:

$$z = 0.001352x + 0.01066(y - 55) - 0.1765 \quad (4-24)$$

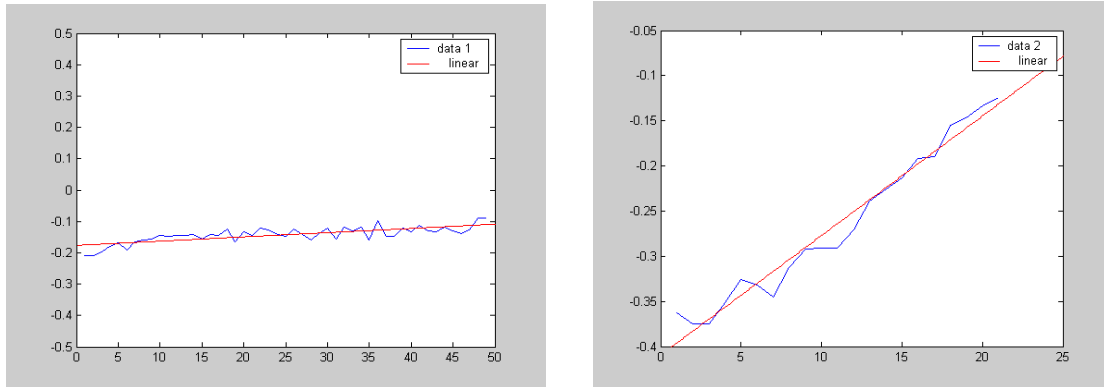


Figure 74. Linear fittings of the line equations for 18B

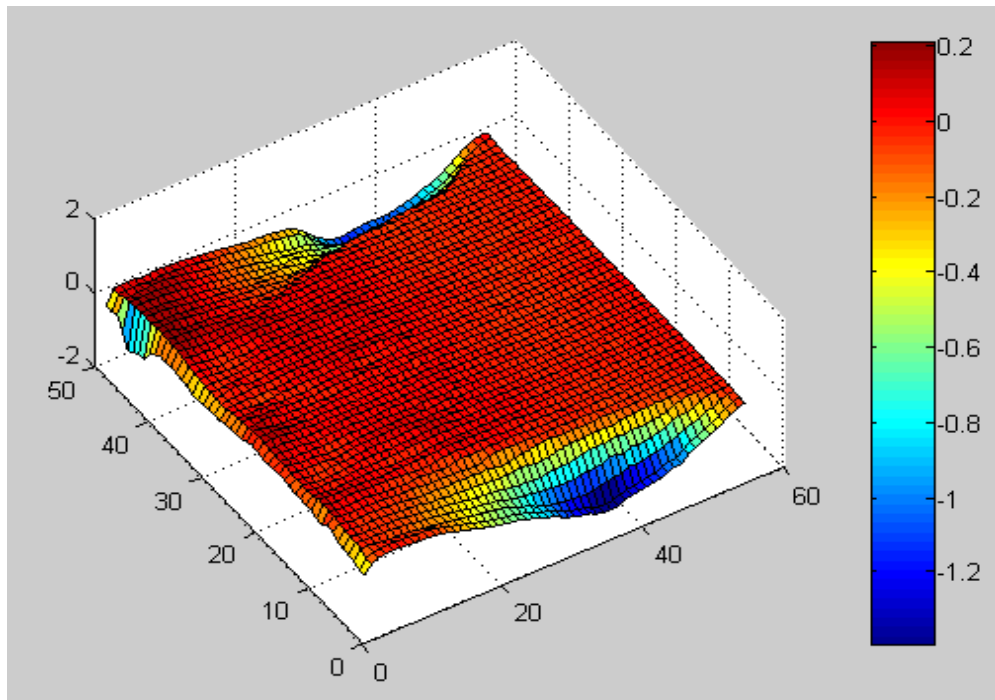


Figure 75. Corrected (3-D) surface plot of 18B

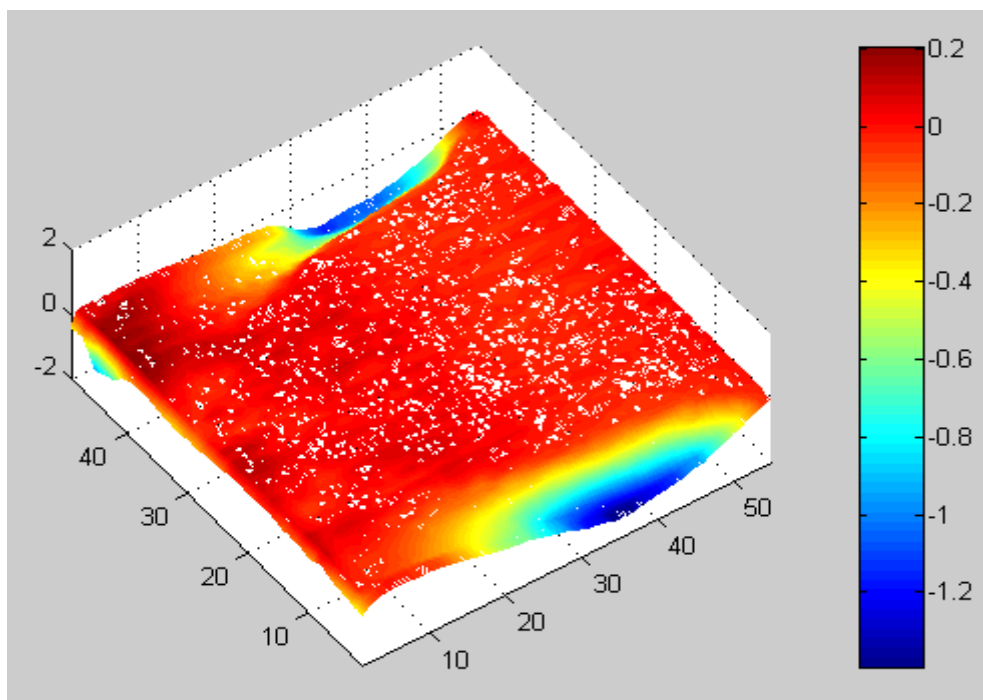


Figure 76. Corrected (3-D) erosion contours of 18B

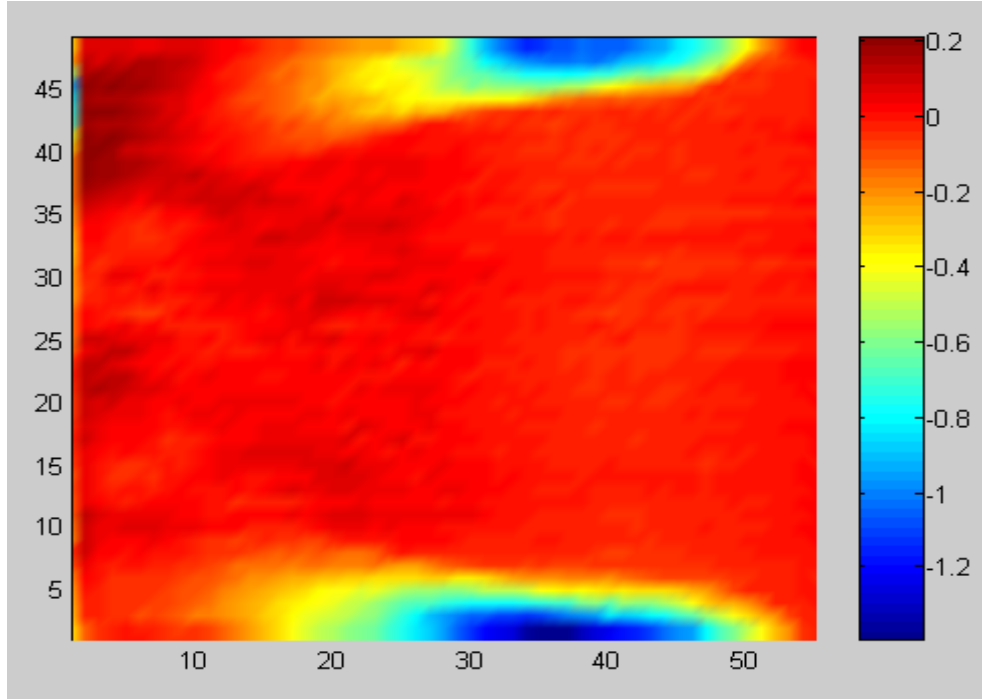


Figure 77. Corrected (2-D) erosion contours of 18b

d. Calculation of Eroded Mass

The total eroded metal volume was found to be 261.6066 mm^3

$$\rho = 2.7 \frac{\text{g}}{\text{cm}^3}$$

$$m = 0.0027 \frac{\text{g}}{\text{mm}^3} \times 261.6066 \text{ mm}^3 = 0.7063 \text{ g}.$$

7. Armature 19 (Surface A)

a. Unpainted Surface Data

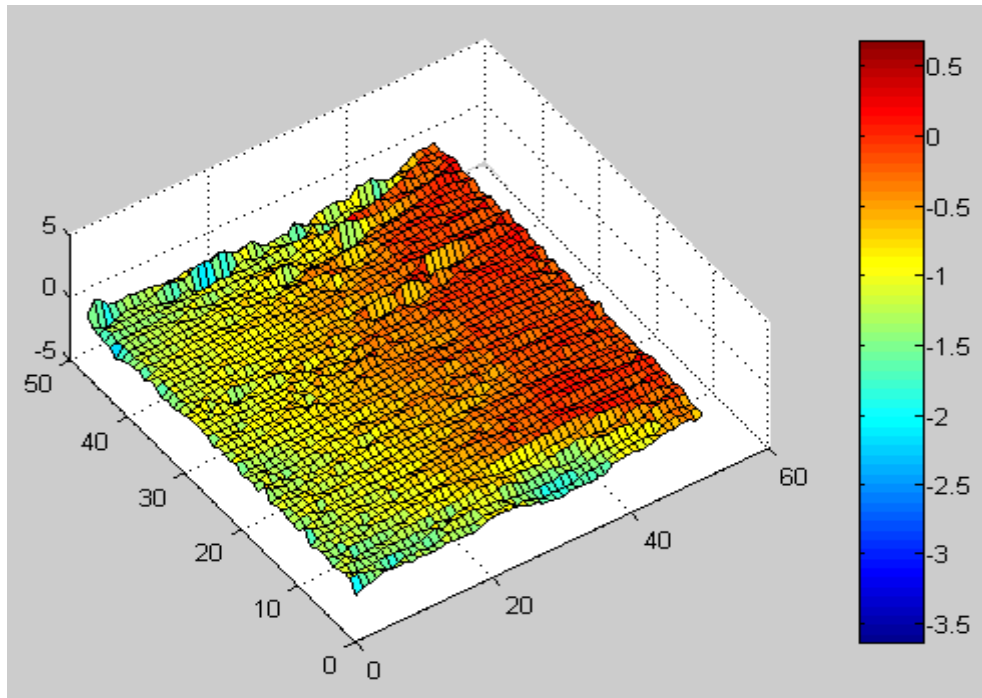


Figure 78. (3-D) Surface plot of 19A

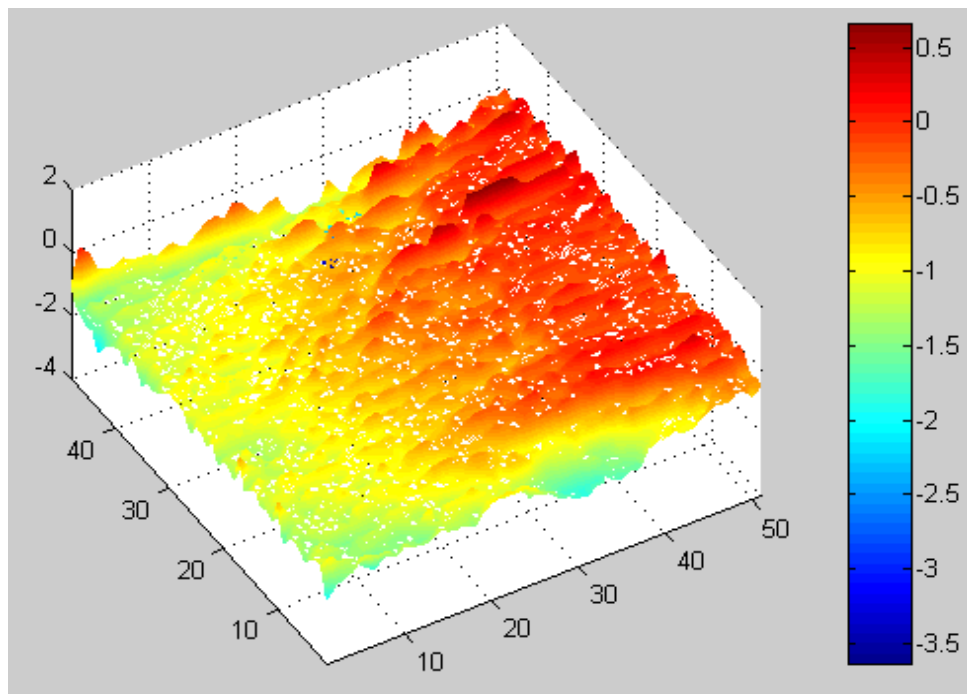


Figure 79. (3-D) Erosion contours of 19A

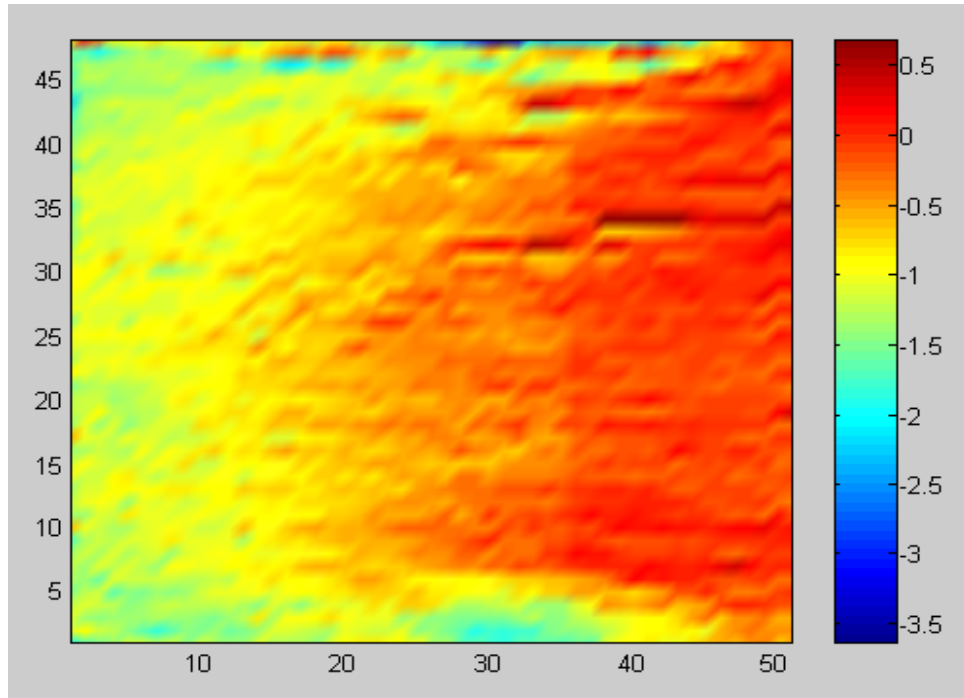


Figure 80. (2-D) Erosion contours of 19A

b. Painted Surface Data

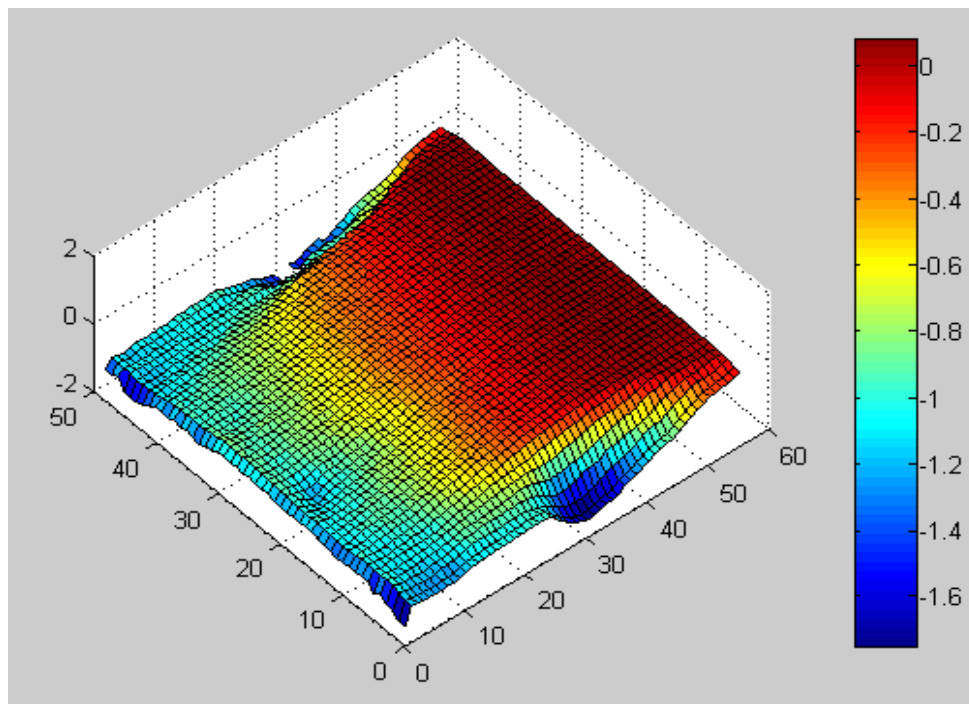


Figure 81. (3-D) Surface plot of 19A

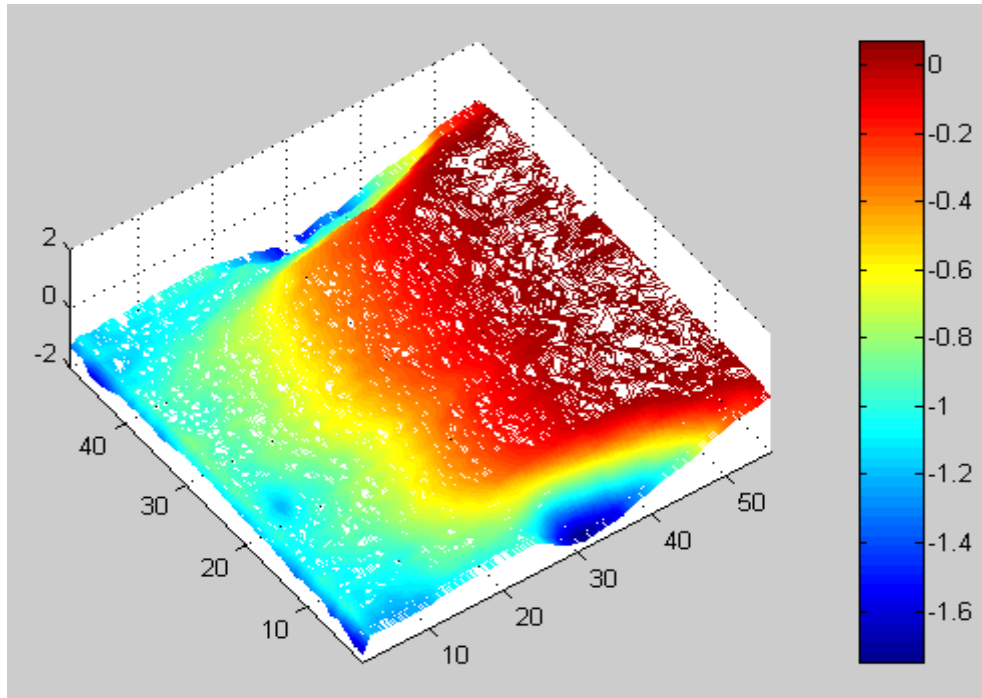


Figure 82. (3-D) Erosion contours of 19A

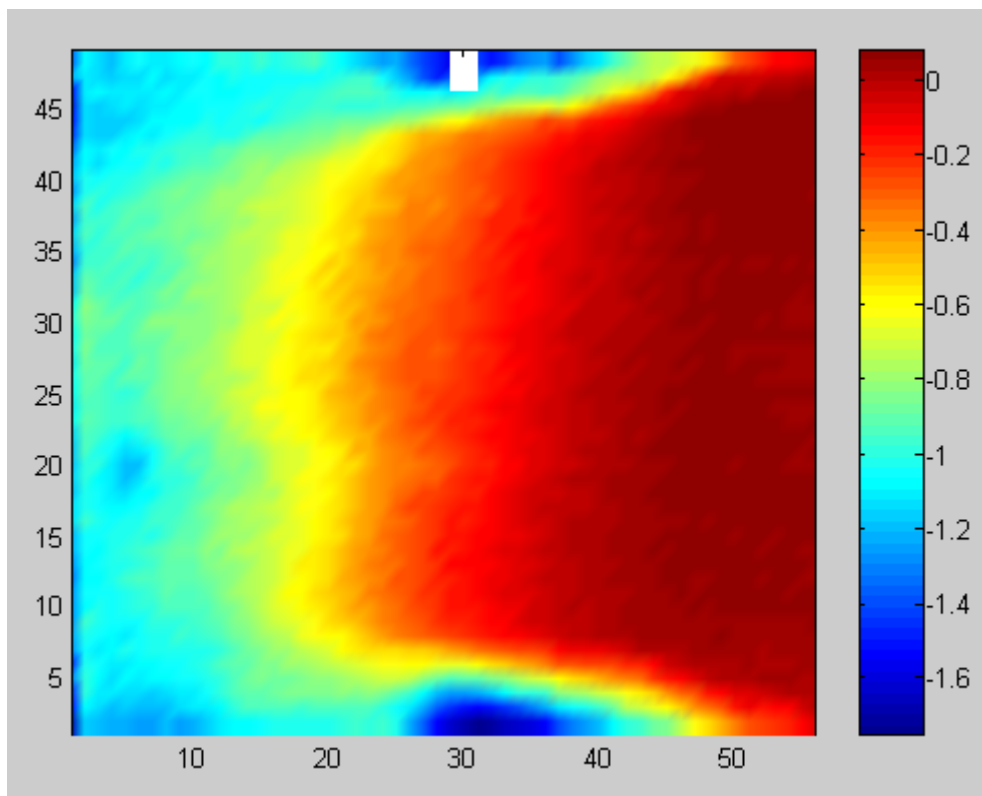


Figure 83. (2-D) Erosion contours of 19A

c. Correction

The region between the 26th column and the last column was not damaged. Lines that adequately represent the area were the part of 26th row after 26th column and column 56 as shown in Figure 84.

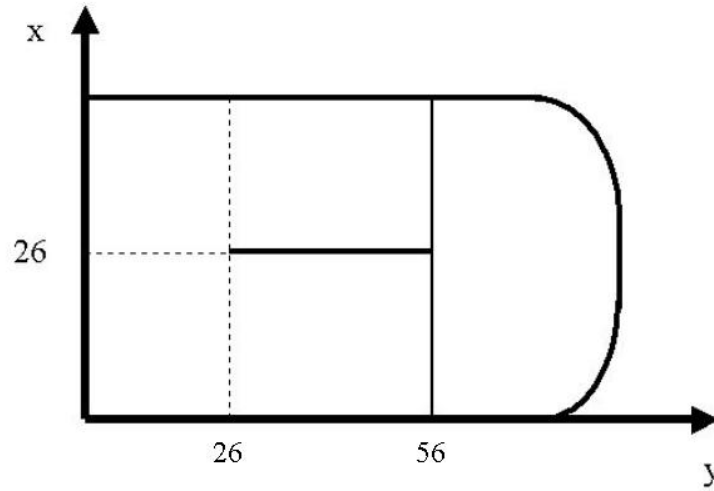


Figure 84. Lines for correction plane of 19A

For 56th column:

$$y = -0.00051x + 0.022 \quad (4-25)$$

For 26th row:

$$y = 0.012x - 0.2403 \quad (4-26)$$

The combination of the two equations above gives us the plane equation.

$$z = 0.00051x + 0.012y + 0.022 \quad (4-27)$$

If the reference system is translated to that shown in Fig. 9, the plane equations becomes as follows:

$$z = 0.00051x + 0.012(y - 56) + 0.022 \quad (4-28)$$

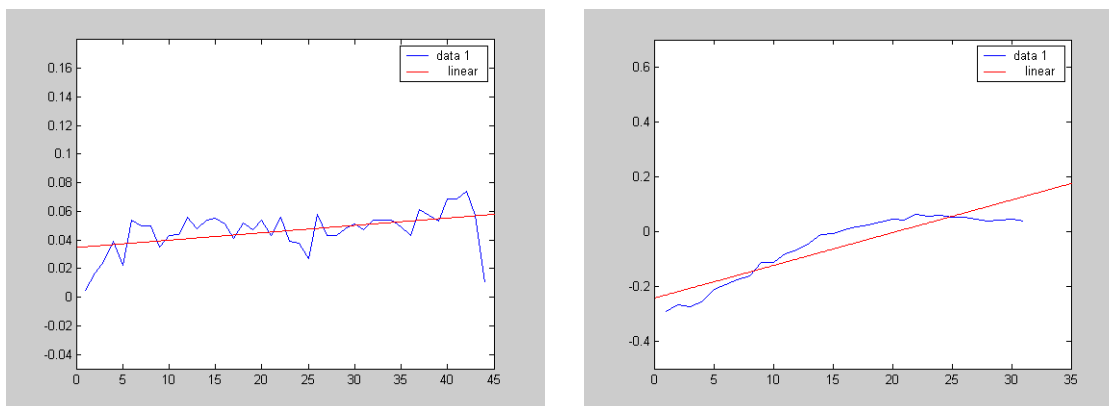


Figure 85. Linear fittings of the line equations for 19A

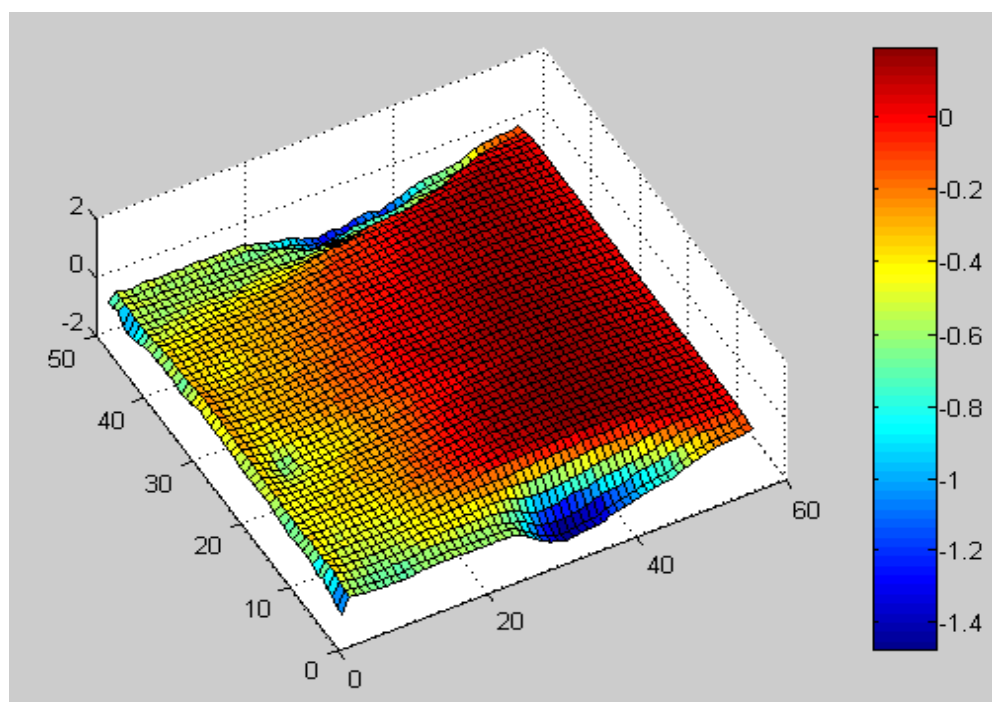


Figure 86. Corrected (3-D) surface plot of 19A

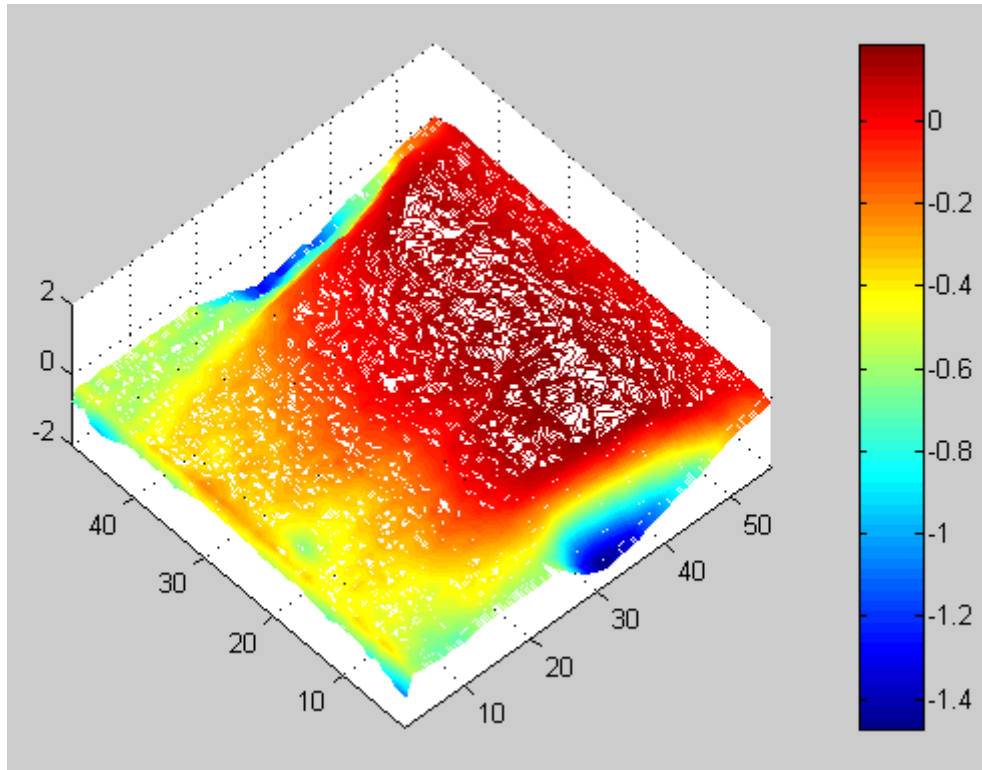


Figure 87. Corrected (3-D) erosion contours of 19A

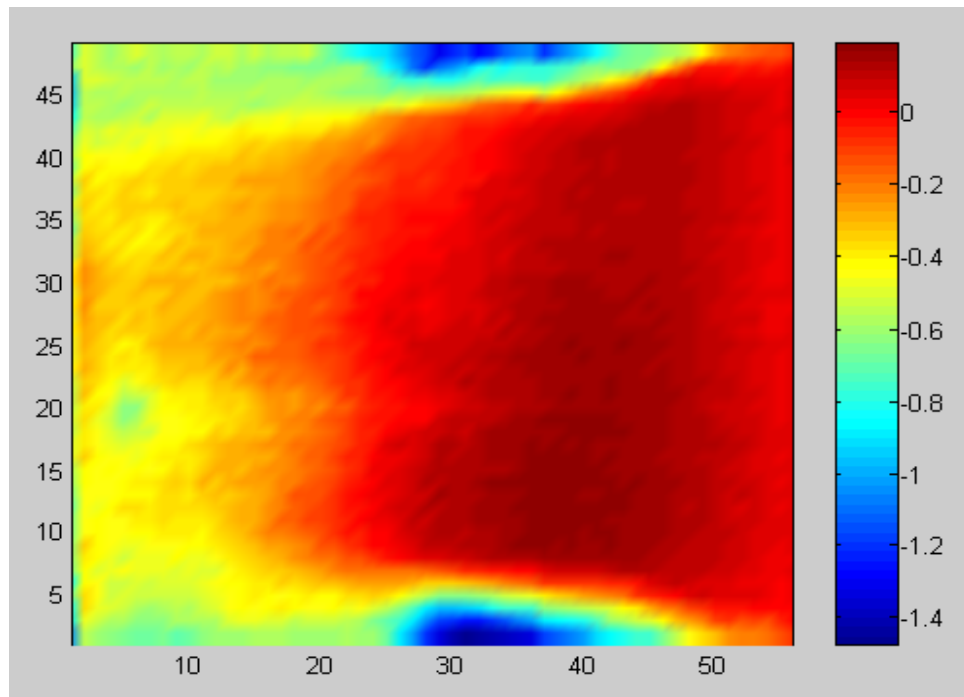


Figure 88. Corrected (2-D) erosion contours of 19A

d. Calculation of Eroded Mass

The total eroded metal volume was found to be 527.1413 mm^3

$$\rho = 2.7 \frac{\text{g}}{\text{cm}^3}$$

$$m = 0.0027 \frac{\text{g}}{\text{mm}^3} \times 527.1453 \text{ mm}^3 = 1.423 \text{ g}$$

8. Armature 19 (Surface B)

a. Unpainted Data

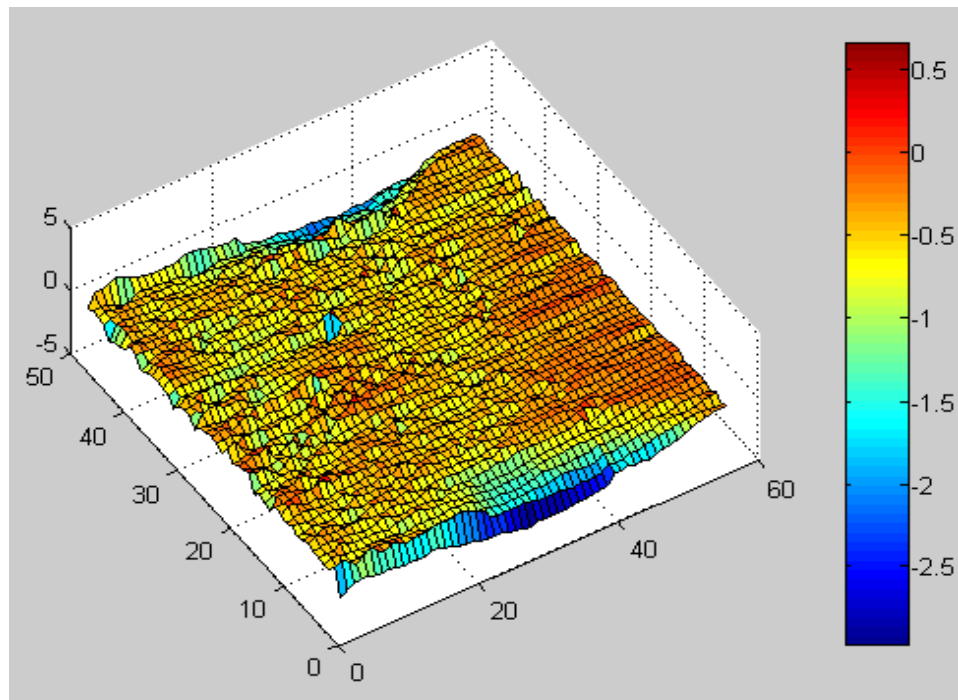


Figure 89. (3-D) Surface plot of 19B

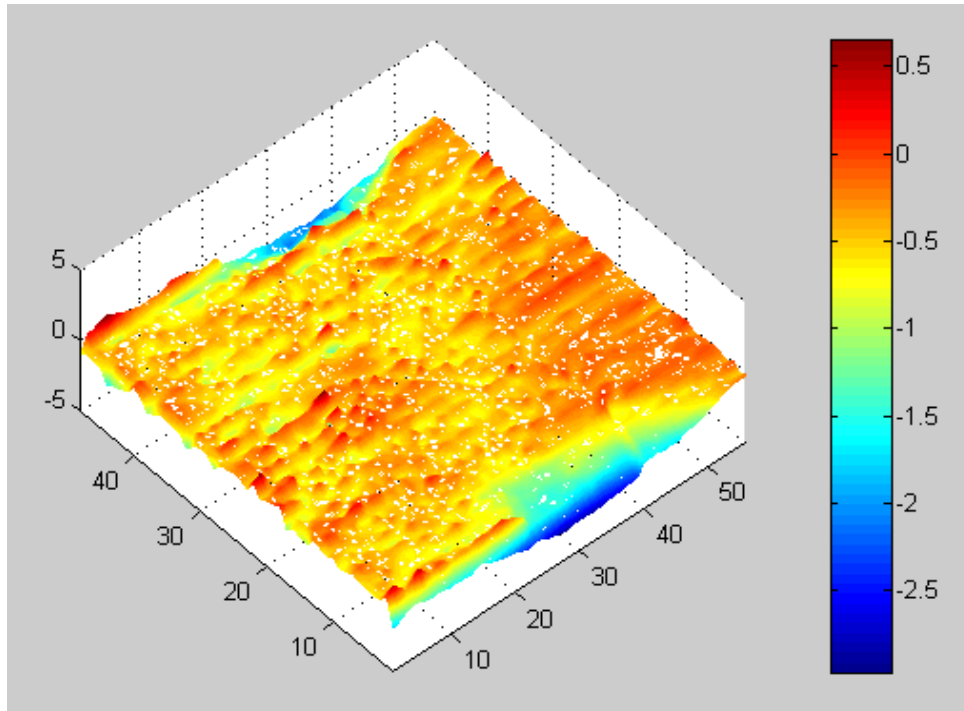


Figure 90. (3-D) Erosion contours of 19B

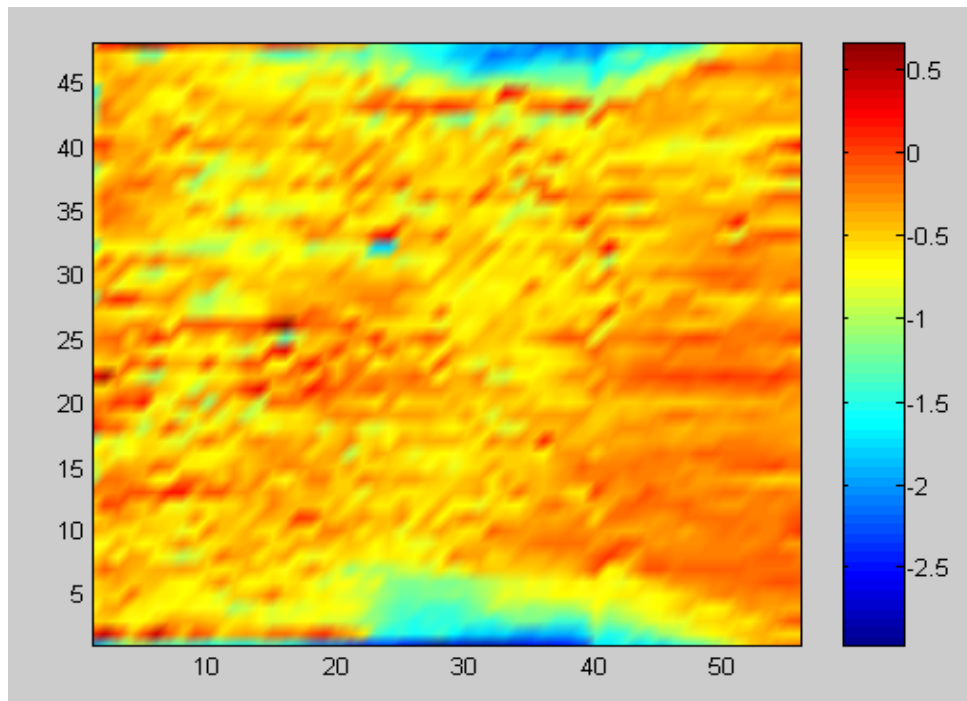


Figure 91. (2-D) Erosion contours of 19B

b. Painted Surface Data

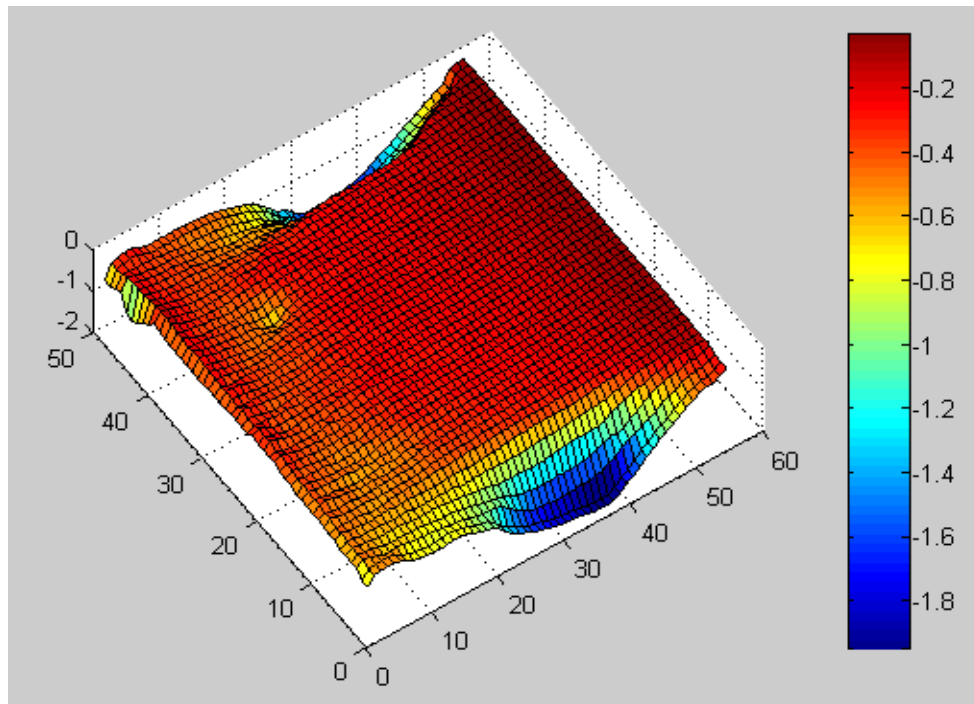


Figure 92. (3-D) Surface plot of 19B

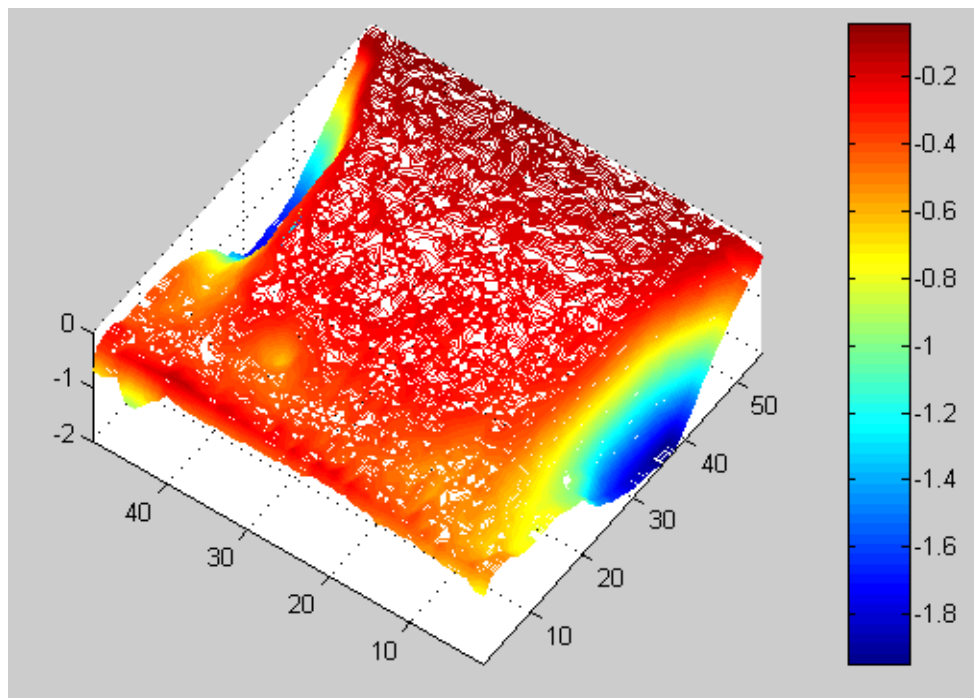


Figure 93. (3-D) Erosion contours of 19B

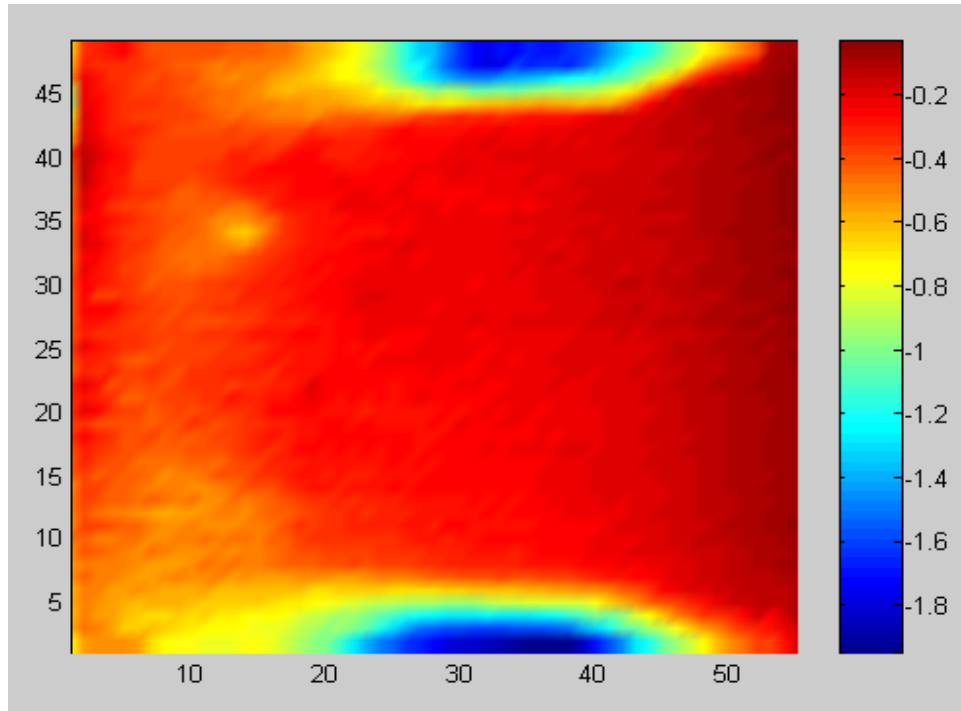


Figure 94. (2-D) Erosion contours of 19B

c. Correction

The region between the 35th column and the last column was not damaged. Lines that adequately represent the area were the part of 26th row after 35th column and column 55 as shown in Figure 95.

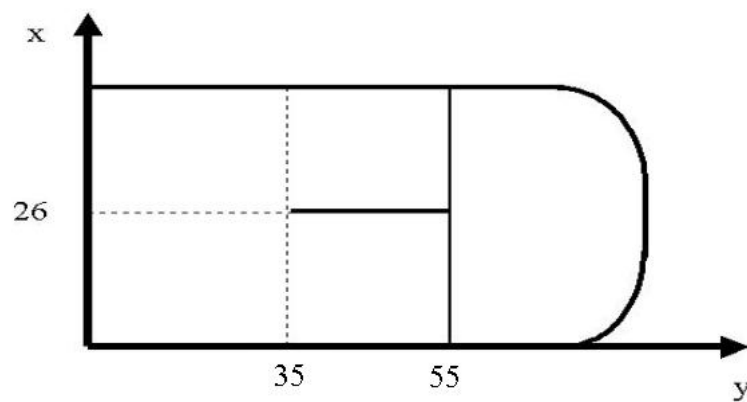


Figure 95. Lines for correction plane of 19A

For 55th column:

$$y = 0.0012x - 0.095 \quad (4-28)$$

For 26th row:

$$y = 0.0087x - 0.2504 \quad (4-29)$$

The combination of the two equations above gives us the plane equation.

$$z = 0.0012x + 0.087y + 0.095 \quad (4-30)$$

If the reference system is translated to that shown in Fig. 9, the plane equations becomes as follows:

$$z = 0.0012x + 0.087(y - 55) + 0.095 \quad (4-31)$$

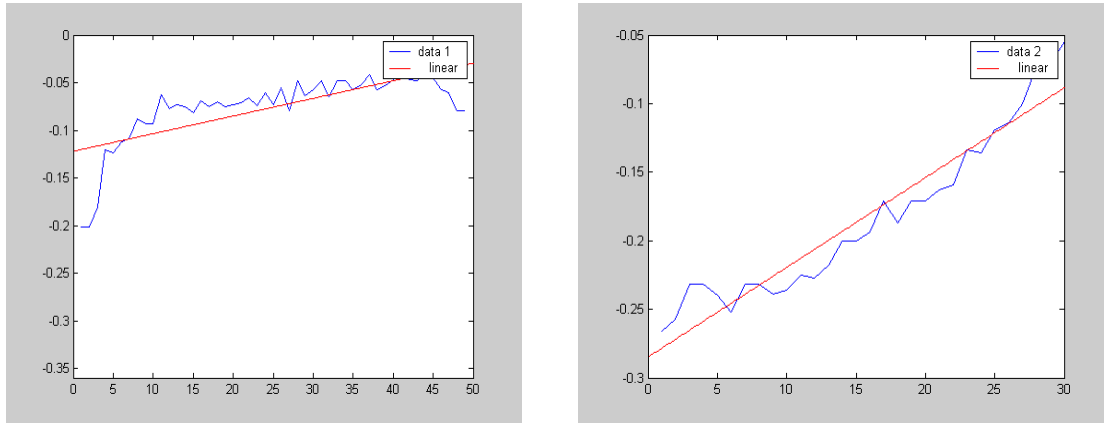


Figure 96. Linear fittings of the line equations for 19B

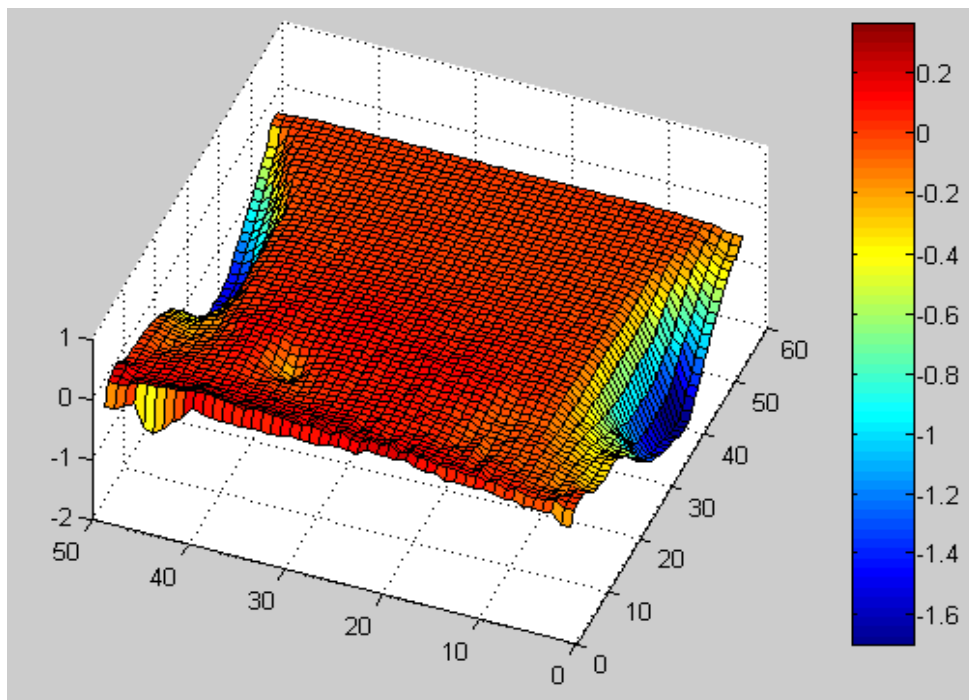


Figure 97. Corrected (3-D) surface plot of 19B

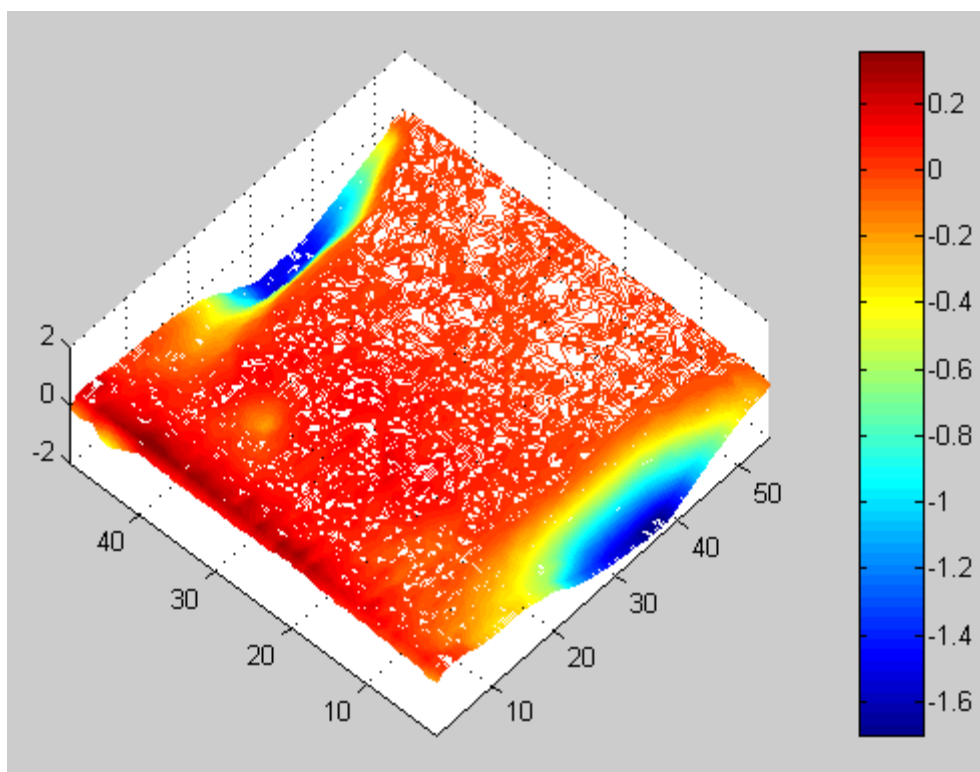


Figure 98. Corrected (3-D) surface plot of 19B

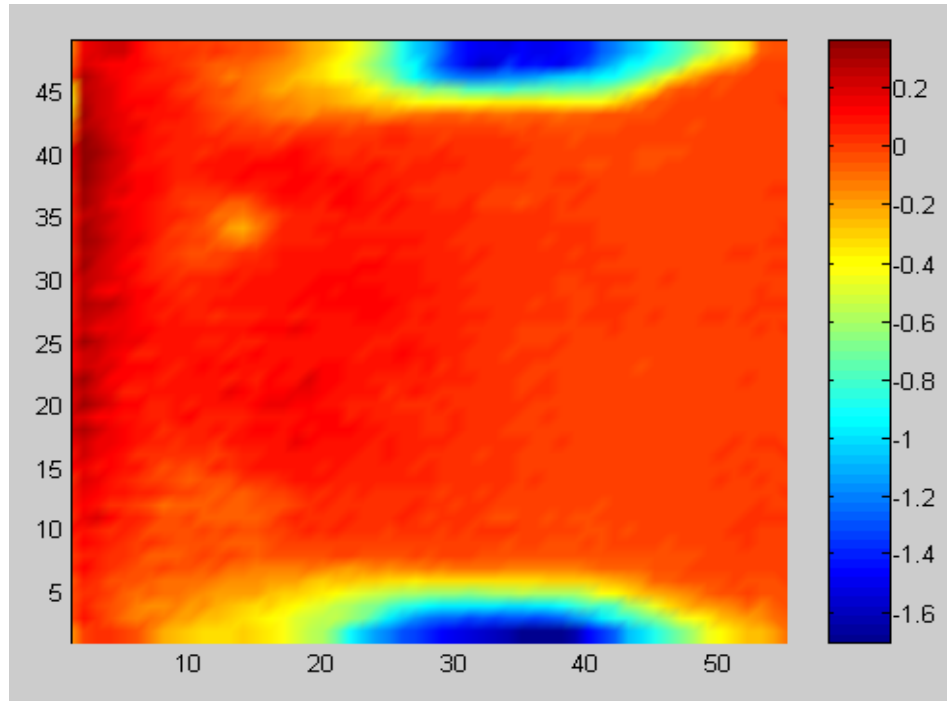


Figure 99. Corrected (2-D) erosion plot of 19B

d. Calculation of Eroded Mass

The total eroded metal volume was found to be 260.4215 mm^3

$$\rho = 2.7 \frac{\text{g}}{\text{cm}^3}$$

$$m = 0.0027 \frac{\text{g}}{\text{mm}^3} \times 260.4215 \text{ mm}^3 = 0.7032 \text{ g}$$

THIS PAGE INTENTIONALLY LEFT BLANK

V. UNCERTAINTIES

A CONTROL ARMATURE SURFACE

We measured the surface of an unfired armature as a control for measurement accuracy. The surface of the unfired armature was painted uniform white and scanned thereafter.

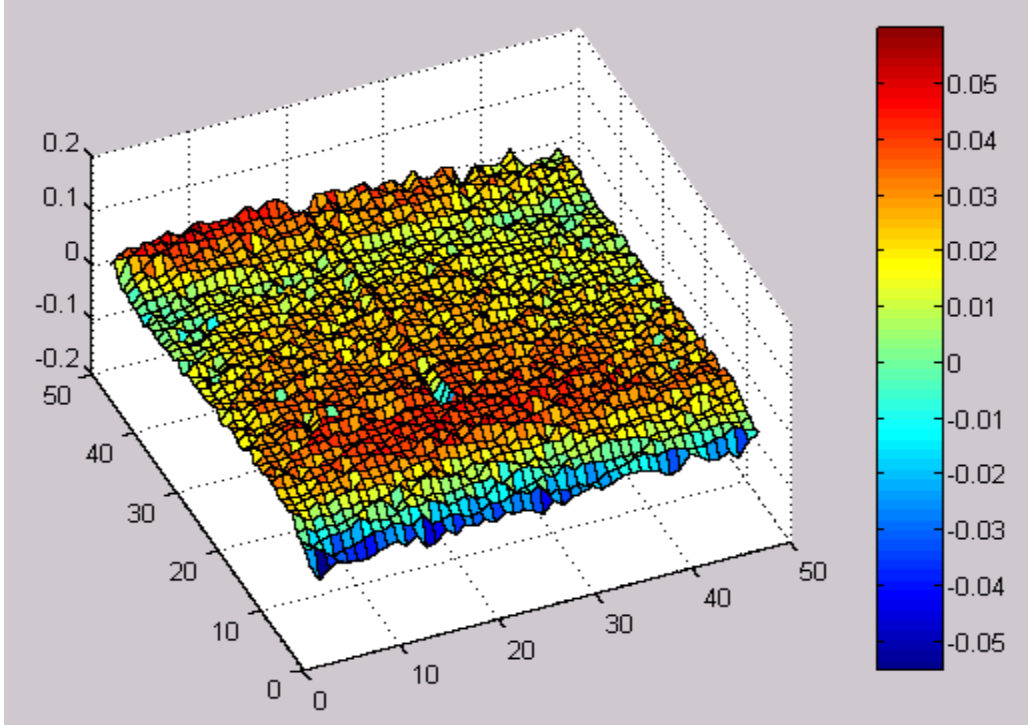


Figure 100. (3-D) Surface plot of unfired armature

The average value of the displacements on this surface is -0.02375 mm which corresponds to a volume loss of 53.591 mm^3 and a mass loss $\Delta m = 0.144 \text{ g}$. The proper value of Δm is zero. The non-zero value of Δm is an artifact of our method and can be taken as an indication of the accuracy of our measurements.

B. COMPARISON OF MASS LOSSES

Measured values of Δm are given in Table 5 for all nine surfaces. Asymmetric mass losses are observed for most armatures and it is important to know if these differences are meaningful. Measured thickness of the paint applied to the armature surfaces were less than $1 \text{ } \mu\text{m}$ and hence should not seriously affect the results.

The values of Δm for different surfaces of some armatures differ by more than the expected uncertainty of our data. On the other hand, we corrected gross deformations of the armatures by equations of the form $z = a + bx + cy$, and it is obvious that some of the armatures have curvatures. Specifically examination of Figs. 64,75, and 90 and of corresponding armatures 11B, 18B, and 19A indicate that second order corrections in x and y were required.

Thus, the symmetries in mass losses in Table 5 from different surfaces of the same armature are not significant and may be artifacts of the data reduction.

ARMATURES	MASS LOSS (g)
10A	1.33
10B	0.0938
11A	0.396
11B	0.452
18A	1.945
18B	0.706
19A	1.42
19B	0.703
Unfired	0.144

Table 5. Mass losses for each armature surface

VI. CONCLUSIONS

Nine armature surfaces were measured. The erosion contours and surface plots are presented. The erosion on these armatures is mostly on the lateral edges of the electrical contact face. Mass losses from unbent surfaces range from 0.4 to 0.7 g and should represent the mass losses accurately. We do not have the operating condition and so cannot correlate mass losses with firing parameters.

THIS PAGE INTENTIONALLY LEFT BLANK

VII. FUTURE WORK

This research provides a basic method to measure the metal erosion on railgun armatures. The following is a list of topics for future research.

- The correlation of eroded mass with firing parameters.
- Second-order correction of armature bending.

THIS PAGE INTENTIONALLY LEFT BLANK

APPENDIX A

Visual Basic code for controlling XY tables

```
Option Explicit
Dim cnt As Integer
Dim pos As Single
Dim t As String
Dim b As String
Dim z As String
Dim s As String
Dim F As Double
Dim datum(2500) As Double
Dim ozcount As Integer
Dim Buf2 As String
Dim j As String
Dim Buf1 As String

Private Sub anzio_Click()

Buf2 = Chr(2) + "MSVLR" + Chr(3)
MSComm2.Output = Buf2
Buf2 = ""
Buf1 = "2LDO 2MN 2A1 2V.5 2D5100 2H- 2G" + vbCrLf
MSComm1.Output = Buf1
Buf1 = ""
End Sub

Private Sub CENTER_Click()
Buf1 = "1LD0 1MN 1A1 1V3 1D458880 1H- 1G 2LD0 2MN 2A1 2V3  
2D205140 2H- 2G" + vbCrLf
MSComm1.Output = Buf1
Buf1 = ""
End Sub

Private Sub cmdGrandTour_Click()
Dim i As Long
'put to home
Buf1 = "1LD0 1MC 1V3 1H+ 1G 2LD0 2MC 2V3 2H+ 2G " + vbCrLf
MSComm1.Output = Buf1
Buf1 = ""
Call control
MsgBox "Move Complete"
'put to center
```

```

Buf1 = "1LD0 1MN 1A1 1V3 1D331380 1H- 1G 2LD0 2MN 2A1 2V3
2D205140 2H- 2G" + vbCrLf
MSComm1.Output = Buf1
Buf1 = ""
Call control
MsgBox "Move Complete"
'Call Read_Click
'Call cmdsavefile_Click
End Sub

```

```

Private Sub cmdsavefile_Click()
    Dim cnt As Integer
    Open "C:\ozkan.dat" For Output As #1
    For cnt = 0 To 25
        Print #1, datum(cnt)
    Next cnt
    Close #1
End Sub

```

```

Private Sub cmdShow_Click()
    Dim cnt As Integer
    For cnt = 0 To 25
        picout.Print (datum(cnt))
    Next cnt
End Sub

```

```

Private Sub DOWN_Click()
    Buf1 = "2LD0 2MC 2A1 2V1 2D11000 2H+ 2G" + vbCrLf
    MSComm1.Output = Buf1
    Buf1 = ""
End Sub

```

```

Private Sub down1step_Click()
    Buf1 = "2LD0 2MN 2A1 2V.5 2D5100 2H+ 2G" + vbCrLf
    MSComm1.Output = Buf1
    Buf1 = ""
End Sub

```

```

Private Sub DOWNMOST_Click()
    Dim e As String
    Buf1 = "2LDO 2MC 2A1 2V.5 2H- 2G" + vbCrLf
    MSComm1.Output = Buf1
    Buf1 = ""

```

```

e = ""
Do Until Mid(e, 2, 2) = "DA"
    Buf2 = Chr(2) + "MSVLR" + Chr(3)
    MSComm2.Output = Buf2
    Buf2 = ""
    e = MSComm2.Input
Loop
Buf1 = "2S" + vbCrLf
MSComm1.Output = Buf1
Buf1 = ""
MsgBox "Red dot is on the down edge of the armature"
Buf1 = "2LDO 2MN 2A1 2V0.5 2D5100 2H+ 2G" + vbCrLf
MSComm1.Output = Buf1
Buf1 = ""
End Sub

```

```

Private Sub left1step_Click()
    Buf1 = "1LDO 1MN 1A1 1V.5 1D5100 1H- 1G" + vbCrLf
    MSComm1.Output = Buf1
    Buf1 = ""
End Sub

```

```

Private Sub LEFTMOST_Click()
    Dim r As String
    Buf1 = "1LDO 1MC 1A1 1V.5 1H+ 1G" + vbCrLf
    MSComm1.Output = Buf1
    Buf1 = ""
    r = ""
    Do Until Mid(r, 2, 2) = "DA"
        Buf2 = Chr(2) + "MSVLR" + Chr(3)
        MSComm2.Output = Buf2
        Buf2 = ""
        r = MSComm2.Input
    Loop
    Buf1 = "1S" + vbCrLf
    MSComm1.Output = Buf1
    Buf1 = ""
    MsgBox "Red dot is on the left edge of the armature"
    'Move small amount away from edge!
    Buf1 = "1LDO 1MN 1A1 1V.5 1D5100 1H- 1G" + vbCrLf
    MSComm1.Output = Buf1
    Buf1 = ""
End Sub

```

```

Private Sub measureUp_Click()
    Buf2 = Chr(2) + "MSVLR" + Chr(3)

```

```

MSComm2.Output = Buf2
Buf2 = ""
Buf1 = "2LDO 2MN 2A1 2V.5 2D5100 2H+ 2G" + vbCrLf
MSComm1.Output = Buf1
Buf1 = ""
End Sub

```

```

Private Sub Positon_Report_Click()
Buf1 = "1PR" + vbCrLf
MSComm1.Output = Buf1
Buf1 = ""
t = ""
End Sub

```

```

Private Sub Proceed1_Click()
Buf2 = Chr(2) + "MSVLR" + Chr(3)
MSComm2.Output = Buf2
Buf2 = ""
Buf1 = "2LDO 2MN 2A1 2V.5 2D5100 2H- 2G" + vbCrLf
MSComm1.Output = Buf1
Buf1 = ""
End Sub

```

```

Private Sub readsave_Click()
Buf2 = Chr(2) + "MSVLR" + Chr(3)
MSComm2.Output = Buf2
Buf2 = ""
End Sub

```

```

Private Sub right1step_Click()
Buf1 = "1LD0 1MN 1A1 1V.5 1D5100 1H+ 1G" + vbCrLf
MSComm1.Output = Buf1
Buf1 = ""
End Sub

```

```

Private Sub up1step_Click()
Buf1 = "2LD0 2MN 2A1 2V.5 2D5100 2H- 2G" + vbCrLf
MSComm1.Output = Buf1
Buf1 = ""
End Sub

```

```

Private Sub UPMOST_Click()
Dim q As String
Buf1 = "2LDO 2MC 2A1 2V.5 2H+ 2G" + vbCrLf
MSComm1.Output = Buf1
Buf1 = ""

```

```

q = ""
Do Until Mid(q, 2, 2) = "DA"
    Buf2 = Chr(2) + "MSVLR" + Chr(3)
    MSComm2.Output = Buf2
    Buf2 = ""
    q = MSComm2.Input
Loop
Buf1 = "2S" + vbCrLf
MSComm1.Output = Buf1
Buf1 = ""
MsgBox "Red dot is on the upper edge of the armature"
Buf1 = "2LDO 2MN 2A1 2V0.5 2D5100 2H- 2G" + vbCrLf
MSComm1.Output = Buf1
Buf1 = ""
End Sub

```

```

Private Sub Form_Load()
    MSComm1.CommPort = 1
    MSComm2.CommPort = 2
    MSComm1.Settings = "9600,N,8,1"
    MSComm2.Settings = "9600,N,8,1"
    'Com event will be triggered when a single character is received.
    MSComm1.RThreshold = 1
    MSComm2.RThreshold = 1
    'Open the port.
    MSComm1.PortOpen = True
    MSComm2.PortOpen = True
    Dim Buf1 As String
    Dim Buf2 As String
    Erase datum
End Sub

```

```

Private Sub HOME_Click()
    Buf1 = "1LD0 1MC 1A1 1V3 1H+ 1G 2LD0 2MC 2A1 2V3 2H+ 2G " + vbCrLf
    MSComm1.Output = Buf1
    Buf1 = ""
End Sub

```

```

Private Sub LEFT_Click()
    Buf1 = "1LD0 1MC 1A1 1V1 1D11000 1H- 1G" + vbCrLf
    MSComm1.Output = Buf1
    Buf1 = ""
End Sub

```

```

Private Sub MIDDLEX_Click()

```



```

Dim HALFMIDI As Double
Dim MIDI As Double
Dim V As String
Dim G As String
Dim r As String
Buf1 = "1LDO 1MC 1A1 1V.5 1H+ 1G" + vbCrLf
MSComm1.Output = Buf1
Buf1 = ""
r = ""
Do Until Mid(r, 2, 2) = "DA"
    Buf2 = Chr(2) + "MSVLR" + Chr(3)
    MSComm2.Output = Buf2
    Buf2 = ""
    r = MSComm2.Input
Loop
Buf1 = "1S" + vbCrLf
MSComm1.Output = Buf1
Buf1 = ""
MsgBox "Red dot is on the left edge of the armature"
'Move small amount away from edge!
Buf1 = "1LDO 1MN 1A1 1V.5 1D3500 1H- 1G" + vbCrLf
MSComm1.Output = Buf1
Buf1 = ""
Call control
Buf1 = "1PR " + vbCrLf
MSComm1.Output = Buf1
Buf1 = ""
MsgBox "WAIT!!"
G = MSComm1.Input
G = Trim(G)
V = Mid(G, 7, 9)
V = Format(V, "#####")
MsgBox "Position = " + V
'Debug.Print V
'MIDI = CSng(V)
'MsgBox V / 5100 + "mm in X dir"

HALFMIDI = Int(MIDI / 2)
'Debug.Print (HALFMIDI)
'MsgBox HALFMIDI
Buf1 = "1LD0 1MN 1A1 1V0.5 1D(HALFMIDI) 1H+ 1G " + vbCrLf
MSComm1.Output = Buf1
Buf1 = ""
End Sub

Private Sub RIGHTMOST_Click()

```

```

Dim w As String
Dim POSITION As String
POSITION = ""
Buf1 = "1PZ 1LDO 1MC 1A1 1V.5 1H- 1G" + vbCrLf
MSComm1.Output = Buf1
Buf1 = ""
w = ""
Do Until Mid(w, 2, 2) = "DA"
    Buf2 = Chr(2) + "MSVLR" + Chr(3)
    MSComm2.Output = Buf2
    Buf2 = ""
    w = MSComm2.Input
Loop
Buf1 = "1S" + vbCrLf
MSComm1.Output = Buf1
Buf1 = ""
MsgBox "Red dot is on the right edge of the armature "
Buf1 = "1LD0 1MN 1A1 1V0.5 1D5100 1H+ 1G" + vbCrLf
MSComm1.Output = Buf1
Buf1 = ""

'Buf1 = "1PR" + vbCrLf
'MSComm1.Output = Buf1
'Buf1 = ""
'Call control
'POSITION = MSComm1.Input
'MsgBox "Position=" + POSITION
End Sub

Private Sub MSComm1_OnComm()
'when a comm event occurs.

'Was it a "receive event? If so, add the received character
'to the Text Box and set the insertion point at the end of
'the text, other events.

Select Case MSComm1.CommEvent
    Case comEvReceive
        s = MSComm1.Input
        If Asc(s) = 13 Then s = vbCrLf
        t = t + s
        Text1.Text = Text1.Text & s
        Text1.SelStart = Len(Text1.Text)
End Select
t = Format(t, "#####")
pos = Val(t)

```

```

Text1.Text = pos
End Sub
Private Sub MSComm2_OnComm()
Dim C As String
Dim D As String
Dim e As String
Dim b As String

'Dim ozcount As Integer
'when a comm event occurs.

'Was it a "receive event? If so, add the received character
'to the Text Box and set the insertion point at the end of
'the text, other events.

Select Case MSComm2.CommEvent
    Case comEvReceive

        MSComm2.InputLen = 0
        Do
            DoEvents
        Loop Until MSComm2.InBufferCount >= 2
        ' Read the "OK" response data in the serial port.
        'Call control
        z = MSComm2.Input
        z = Trim(z) 'trim returns string without spaces
        'MsgBox z
    End Select

    b = Mid(z, 4, 7)
    C = LEFT(z, 1) 'take the first char of the input str
    If Asc(C) <> 6 Then 'Test if first character is line
        D = LEFT(z, 2) 'if not take the two chars left
        e = Mid(z, 7, 5) 'take rightmost 5 chars
        b = e & D 'concatenate them
        D = ""
    End If
    F = Val(b)
    'MsgBox F
    Upscale F
End Sub

Private Sub Read_Click()
DownScale

'Dim u As Integer

```

```

'For u = 1 To 2
'Dim o As Double
'Buf2 = Chr(2) + "MSVLR" + Chr(3) 'Request distance measurement
'MSComm2.Output = Buf2
'Buf2 = ""
'For o = 1 To 50000000 'Delay 5 seconds
'Next o
'Buf1 = "2LDO 2MN 2A1 2V.5 2D5100 2H- 2G" + vbCrLf
'MSComm1.Output = Buf1 'Move 1mm
'Buf1 = ""
'Next u
End Sub

```

```

Private Sub Revision1_Click()
Buf1 = "1RV" + vbCrLf
MSComm1.Output = Buf1
Buf1 = ""
End Sub

```

```

Private Sub Revision2_Click()
Buf1 = "2RV" + vbCrLf
MSComm1.Output = Buf1
Buf1 = ""
End Sub

```

```

Private Sub RIGHT_Click()
Buf1 = "1LDO 1MC 1A1 1V1 1D11000 1H+ 1G" + vbCrLf
MSComm1.Output = Buf1
Buf1 = ""
End Sub

```

```

Private Sub SAVE_Click()
Dim counter As Integer
For counter = 1 To 5
Call Read_Click
datum(counter) = F
MsgBox datum(counter)
Next counter
End Sub
Private Sub STOP_Click()
Buf1 = "1S 2S" + vbCrLf
MSComm1.Output = Buf1
Buf1 = ""
End Sub

```

```

Private Sub Test_Click()
Buf1 = "TEST" + vbCrLf
MSComm1.Output = Buf1
Buf1 = ""
End Sub

```

```

Public Sub Text1_KeyPress(KeyAscii As Integer)
'Add the key to the buffer.
    Buf1 = Buf1 + Chr$(KeyAscii)
'if it was a carriage return, send the buffer contents
'to the Comm control and empty the buffer.
    If KeyAscii = 13 Then
        MSComm1.Output = Buf1
        Buf1 = ""
    End If
    'Asc(9)=Tab Key
    If KeyAscii = Asc(9) Then
        Form_Quit
    End If
End Sub

```

```

Public Sub Form_Resize()
'Set text box to fill the form.
Text1.Width = Form1.ScaleWidth
Text1.Height = Form1.ScaleHeight
Text1.LEFT = 0
Text1.Top = 0
End Sub

```

```

Public Sub Form_Quit()
'Close the Port
MSComm1.PortOpen = False
MSComm2.PortOpen = False
End
End Sub

```

```

Private Sub UP_Click()
Buf1 = "2LD0 2MC 2A1 2V1 2D11000 2H- 2G" + vbCrLf
MSComm1.Output = Buf1
Buf1 = ""
End Sub

```

```

Public Sub control()
Dim j As String
j = ""
Do Until Mid(j, 2, 2) = "00"
Buf1 = "1PR" + vbCrLf
MSComm1.Output = Buf1
Buf1 = ""
j = MSComm1.Input
Loop
End Sub

```

```

Public Sub don()
Open "C:\ozkan.dat" For Output As #1
Print #1, datum(ozcount)
Close #1
End Sub

```

```

Public Sub DownScale()
'Dim i As Integer
'Dim p As Double
'For i = 1 To 2
Buf2 = Chr(2) + "MSVLR" + Chr(3)
MSComm2.Output = Buf2
Buf2 = ""
'picout.Print "Loop#1"
'For p = 1 To 10000000
'Next p
'Buf2 = Chr(2) + "MSVLR" + Chr(3)
'MSComm2.Output = Buf2
'Buf2 = ""
'picout.Print "Loop#2"
'picout.Print F
'Next i
End Sub
Public Sub Upscale(F As Double)
Open "C:\ozkan.dat" For Append As #1
Write #1, F
Close #1
Debug.Print F
picout.Print F
'Call cmdsavefile_Click
End Sub

```

THIS PAGE INTENTIONALLY LEFT BLANK

LIST OF REFERENCES

- [1] Ogorkiewicz, R.M., In search of Lighter, “Smaller Electric Guns for Future Tanks”, Jane’s International Defense Review, Vol. 032, Issue: 001,pp. 1-6,1999
- [2] W.A. Walls, W.F. Weldon, S.B. Pratab, Palmer and D. Adams, “Applications of Electromagnetic guns to future naval platforms” IEEE Trans.Magn.,January 1999,pp.262-267
- [3] Ian R.McNab, IEEE, Scott Fish, Francis Stefani, “Parameters for an Electromagnetic Naval Railgun”, Institute for Advanced Technology, The University of Texas at Austin, 1999
- [4] Luke,I.T. and Stumborg ,M.F., “ The operational value of Long Range Land Attack EM Guns to Future Naval Forces”,IEEE Trans. Magn.,pp.3-15,1998
- [5] A.Marshall, Richard, “Railgun Bore Geometry, round or square?”IEEE Trans.Magn.,Vol.35 No. 1
- [6] Stefani, Francis and Parker, Jerry, “Experiments to measure Armature Wear Part1:Wear Measurements on the KJ202 Armature”, 1997
- [7] Grant M.G. Hainsworth and David C. Haugh, “Erosion Observations on Recovered Large Caliber Armatures” IEEE Trans.Magn., 1 January 2001,vol.37,No.1, page 73
- [8] The armatures were obtained from Francis Stefani, Institute of Advanced Technology, Austin-Texas, May 2001
- [9] J.F. Kerrisk, “Current Distribution and Inductance Calculation for railgun Conductors” Los Alamos National Laboratory report LA-9092-MS, October 1980

THIS PAGE INTENTIONALLY LEFT BLANK

INITIAL DISTRIBUTION LIST

1. Defense Technical Information Center
Ft. Belvoir, Virginia
2. Dudley Knox Library
Naval Postgraduate School
Monterey, California
3. Turkish Army Headquarters Library
(Kara Kuvvetleri Komutanligi Kutuphanesi)
Bakanliklar-ANKARA
TURKEY
4. 1LT Ozkan Gurhan
Yeni Mah. Kemal Sedele Sok. No:8/14
Elazig
TURKEY
5. Professor William Maier II
Department of Physics
Naval Postgraduate School
Monterey, California
6. Francis Stefani
Institute of Advanced Technology
University of Texas at Austin
3925 W. Braker Ln. Ste. 400
Austin, Texas